INFLUENCE OF SPRUCE BUDWORM DEFOLIATION ON STREAM MICROBIOMES

THE INFLUENCE OF SPRUCE BUDWORM DEFOLIATION ON STREAM MICROBIOME STRUCTURE AND FUNCTION

MADISON MCCAIG, BSc.

A Thesis Submitted to the School of Graduate Studies in Partial Fulfilment of the Requirements for the Degree Master of Science

McMaster University MASTER OF SCIENCE (2023) Hamilton, Ontario (Biology)
TITLE: The influence of spruce budworm defoliation on stream microbiome structure and function
AUTHOR: Madison L McCaig, B.Sc. (University of Ottawa)
SUPERVISORS: Dr. K. Kidd and Dr. E. Emilson
NUMBER OF PAGES: xv, 100

Lay Abstract

Terrestrial and aquatic landscapes are tightly linked, and forest disturbances can influence stream ecosystems. Insect pests defoliate millions of hectares of forests each year, but the resulting impacts on stream ecosystems are poorly understood. This study investigated the effects of a spruce budworm outbreak on water quality and microbial communities in streams in Gaspésie, QC, Canada. Microbial communities are critical to the functioning of stream ecosystems as they convert energy (e.g., carbon) into useable forms for other organisms. Results indicate that defoliation altered stream flow rates, temperatures, and carbon composition, as well as the microbial communities involved in carbon cycling processes. Carbon is essential to aquatic food webs and this improved understanding of how carbon flow is altered by a widespread forest disturbance can inform pest management decisions for spruce budworm outbreaks.

Abstract

Insect pests are the most widespread disturbance in Canadian forests, but resulting impacts of forest defoliation on stream ecosystem functions are poorly understood. This study investigated the effects of a spruce budworm outbreak on water quality and the structure and function of microbial communities in streams of 12 catchments across a gradient of cumulative defoliation severity in the Gaspésie Peninsula, Québec, Canada. Bi-weekly stream habitat sampling was conducted spring to fall 2019-2021, with stream flow rates measured and water samples collected and analyzed for water chemistry parameters, nutrients, and dissolved organic matter (DOM) structure and quality. Algal communities were assessed at the same time by measuring in-situ biomass. Bacteria and fungi communities on leaf packs were assessed by incubating six leaf packs for five weeks (mid-August- late September) in one stream reach per watershed. Microbial community composition of leaf packs was determined using metabarcoding of 16S and ITS rRNA genes, and functions were examined using extracellular enzyme assays, leaf litter decomposition rates, and taxonomic functional assignments. This study determined that cumulative defoliation increased stream temperatures, flow rates, and SUVA (DOM aromaticity), but not nutrients. It increased algal biomass and altered microbial community composition, with a stronger influence on bacteria than fungi. The observed increases in SUVA and algal biomass corresponded with changes to bacteria carbon cycling functions, which indicated that microbes were preferentially selecting carbohydrates produced by algae rather than the aromatic compounds from increased terrestrial inputs. There were no changes to other bacteria or fungi functions and no changes to taxonomic or functional diversity. Overall, results indicate that forest pest outbreaks alter carbon inputs to streams and the structure and function of stream microbial communities associated with carbon cycling.

Acknowledgments

I am extremely grateful for the support and guidance of both of my supervisors, Dr. Karen Kidd and Dr. Erik Emilson. Your expertise, feedback, encouragement, and kindness made this a very enjoyable experience for me and allowed me to learn and grow as a scientist. I would also like to thank Dr. Herb Schellhorn for being a part of my advisory committee and providing feedback on my methods and results.

This project would not have been possible without the help of everyone in the Watershed Ecology Team (WET) at Natural Resources Canada, Great Lakes Forestry Centre – Joe Schadenberg, Derek Chartrand, Scott Capell, Brian Kielstra, and Caroline Emilson. Special thank you to Emily Smenderovac for managing the overall project data, teaching me all about DNA, bioinformatics, and microbes, and always being there to give me a hand when I needed it.

Thank you to everyone at the Kidd Lab at McMaster for their support – it has been a pleasure to work with such a welcoming and passionate group of people. I am especially grateful for everyone who helped with field work and provided support and advice throughout my degree (Sally Ju, Harvinder Sidhu, Cora Bilhorn, Jenni Velichka, and Celine Lajoie). Special thank you to Brittany Perrotta for being an excellent teacher and providing guidance and suggestions for my data analyses.

I would also like to acknowledge the funding sources (NRCan, NSERC, and The Jarislowsky Foundation) and collaborations (University of New Brunswick and Québec Ministère des Forêts, de la Faune et des Parcs) that made this project possible.

Finally, thank you to my partner and my family for the support and encouragement to pursue my passions and dreams.

Table of Contents

List of Figures

List of Tables

List of Abbreviations

Abbreviation	Definition
Bix	Biological index
Btk	*Bacillus thuringiensis* var. *kurstaki*
Clr	Centre log transformed
CoDA	Compositional Data Analysis
DEM	Digital Elevation Model
DOC	Dissolved organic carbon
DOM	Dissolved organic matter
EEMs	Fluorescence excitation-emission matrices
EIS	Early Intervention Strategy
ESV	Exact Sequence Variant
GIS	Geographic Information Systems
HAiFLO	hydrologically active, inverse distance weighted metric
Hix	Humification index
MFFP	Ministère des Forêts de la Faune et des Parcs
NAG	N-acetyl-β-D-glucosaminidase
NMDS	Non-metric Multidimensional Scaling
NRCan -GLFC	Natural Resources Canada, Great Lakes Forestry Centre
PCA	Principal Component Analysis
PCoA	Principle Coordinate Analysis
PERMANOVA	Permutational multivariate analysis of variance
PHOS	Phosphatase
RDA	Redundancy Analysis
SOPFIM	La Société de Protection des Forêts Contre les Insectes et Maladies
SUVA	Specific ultraviolet absorbance at 254 nm
XY	Xylosidase

Declaration of Academic Achievement

This thesis was designed and written by Madison McCaig under the supervision of Dr. Erik Emilson and Dr. Karen Kidd. The overall project study design for stream sampling of the watersheds in the Gaspésie was created and implemented by Dr. Erik Emilson, Dr. Michael Stastny, and Dr. Karen Kidd. The field and laboratory study design for this thesis was developed by Dr. Erik Emilson and Dr. Karen Kidd. Field sampling for water quality, stream flow, and algal biomass was conducted by Holly Campbell in 2019 and by Marc-Antoine Allard in 2020 and 2021. Field sampling of leaf packs, sediment tubes, and temperature loggers was conducted by the WET Lab (NRCan-GLFC) in 2019, the Kidd lab in 2020, and Madison McCaig with assistance from the Kidd lab in 2021. Laboratory processing of sediment tubes and leaf litter decomposition was conducted by Scott Capell (WET Lab). Extracellular enzyme assays and DNA extractions were conducted by Derek Chartrand (WET Lab) for 2019 and 2020 samples and Madison McCaig for 2021 samples, with protocols established by Caroline Emilson. Illumina sequencing was performed on an Ilumina MiSeq at the National Research Council Canada, Saskatoon as supported through the Genomics Research and Development Initiative. Bioinformatic processing of DNA sequence data was performed by Emily Smenderovac (WET Lab) on the 2019 and 2020 data and Madison McCaig on the 2021 data. Data analysis and interpretation were completed by Madison McCaig with advice from Erik Emilson, Karen Kidd, Emily Smenderovac, Brittany Perrotta, and Caroline Emilson. I, Madison McCaig, declare that this thesis is an original report of my research

1.0 Introduction

Forests are impacted by many natural disturbances such as wildfires, drought, windthrow, parasites, disease, and insect pests and are managed to enhance resilience to these threats. Insect pests are the most widespread disturbance type in Canadian forests, impacting over 17 million hectares in 2020, with 40% of the damage caused by the eastern spruce budworm (*Choristoneura fumiferana)* (Natural Resources Canada, 2022). This native insect pest feeds upon and defoliates balsam fir (*Abies balsamea)* and white spruce (*Picea glauca)* trees and causes changes to forest ecosystems through frass production, tree needle loss, reduced tree growth, and eventually tree mortality (De Grandpré et al., 2022; D. R. Gray & MacKinnon, 2006). Outbreaks of spruce budworm occur cyclically every 30 – 40 years and are predicted to expand their range and increase in duration and severity as climate change progresses (Candau & Fleming, 2011; David R. Gray, 2008). On the terrestrial landscape, spruce budworm defoliation threatens many of the essential ecosystem services Canada's boreal forests provide as it causes wildlife habitat loss, a reduction in forest carbon sequestration, and billions of dollars in economic losses for the commercial forestry industry (Johns et al., 2019; E. Y. Liu et al., 2019; Z. Liu et al., 2020; Schowalter, 2012). However, the influence of spruce budworm defoliation on aquatic ecosystems within forested watersheds is poorly understood.

Forest and aquatic ecosystems are tightly connected and forest disturbances can alter stream ecosystem conditions, but the nature of these responses depends on the specific changes occurring in the forests (Kreutzweiser et al., 2008; Paul et al., 2022; Warren et al., 2016). The loss of foliage and tree mortality associated with spruce budworm defoliation could lead to multiple physical changes in stream conditions. It can increase light levels, resulting in increased water temperatures, increased snow melt rates, and reduced evapotranspiration rates, leading to

increased runoff and stream flow rates (Jenicek et al., 2018; Sidhu et al., in prep.; Warren et al., 2016). Furthermore, the litter and frass inputs from spruce budworm defoliation increase nutrient inputs to the forest floor, which could be transferred through runoff to stream ecosystems (De Grandpré et al., 2022). These increased terrestrial inputs can also have implications for the quantity and quality of the dissolved organic matter (DOM) pool in streams, with increased aromaticity and humic content of DOM increasing with more terrestrial runoff (Jaffe et al. 2008; LoRusso et al. 2021). Despite the potential for effects, to date no studies have specifically tested the impacts of spruce budworm defoliation on stream ecosystem responses.

These altered stream conditions can also have implications for the aquatic food web, including the stream microbiome, which is essential to stream ecosystem functioning. Bacteria, fungi, and algae communities play particularly critical roles in the flow of energy and nutrients though stream food webs as they are important contributors to both primary and secondary productivity (Findlay, 2010). Primary productivity in these systems is largely driven by the photosynthetic production by algal communities, where inorganic carbon is converted into simple organic carbon that is easily accessible for consumers (Findlay, 2010). Secondary productivity is typically driven by bacteria and fungi communities which decompose organic matter and mineralize inorganic nutrients, making these resources accessible to consumers in higher trophic positions (Allan et al., 2021; Emilson et al., 2016; Findlay, 2010). This is critical for stream ecosystem functioning as DOM is their largest source of organic carbon and without microbial decomposition, it would be inaccessible to the rest of the food web (Findlay, 2010).

Stream microbiomes are comprised of a wide diversity of organisms which perform key biogeochemical functions for stream ecosystems, and their structure and function are influenced by both regional (e.g., dispersal and landscape characteristics) and local environmental

conditions (e.g., temperature, nutrient concentrations, DOM composition, flow rates, pH levels, and metal concentrations) (Besemer, 2016; Emilson et al., 2016; Zeglin, 2015). For example, microbiome composition and diversity are positively associated with gradients of landscape heterogeneity and stream flow due to increased dispersal of microbial taxa and associated increases in transfers of nutrients, carbon, and oxygen (Besemer, 2016; Besemer et al., 2009; Woodcock et al., 2013). Changes in the quality of DOM often results in shifts in bacteria functions as they preferentially select the most easily accessible carbon compounds (Cunha et al., 2010; Gorke & Stulke, 2008). Furthermore, is important to consider the complex relationship between microbiome structure and function as this can provide a more complete understanding of stream ecosystem functioning (Findlay, 2010; Grossart et al., 2020). In some cases, structure and function are linked, whereas in others, differences in community structure have been observed along environmental gradients while functions remain stable (i.e., functional redundancy) (Grossart et al., 2020). Characterizing the structure and function of stream microbiomes along environmental gradients is critical as freshwater ecosystems are increasingly threatened by stressors such as climate change, urbanization, and forest change (Dudgeon et al., 2006; Reid et al., 2019).

Natural and anthropogenic disturbances often change stream habitat conditions which can alter the structure and function of stream microbiomes (Burdon et al., 2020; Emilson et al., 2016; Laperriere et al., 2020). Shifts in stream microbiome species composition are often observed after a disturbance, while species richness and species diversity are not typically altered (Emilson et al., 2016; Lau et al., 2015; Simonin et al., 2019). Disturbances that increase stream temperatures and nutrient concentrations can enhance microbial decomposition (Burdon et al., 2020; Emilson et al., 2016; Fernandes et al., 2014), while alterations to carbon quality (e.g.,

specific ultraviolet absorbance (SUVA)) can increase extracellular enzyme activities (Cunha et al., 2010) and bacteria functions associated with the processing of aromatic compounds (Fasching et al., 2020). The response of stream microbiomes to disturbance has been investigated for urban and agricultural land use (Laperriere et al., 2020; Simonin et al., 2019), wastewater treatment plant discharges (Burdon et al., 2020), and fire, logging, and mining (Emilson et al., 2016), but the influence of forest pest defoliation on stream microbiome structure and function has not been previously investigated.

A large-scale spruce budworm outbreak has been ongoing in the Gaspésie Peninsula of Québec, Canada, since 2016. A multidisciplinary project was initiated in 2018 to investigate the ecological risks and benefits of defoliation at the forested watershed scale to inform forest pest management decisions. Two forest pest management strategies are typically used in the Atlantic region to mitigate the impacts of spruce budworm outbreaks – the more traditional reactive strategy, and a recently introduced proactive strategy called the Early Intervention Strategy (EIS). The reactive approach focuses on foliage protection of only the most valuable resources using insecticides, whereas EIS aims to suppress spruce budworm populations prior to major defoliation through targeted applications of insecticides in hotspot areas (Johns et al., 2019). EIS generally results in less defoliation and has been found to reduce tree mortality and economic losses of forest resources; however, the risks and benefits of EIS to broader ecosystem processes through suppression of defoliation and mortality within forested watersheds have not been explored.

The objective of the current study is to assess how spruce budworm defoliation in the Gaspésie impacts the structure and function of stream microbiomes in forested watersheds. We used leaf packs as the substrate for microbiome establishment to assess fungal and bacteria

communities in 12 forested watersheds across a gradient of defoliation severity. To assess microbiome structure, we used next generation sequencing and to assess microbiome function we used hydrolase enzyme activities, leaf litter decomposition rates, and taxonomic functional assignments. We predict that cumulative defoliation will have three main influences on the stream microbiome. First, we predict that it will alter the stream microbiome through changes to stream habitat, specifically by increasing nutrient levels, water temperature, and flow rates, and by altering dissolved organic matter quality. Second, we predict that stream microbiome composition will be altered by cumulative defoliation (through changes to stream habitat), but species richness (16S and ITS) and diversity (16S) will not change. Finally, we predict that cumulative defoliation (through changes to stream habitat) will alter stream microbiome functions (hydrolase enzyme activity, decomposition, and taxonomic functional assignments). The insights gained from this project will provide a more comprehensive understanding of the ecological risks and benefits of forest pest management.

2.0 Methods

2.1 Study Design

This study was done in the Gaspésie Peninsula of eastern Québec, Canada (Figure 1). It is a rugged and mountainous area that forms part of the Appalachian Mountain range. Land cover in the area is primarily forested with an abundance of streams and rivers and few lakes (Berger & Blouin, 2004). The most important industries are forestry and recreational tourism, particularly Atlantic salmon fishing. The Gaspésie Peninsula has a history of forest disturbances, including fire, logging, and insect outbreaks (Berger & Blouin, 2004). It is currently experiencing a spruce budworm outbreak which began in 2016 and is impacting white spruce and balsam fir trees (Ministère des Ressources naturelles et des Forêts, 2022).

Twelve forested watersheds in the Gaspésie Peninsula were selected for this study (Figure 1). The selection process involved first delineating all watersheds between 6 – 10 km^2 using a digital elevation model (DEM) at 20 m resolution (acquired from the Canadian DEM open dataset). Candidate watersheds were further restricted to those with a minimum of 90% forested land cover, a minimum 65% spruce and fir cover, a maximum 15% watershed area harvested in the last 15 years, and an outflow within 300 m of a road. All candidate sites were visited and further restricted to 17 suitable watersheds that were easily accessible and had comparable stream substrates (pebble and rock). The final 12 watersheds were selected based on discussions with the Québec Ministère des Forêts, de la Faune et des Parcs (MFFP) about regional management plans and all harvesting activity in the watersheds was stopped during the study period. The study watersheds were divided into three regional groupings based on latitude, with upper (U01, U02, U03), central (C04, C05, C06, C07), and lower (L08, L09, L10, L11, L12) sites (Figure 1). Watershed size ranged from 6.33 to 9.85 km^2, and mean elevation ranged from 281 to 775 m above sea level (Table 1). All GIS spatial layers used in the screening process (roads, forest resource inventory, and land cover) were provided by MFFP and all spatial analyses were conducted in R 3.5.1 (R Development Core Team, 2021) with RSAGA 1.2.0 (Brenning et al., 2018).

Eight of the study watersheds (U01, U02, U03, C04, C05, C06, C07, and L08) are in the boreal forest ecozone, while the remaining 4 watersheds (L09, L10, L11, L12) are in the hemi boreal ecozone (Brandt, 2009). The watersheds in the boreal ecozone are characterized by medium to high elevations (200 – 900 m), average annual temperatures of 0 – 2.5°C, average annual precipitation of 1000 – 1300 mm, short to very short growing seasons, and conifer forest stands comprised of balsam fir, white spruce, black spruce, tamarack, and white cedar (Berger &

Blouin, 2006). The watersheds in the hemi boreal region are characterized by low to moderate elevations (0 – 400 m), average annual temperatures of 1.5 – 3.5°C, average annual precipitation of 900 – 1300 mm, and short to moderately long growing seasons (Berger & Blouin, 2004). Forest stands in this area tend to have a mixed composition, with balsam fir, white spruce, yellow birch, sugar maple, red maple, black ash, and white cedar. The study watersheds drain into 3 large rivers, the Cascapédia (U01, C04), Petite Cascapédia (U02, U03, C05, C06, C07, L09, L10), or Bonaventure (L08, L11, L12). A second- or third- order stream reach (25-60 m) was selected in each watershed for stream habitat and microbiome community sampling.

Six watersheds (U02, U03, C06, L08, L10, L12) were treated with Btk (*Bacillus thuringiensis kurstaki*) insecticide in 2020 and 2021 through aerial applications coordinated by MFFP and La Société de Protection des Forêts contre les Insects et Malades (SOPFIM), to supress defoliation (Table 1). This was to ensure a gradient of defoliation severity across watersheds. The Btk spray was not intended to establish a control/treatment experiment, but rather to ensure a gradient of defoliation intensities across watersheds, from lightly to heavily defoliated. Furthermore, the influence of Btk on microbial communities was not evaluated, as previous research has indicated it has no influence on microbial community function (Kreutzweiser et al., 1996)

Table 1. Landscape characteristics of the 12 forested watersheds studied in Gaspésie, Québec, Canada.

Watershed	Latitude	Longitude	Mean Elevation (m)	Catchment Area (km^2)	% Spruce-Fir	Slope (°)	Aspect (°)	% Wetland Area	Cumulative Defoliation (2019)	Cumulative Defoliation (2020)	Cumulative Defoliation (2021)
U01	48.77749	-66.1344	607	7.83	90	14.8	169	0.9	7.9	10.4	13.0
U02	48.84763	-65.9559	775	8.11	95	11.4	142	0	7.6	10.3	11.0
U03	48.87196	-65.8299	678	6.33	96	10.9	175	2.5	5.6	7.5	8.9
C04	48.52692	-66.1021	462	9.85	80	17.4	192	0	6.4	8.6	10.9
C05	48.53386	-65.8709	435	8.75	83	12.8	216	0	5.7	7.6	10.0
C06	48.56082	-65.7826	489	8.06	94	8.1	174	1	4.8	6.2	7.8
C07	48.58588	-65.7632	520	7.83	91	5.7	148	1.8	4.6	6.5	8.9
L08	48.40672	-65.6125	333	7.71	69	10.6	198	1.2	2.1	2.9	4.1
L09	48.30158	-65.7219	281	7.84	65	19.2	199	0	1.9	2.8	4.2
L10	48.28294	-65.6737	281	7.98	62	17.2	174	0	1.8	2.5	3.2
L11	48.30726	-65.5456	315	7.97	77	13.9	170	0.5	2.2	3.4	5.3
L12	48.30666	-65.5431	274	8.46	82	11.2	195	0.9	1.6	2.6	3.8

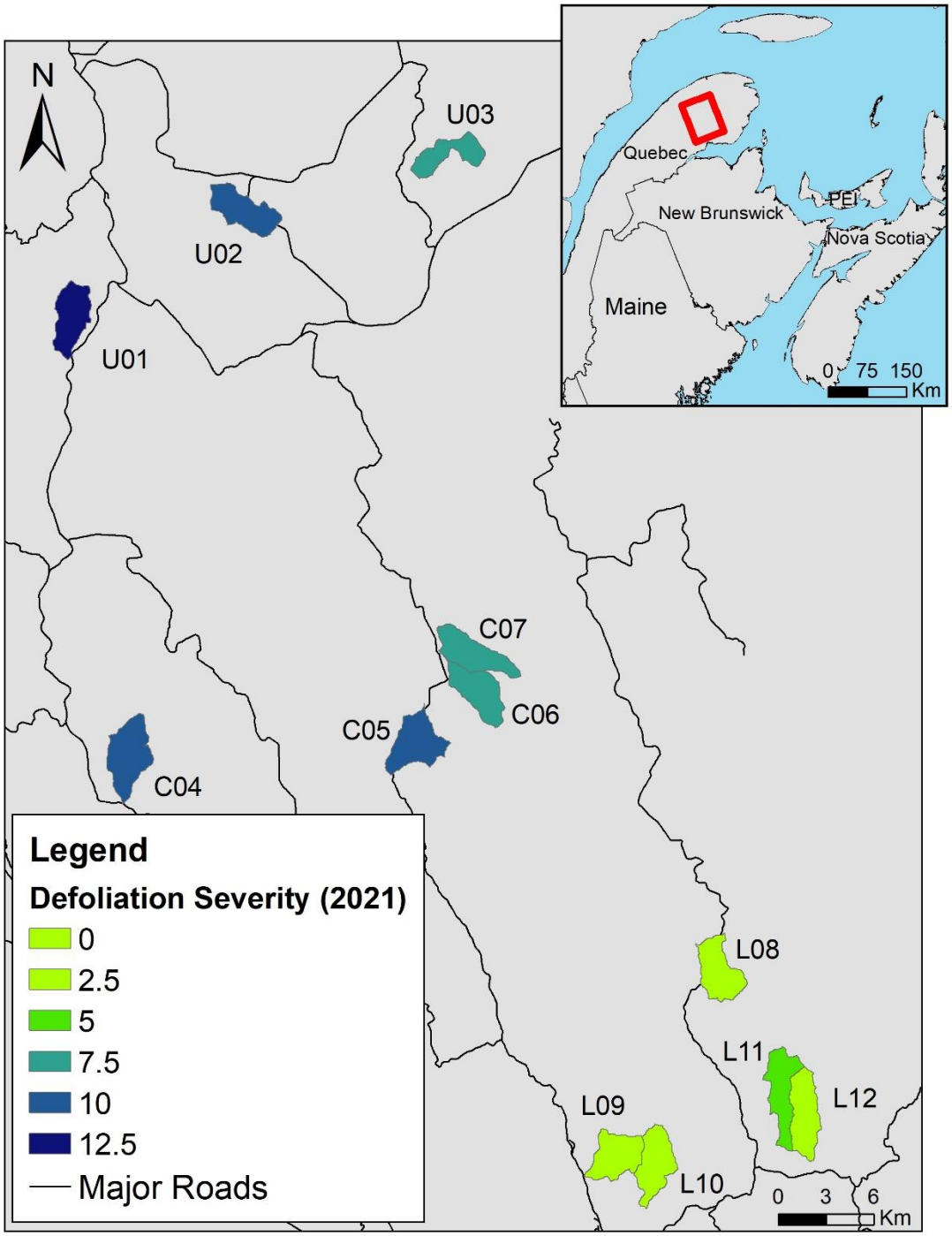

Figure 1. Map of the study area in Gaspésie, Québec, Canada, with 12 forested watersheds coloured with the associated 2021 cumulative defoliation intensity gradient (light green = light defoliation, dark blue = heavy defoliation). Cumulative defoliation was calculated by taking the sum of the annual hydrologically active, inverse distance weighted (HAiFLO) defoliation metric from the start of the outbreak in 2016 to the current year (see Methods for more detail).

2.1.1 Defoliation Intensity Index

The level of annual defoliation intensity in each watershed was determined through a combination of provincial surveys and targeted surveys. Beginning in 2016, the MFFP coordinated standardized aerial surveys (conducted by SOPFIM) using a fixed-wing aircraft and rated watershed defoliation on a scale of 0 – 3 (0 = no defoliation, 1 = low, 2 = moderate, and 3 = severe) (MacLean & MacKinnon, 1996). In 2020 and 2021, additional targeted aerial surveys were conducted using a helicopter to obtain defoliation intensity data with increased accuracy and resolution. These surveys obtained estimates on the same 0 – 3 scale as the provincial data, with 3 additional categories (0.5 = null-low, 1.5 = low-moderate, and 2.5 = moderate-severe). The provincial survey data were used for 2016 – 2019 and targeted survey data were used for 2020 and 2021.

We weighted the defoliation data in two ways. Both aerial survey methods quantify visible defoliation without consideration of the underlying vegetation type, so the defoliation index values were first weighted by the proportion of spruce and fir trees in each underlying forest stand. The spruce-fir content in each watershed was determined using Forest Resource Inventory stand data obtained from MFFP and binned by 10% content. We also expected that defoliation closer to water flow paths and streams would have a greater impact on stream habitat and microbiomes, so we weighted the spruce-fir adjusted defoliation data as in Sidhu et al (in prep) using the R package *hydroweight* (version 1.1.0) (Kielstra et al., 2021). Briefly, *hydroweight* spatially weights by the straight line or flow-path distances of landscape features to a given target (e.g., streams or sites along a stream network) based on concepts in Peterson et al. (2011). We used a hydrologically active weighting scheme, HAiFLO – where the influence of each point on the landscape is inversely proportional to the distance from the stream outlet (or stream survey site) and proportional to flow accumulation values (Peterson et al., 2011). We

then used this weighted metric (on the same 0 – 3 defoliation intensity scale) to calculate annual averages for each watershed. A cumulative defoliation intensity metric was then calculated for each year by taking the sum of the annual defoliation intensity metrics from the current year and all previous years since the start of the outbreak in 2016 (i.e., 2021 = sum of 2016 – 2021). This cumulative defoliation metric ranges from 0 (no defoliation) to 15 (very high defoliation) and was used for all subsequent data analyses (Figure 1). Cumulative defoliation was used instead of annual defoliation because a single year of defoliation does not have much influence on tree conditions, whereas several years of repeated defoliation results in large growth declines and mortality (Natural Resources Canada, 2018). The cumulative defoliation data were grouped into two groups for some categorical analyses (sites with 0 – 7.5 in low and 7.5 – 15 in high).

The helicopter surveys also capture the amount of tree top mortality, which we used to calculate % mortality area for each watershed. The mortality data were weighted with the same tree composition and *hydroweight* methods as the defoliation data, to provide annual % mortality value for each watershed. Mortality was mainly used as a supporting metric to visually assess trends as it was only present in 1 watershed in 2020 (U02) and 3 watersheds in 2021 (U01, U02, and C05).

2.1.2 Precipitation Data

Precipitation data were used to explore potential causes of the interannual variability observed in some stream habitat conditions. Daily precipitation data were extracted from the Environment and Climate Change Canada (ECCC) Historical Climate Data web site for the New Richmond East weather station in Québec (latitude: 48.15640667, longitude: -65.84194500) (ECCC, 2022). Precipitation data were analyzed cumulatively for each year starting on Nov 1st of the previous year and ending on Oct 31st to account for winter snowpack amounts (i.e., 2019 =

Nov 1st, 2018, to Oct 31st, 2019). This weather station is the closest available data source to the watersheds and is about 20 km south of the lower watersheds, 50 km south of the central watersheds, and 80 km south of the upper watersheds. In addition to the increasing latitudinal gradient from the weather station to the upper sites, there is also an increasing elevation gradient from south to north. The distance from the weather station and increasing latitudinal and elevational gradients likely influences weather patterns. As such, precipitation data were only used to provide an approximation of broad differences in annual precipitation patterns in the overall study area.

2.2 Stream Habitat Sampling

To investigate the influence of cumulative defoliation on stream habitat, we collected water chemistry, flow, temperature, and sediment deposition measurements from one stream reach in each of the 12 watersheds. Water chemistry grab samples (500 mL) were collected every 2 – 3 weeks from May to October in 2019 (n=8), 2020 (n=10), and 2021 (n=10) from all 12 stream reaches. Stream flow was measured with an Ott MF Pro flow meter through a standard area/velocity cross-section method, at the same time as each grab sample collection. All water samples were kept refrigerated and in the dark until they were shipped to Natural Resources Canada, Great Lakes Forestry Centre (NRCan-GLFC) in Sault Ste Marie, ON, Canada, except those collected in 2021, which were frozen prior to shipment due to COVID-related laboratory backlogs at NRCan-GLFC. Water samples were analyzed for nutrients (TP, TN, SRP, NO_2-NO_3, NH_4) and dissolved organic carbon (DOC), as well as a suite of other water chemistry variables (metals, dissolved inorganic matter, cations (Ca, K, Mg, Na) and anions (Cl, SO_4, SiO_2)) at the NRCan-GLFC Central Water Chemistry Lab using standard methods (Hazlett et al., 2008). Water chemistry variables, abbreviations, and detection limits are summarized in Table A1. Any

values below detection limits were replaced by a value of half the detection limit, and any variable with greater than 50% of the values below the detection limits were excluded from further analyses.

Dissolved organic matter (DOM) metrics were generated from a split of the grab sample that was further filtered to 0.45 µm. Fluorescence excitation-emission matrices (EEMs) were generated from three-dimensional fluorescence scans at 5-nm excitation steps from 250 to 450 nm and 2-nm emission steps from 300 to 600 nm using a Cary eclipse fluorescence spectrophotometer, and absorbance was measured with a Cary 60 ultraviolet visible absorbance spectrophotometer. To determine whether there was a change in the degree of DOM degradation and bioavailability in response to cumulative defoliation, we calculated the humification index (hix) and biological index (bix) from spectrally-corrected EEMs, and the specific ultraviolet absorbance at 254 nm (SUVA) from DOC-adjusted absorbance scans. These DOM metrics provide information about the quality of the DOM pool. Hix provides an indication of humic content of DOM, with humification typically associated with greater terrestrial DOM inputs (Huguet et al., 2009; Ohno, 2002). Bix provides an estimate of the amount of recent autochtonous (microbial derived) contributions to the DOM pool (Huguet et al., 2009). Finally, SUVA is an indicator of the aromaticity of the DOM pool, with higher aromatic content suggesting greater terrestrial contributions as terrestrial vegetation is high in aromatic compounds (Weishaar et al., 2003).

We measured full season (May – October) water temperatures each year in all 12 stream reaches using Solinst Level Loggers (Model 3001) set to measure temperature every 15 minutes. We also measured late summer (mid-August – end September) stream temperatures associated with each leaf pack (used as the substrate to assess microbial communities, see Section 2.3.1

Microbiome Sample Collection). These temperatures were measured using HOBO Pendant MX Water Temperature Data Loggers (6 loggers per stream reach) which were attached to the brick used to hold leaf packs in place and set to record at 10-minute intervals.

We also measured sedimentation rates in the stream reaches during the leaf pack incubation period (mid-August to end of September) of each year. Sediment was collected in 6 tubes per stream, placed at approximately 10 cm from the stream bottom and held in place with the same brick used for leaf packs and temperature loggers. After incubation, tubes were removed from the stream and preserved with 5 mL of formaldehyde. In the lab, the accumulated sediment was poured through a 250-um sieve to obtain the coarse sediment material (Erdozain et al., 2018). The filtrate was retained and further filtered through pre-ashed 1.2 um filters to obtain the fine sediment material. To calculate ash-free dry mass, the coarse sediment and fine sediment filters were dried for 48 hours at 60 ^{o}C and ashed for 2 hours at 500 ^{o}C (Erdozain et al., 2018). The ash-free dry mass represents the amount of inorganic sediment accumulation, and the difference between the total mass and ash-free dry mass represents the amount of organic sediment accumulation. All sediment accumulation values were divided by the incubation time in days to obtain values in grams per day.

2.3 Stream Microbiome Structure and Function

2.3.1 Microbiome Sample Collection

To explore the response of stream microbiome structure and function to cumulative defoliation and associated stream habitat changes, we incubated leaf packs as substrates for microbial colonization. Leaf packs provide a standardized substrate that allows for comparisons of microbial communities of the same age across all stream sites. The leaf packs were constructed and filled with alder leaves (*Alnus incana ssp. rugosa*) and enclosed in 500 µm

fibreglass mesh bags to exclude macroinvertebrates and focus on microbial decomposition. Alder is common in all boreal riparian forests and is a ubiquitous substrate for colonization by stream microbial communities. Each leaf pack contained two compartments; the first compartment with 10-15 leaves to provide at least 3 g wet mass leaf material for DNA extractions and extracellular enzyme assays and the second compartment with a single pre-weighed leaf used to assess microbial decomposition (mass loss) rates. Leaves in the first compartment were rinsed prior to leaf pack creation and leaves in the second compartment were washed and dried for two days at 30°C, and dry weights were recorded. Six replicate leaf packs were placed in the downstream-most stream reach in each of the 12 watersheds, for a total of 72 leaf packs. Leaf packs were secured with zip ties to a brick placed among the natural stream substrates. They were deployed in August of each year (2019, 2020, and 2021), incubated for four to five weeks, and removed from streams in September, to align with peak in-stream productivity and the start of natural leaf litter inputs to streams. Upon removal from the streams, leaf packs were stored at -20°C until analysis.

To obtain estimates of the algal community response to cumulative defoliation and accompanying changes in stream habitat, in-situ measurements of benthic algal production were taken at the same time as the stream habitat data. Benthic algal production was measured in 2019 (n=8) and 2021 (n=10) using a bbe Moldaenke BenthoTorch, which measures the intensity of chlorophyll fluorescence to determine the benthic production of green algae, cyanobacteria, and diatoms. Algal measurements were not available in 2020 due to COVID-related delays in BenthoTorch repairs.

2.3.2 Microbiome Structure: Metabarcoding

To obtain information about the fungi and bacteria community structure, DNA was extracted from leaves in the first compartment of all leaf packs (n = 72 in 2019, n = 72 in 2020, and n = 71 in 2021) using the Qiagen DNeasy Powersoil Kit (Qiagen, 2017) and a Qiacube. The kit includes a procedure to remove PCR inhibitors from samples, including humic substances and brown colours. The extracted DNA was then amplified using the base primer targets outlined in Table 2. Paired-end sequencing for the 16S (targeting variable regions v4 and v5) and ITS (targeting ITS2) rRNA genes were completed on the Illumina MiSeq 300 platform at the at the National Research Council Canada in Saskatoon, Saskatchewan.

Table 2. Base primers used for 16S and ITS sequence amplification from leaf packs incubated in streams in Gaspésie, QC, Canada.

	Target	Forward	Reverse
16S	16S v4-v5	"515F" Sequence = GTGCCAGCMGCCGCGGTAA	"926R" Sequence = AAACTYAAAKRAATTGRCGG
ITS	ITS2	"fITS9" Sequence: =GAACGCAGCRAAIIGYGA	"ITS4" Sequence = TCCTCCGCTTATTGATATGC

The raw sequence data were processed into ESVs (Exact Sequence Variants) using the MetaWorks pipeline (v1.10.0) (Porter, 2020; Porter & Hajibabaei, 2022). Raw paired-end reads were combined using SEQPREP (v1.3.2) with a minimum Phred quality score of 13 in the overlap region and a minimum overlap of 25 base pairs (St. John, 2016). Primers were trimmed using CUTADAPT (v4.1) with a minimum Phred quality score of 20 at the ends and a minimum trimmed read length of 150 base pairs (Martin, 2011). VSEARCH (v2.21.1) was used for dereplication (Rognes et al., 2016), denoising (singleton and doubleton removal) (Edgar, 2016b), the removal of chimeric sequences (Edgar, 2016a), and ESV table creation (Rognes et al., 2016).

For ITS reads, the ITS2 variable spacer was extracted using ITSx (v1.1.3) (Bengtsson-Palme et al., 2013). Taxonomic assignments were performed using the native RDP Classifier database v2.13 for the 16S data (Wang et al., 2007) and the Fungal UNITE database v8.2 for the ITS data (Abarenkov et al., 2021; Porter, 2021). The resulting datasets contain the ESV taxonomy and the ESV levels were used for subsequent data analyses. Sequences that were not identified to the Bacteria or Archaea domains were removed from the 16S data and sequences that did not belong to the Fungi kingdom were removed from the ITS data. One sample (2020, site L08, rep 2) was removed from the ITS dataset due to a low read count (<1000 reads). Rarefaction curves showed that most unique ESV sequences were likely identified at the sequencing depths achieved, as simulated resampling showed minimal improvement in the number of unique ESV sequences detected by improved read depths. As such, there was no need to subsample to achieve similar community coverages (i.e., rarefy) prior to analysis (Figure A1;Figure **A2**).

2.3.3 Microbiome Function: Extracellular Enzyme Assays and Decomposition Rates

Extracellular enzyme activities for three hydrolase enzymes (xylosidase (XY), N-acetyl-β-D-glucosaminidase (NAG), and phosphatase (PHOS)) were measured to obtain estimates of microbial community functions. Enzyme activities were measured under controlled conditions following the protocol developed at NRCan-GLFC (Muto & Emilson, 2018). Leaves from the first compartment of each leaf pack (n = 72 in 2019, n = 72 in 2020, and n = 71 in 2021) were broken down and homogenized. One gram of leaf material from each leaf pack was mixed with 100 mL of acetate buffer and used as the sample to assess activities. Microplates were set up with a negative control (acetate buffer and enzyme substrate), standard (acetate buffer and MUB standard), buffer (acetate buffer), quench (MUB standard and sample), and blank (sample and acetate buffer). Separate plates were used for each type of enzyme assay, with three samples run on each plate. After a 1-hour incubation period, 10 µL of 0.5 M NaOH was added to each well

and fluorescence readings were measured immediately after using a Biotek (Agilent) Gen5 H1 Plate Reader. All enzyme activities were expressed as nmol per hour per gram of substrate.

The single leaf in the second compartment of each leaf pack (n = 72 in 2019, n = 72 in 2020, and n = 71 in 2021) was used to obtain estimates of microbial decomposition rates. After leaf pack incubation, leaves were washed, dried (two days at 30°C), and weighed. The weights before and after leaf pack incubation were used to calculate percent mass loss. To account for slight differences in incubation times, the percent mass loss was divided by the incubation time in days, with the percent mass loss per day used as an estimate of microbial decomposition.

2.4 Statistical Analysis

All data analysis was performed in R (version 4.2.2) with coding structure following the *tidyverse* (1.3.2) package. Each year of data was analyzed separately because of the expectation that there would be yearly differences in cumulative defoliation among watersheds due to natural annual fluctuations as well as the Btk spraying of the watersheds beginning in 2020.

2.4.1. Stream Habitat Data Analysis

All stream habitat data were plotted over time to look for extreme outliers. One extreme outlier was detected for SUVA in 2019 which is likely due to sample contamination and was removed from the dataset. Three extreme outliers were detected in the stream flow data with flow rates 15 – 400 times greater than the mean values and were removed from the dataset. One extreme outlier was detected for the sediment deposition data, which was likely due to field contamination and was removed from the dataset. All stream habitat data were then averaged per site and year for subsequent analysis (n=8 in 2019, n=10 in 2020, and n=10 in 2021 for water chemistry parameters, DOM metrics, and flow rates, and n=6 replicates per site per year for sediment deposition rates).

Stream habitat data analysis was focused on the response variables that we predicted to change with increased cumulative defoliation, including nutrients (TN, $N0_2$-NO_3, TP), stream flow rates, stream temperature, and several DOM quality and quantity metrics (DOC, hix, bix, fi, and SUVA). These variables were assessed for relationships with cumulative defoliation using the average of the full season of stream habitat measurements (n=8 in 2019, n=10 in 2020, and n=10 in 2021) (Figure A3) and the average of late summer season measurements (n=3 per year) (Figure A4), and the period with the strongest relationship for each variable was used for subsequent analyses. The late summer period was during leaf pack incubation (4–5-week period from mid-August-end of September) which aligns with peak stream productivity. All response variables showed the same directionality regardless of time period, but the magnitude and significance of the response was stronger with the full season of data for SUVA and flow rates, and with the summer season of data for regional temperatures. As such, average values of the full season of data were used for subsequent analyses of all parameters except for temperature, where the average of the summer temperature data were used. To ensure that relationships between cumulative defoliation and the evaluated stream habitat parameters were not due to spurious correlations with other measured stream habitat variables, we conducted exploratory analysis of all measured variables using boxplots and Pearson correlation plots (Figure A5; A6; A7).

We used hierarchical partitioning (HP) to compare the relative importance of cumulative defoliation to other potential landscape drivers on stream habitat variables and used Pearson correlations to visualize the resulting relationships. HP was used because it allows for the inclusion of colinear variables and many of the landscape characteristics were colinear. It uses all possible model combinations to determine both the shared and unique variance explained for each landscape variable and was completed using the *rdacca.hp* (1.0-8) package (Lai et al.,

2022). We created hierarchical partitioning models for flow, temperature, and SUVA as these response variables had significant relationships with cumulative defoliation. The landscape variables used in the models were selected based on their potential to influence the response variable (Table 3). Cumulative defoliation, elevation, and spruce-fir composition were included in all 3 models and were all correlated to one another (Figure A8). Elevation was strongly correlated to latitude ($r=0.98$, $p<0.0001$) and was chosen as the explanatory variable to represent differences in climate, geology, and solar radiation among the study watersheds. The amount of spruce-fir composition in the watersheds was included as it can influence light availability, evapotranspiration rates, and litter deposition rates. Catchment area was used as a predictor for SUVA and flow as the length of flow paths can influence these variables. Aspect was used instead of catchment area for the stream temperature models as it can influence solar radiation. Wetland area was used as a predictor for SUVA and temperature as decomposition rates and water residence times within wetlands can influence these variables. Slope was used in place of wetland area for the flow models as it can have a strong influence on hydrology.

Table 3. Response variables used for three hierarchical partitioning models created for SUVA, flow, and temperature in streams in the Gaspésie Peninsula, QC, Canada.

	Response Variable		
	SUVA	**Flow**	**Temperature**
Explanatory Variables	Cumulative defoliation	Cumulative defoliation	Cumulative defoliation
	Elevation	Elevation	Elevation
	Spruce-fir composition	Spruce-fir composition	Spruce-fir composition
	Wetland area	Slope	Wetland area
	Catchment area	Catchment area	Aspect

2.4.2 Microbiome Community Structure Data Analysis

16S and ITS ESV sequence data were analyzed using the *phyloseq* (1.38.0) package in R and samples were grouped by site and year. Relative abundance plots were created for the phylum and class taxonomic levels using all replicates (n=6) per site and the average across replicates at each site. The relative abundance plots were visually examined for broad patterns along the cumulative defoliation intensity gradients.

Alpha diversity metrics (richness, Shannon diversity, inverse Simpson, and evenness) were calculated at the ESV level using the *vegan* (2.6-2) package. Bacteria communities were assessed as relative abundance (Bray-Curtis distances), while fungi communities were assessed as presence-absence (Jaccard distances) because estimates of fungi abundance are less reliable than those for bacteria (Lofgren et al., 2019). This is due to a difference in gene copy numbers per organism, which are an order of magnitude higher for ITS than 16S (Lofgren et al., 2019). Pearson's correlations were used to assess relationships between diversity metrics (n=6 replicates per site were averaged) and cumulative defoliation or stream habitat variables. HP models were created to assess the relative importance of each stream habitat variable to diversity metrics.

To assess beta diversity along the cumulative defoliation gradient, a compositional data analysis (CoDA) approach was used at the ESV level. Data were transformed using a centered log ratio (clr) using the *microbiome* (1.20) package and principal component analyses (PCAs) were performed on all years combined as well as each year individually. Significant differences between sites and cumulative defoliation categories (low vs high cumulative defoliation) were evaluated using PERMANOVA performed with the *vegan* package. Additional beta diversity ordinations were created (Principal coordinate analysis (PCoA) and non-metric multidimensional scaling (NMDS)) on Bray-Curtis distances for bacteria and Jaccard distances for fungi (both at

ESV level) and outputs were similar to the CoDA PCA output. Beta diversity was also assessed at different taxonomic levels (from genus to phylum) using CoDA PCAs and diversity was similar across taxonomic levels. As such, only the CoDA PCAs at the ESV level are presented.

Comparative RDA plots were used to assess if the changes in beta diversity were occurring along the cumulative defoliation gradient due to the influence of cumulative defoliation on stream habitat. RDAs were performed on the clr data, with one RDA constrained by cumulative defoliation, and the other constrained by stream habitat variables found to be influenced by defoliation (stream flow, stream temperature, and SUVA).

Differential abundance analysis was conducted using the ALDEx2 (1.30.0) package to evaluate changes between low and high cumulative defoliation categories at the individual ESV level. The output was restricted to ESVs with a p-value of 0.05 or less and a minimum effect size of 1. Bacteria community outputs are displayed at the genus level because most ESVs had confident taxonomic identifications at this level (using accepted bootstrap support cut-off value of 0.5 to ensure 95% of EVS are correctly assigned) (Wang et al., 2007). In contrast, fungi community outputs are displayed at the family level because many ESVs were not confidently identified at the genus level (using the accepted bootstrap support cut-off value of 0.7 to ensure 80% correct taxonomic assignments) (Abarenkov et al., 2021; Porter, 2021).

To assess relationships between algal biomass parameters (green, cyanobacteria, diatoms, and total biomass) and cumulative defoliation, the three algal measurements taken throughout the leaf pack incubation period were averaged. For any algal parameter related to cumulative defoliation in both years, HP models were used to determine if this relationship was mediated through changes to stream habitat (full season stream flow and SUVA and late summer stream temperatures).

2.4.3 Microbiome Community Function Data Analysis

Extracellular enzyme assay and decomposition replicates (n=6) were averaged per site per year and Pearson's correlations were used to assess their relationships with cumulative defoliation or stream habitat variables. Hierarchical partitioning models were not created for these parameters as there were no significant relationships with cumulative defoliation.

Taxonomic functional assignments were predicted for the bacteria (16S) gene sequences using the PICRUSt2 software (Douglas et al., 2020). The input for the software is the ESV sequence matrix with abundance data, and it uses a reference database and phylogenetic placements to predict the metabolic pathways for all sequences. The MetaCyc metabolic pathway abundance output was used to explore potential functional changes (Caspi et al., 2018). The pathways were first sorted into functional groups using the MetaCyc pathway type ontology by summing the pathway relative abundance (Karp et al., 2004). Any pathways identified as potentially belonging to multiple groups were sorted into all possible groups, and as such, total relative abundance of all functional groups in the dataset is greater than 100%. To assess which functional groups were changing with cumulative defoliation, they were filtered down to those with a minimum of 2 pathways per functional group that had a significant linear relationship with cumulative defoliation. Given the large number of groups tested (35 groups), significance was limited to p-values < 0.01 and any functional groups with significant relationships in all three years were explored further. The same filtering process was used on all pathways within each of the significant functional groups and pathways with a significant ($p<0.01$) linear relationship with defoliation are shown.

Taxonomic functional assignments were predicted for the fungi (ITS) gene sequences using the FUNGuild (1.1) software (Nguyen et al., 2016). This software groups fungi ESVs into

ecological guilds (or functional groups) by matching them to a reference database and provides three confidence rankings with each assignment (highly probable, probable, and possible). The FUNGuild software assigned 60% of the dataset to a functional guild, with 40% unassigned. The data were further restricted to confidence rankings of only highly probable and probable, with any possible rankings removed (16% of the dataset). The resulting dataset used for subsequent analyses contained 52% of the initial fungi ESVs. Any ESVs identified as potentially belonging to multiple guilds were sorted into all possible guilds, and as such, total relative abundance of the dataset is greater than 100%. The same filtering process used with the bacteria taxonomic assignments was applied here (groups with significant ($p<0.01$) relationships with cumulative defoliation were explored further).

Bacteria and fungi functional diversity metrics (richness, Shannon diversity, evenness, and inverse Simpson's) were calculated in the *vegan* package using the taxonomic functional assignment outputs (pathways for bacteria and guilds for fungi). Pearson's correlations were used to assess relationships between functional diversity metrics (replicates (n=6) averaged per site) and cumulative defoliation or stream habitat variables.

3.0 Results

3.1 Stream Habitat

Of the stream habitat variables that were predicted to change with increasing cumulative defoliation, significant positive relationships were found for SUVA, stream flow rates, and stream temperature, for some or all years (see below for more details). No significant relationships were found between cumulative defoliation and nutrients (TP, TN, and NO_2-NO_3) or the other DOM metrics (hix, bix, fi, and DOC) (Figure A3).

3.1.1 Nutrients

TP concentrations were generally low in these streams, with means ranging from 0.0005 – 0.0050 mg/L in 2019 and 2021, and 0.0005 – 0.0200 in 2020 (Table A2). Mean NO_2-NO_3 levels ranged from 0.02 – 0.43 mg/L and were similar across years in each site, except for site U02 which increased in 2020 and 2021 (Figure 2). Mean TN ranged from 0.07 – 0.49 mg/L and showed the same patterns as NO_2-NO_3, and changes in TN were due to NO_2-NO_3, not NH_3. Site U02 was the only watershed with substantial tree top mortality, covering 25% of the watershed in 2020 and 32% in 2021. All other watersheds had no recorded top mortality in 2020 and 2021, except 3 watersheds that had less than 5% area with mortality in 2021.

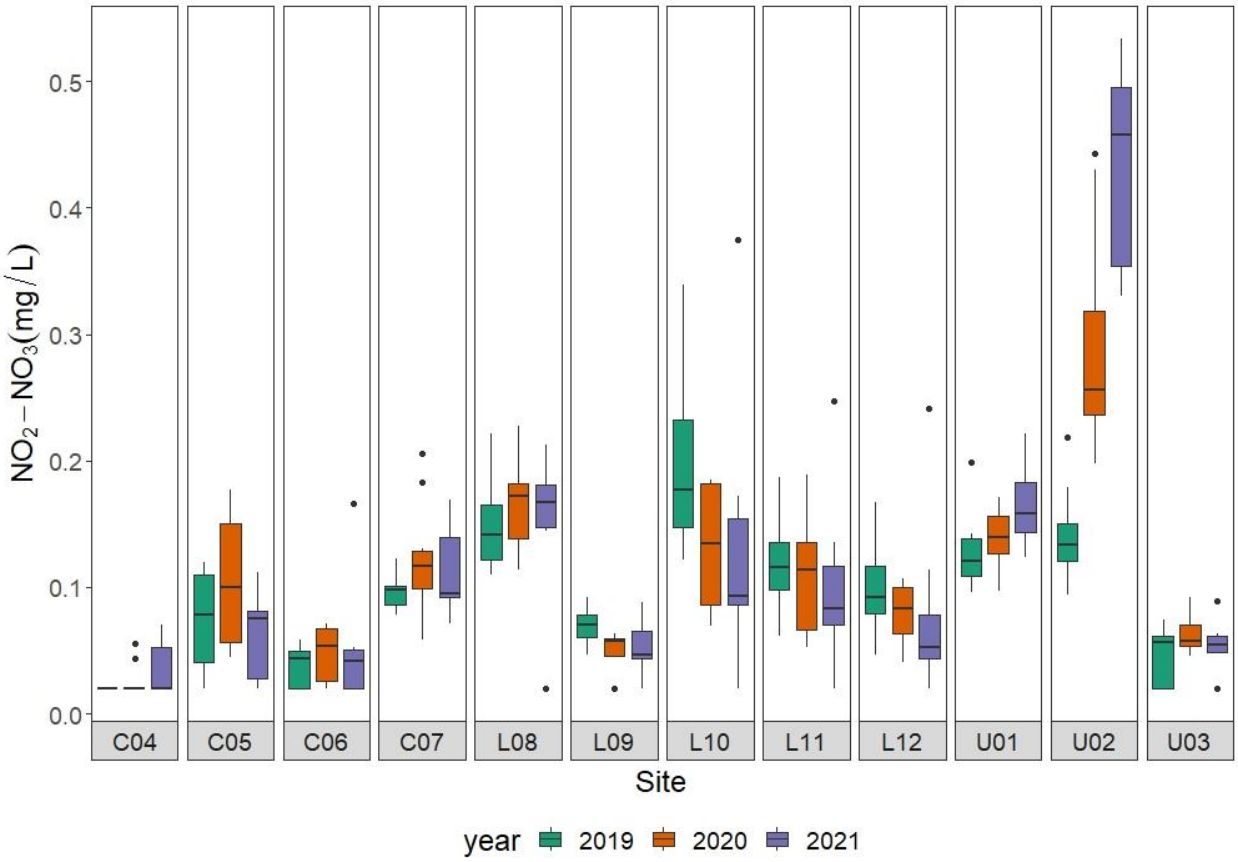

Figure 2. NO_2-NO_3 concentrations (mg/L) in stream water samples taken from streams in the Gaspésie Peninsula, QC, Canada during the open water season (May – October) of 2019 (n=8), 2020 (n=10), and 2021 (n=10).

3.1.2 Dissolved Organic Matter

Mean SUVA values were similar in 2019 (2.5 – 4.4 mg-$L^{-1}m^{-1}$) and 2021 (3.2 – 6.3 mg-$L^{-1}m^{-1}$), with similar positive relationships to cumulative defoliation (Figure 3A). In contrast, 2020 had lower SUVA values (1.7 – 3.7 mg-$L^{-1}m^{-1}$) and a nonsignificant relationship ($p=0.062$) with cumulative defoliation. Cumulative defoliation was the strongest contributing landscape variable to SUVA in 2019 and 2021, while in 2020, the strongest predictor of SUVA was elevation (Figure 3B). Further, in 2019 most of the explained variation was shared between elevation and cumulative defoliation, whereas in 2021, most of the explained variation was unique to cumulative defoliation (Table 4). These among-year differences could be attributed to differences in cumulative precipitation (measured from Nov 1st in the previous year to Oct 31st to account for snow accumulation), as 2020 had lower values than 2019 and 2021 (Figure A9).

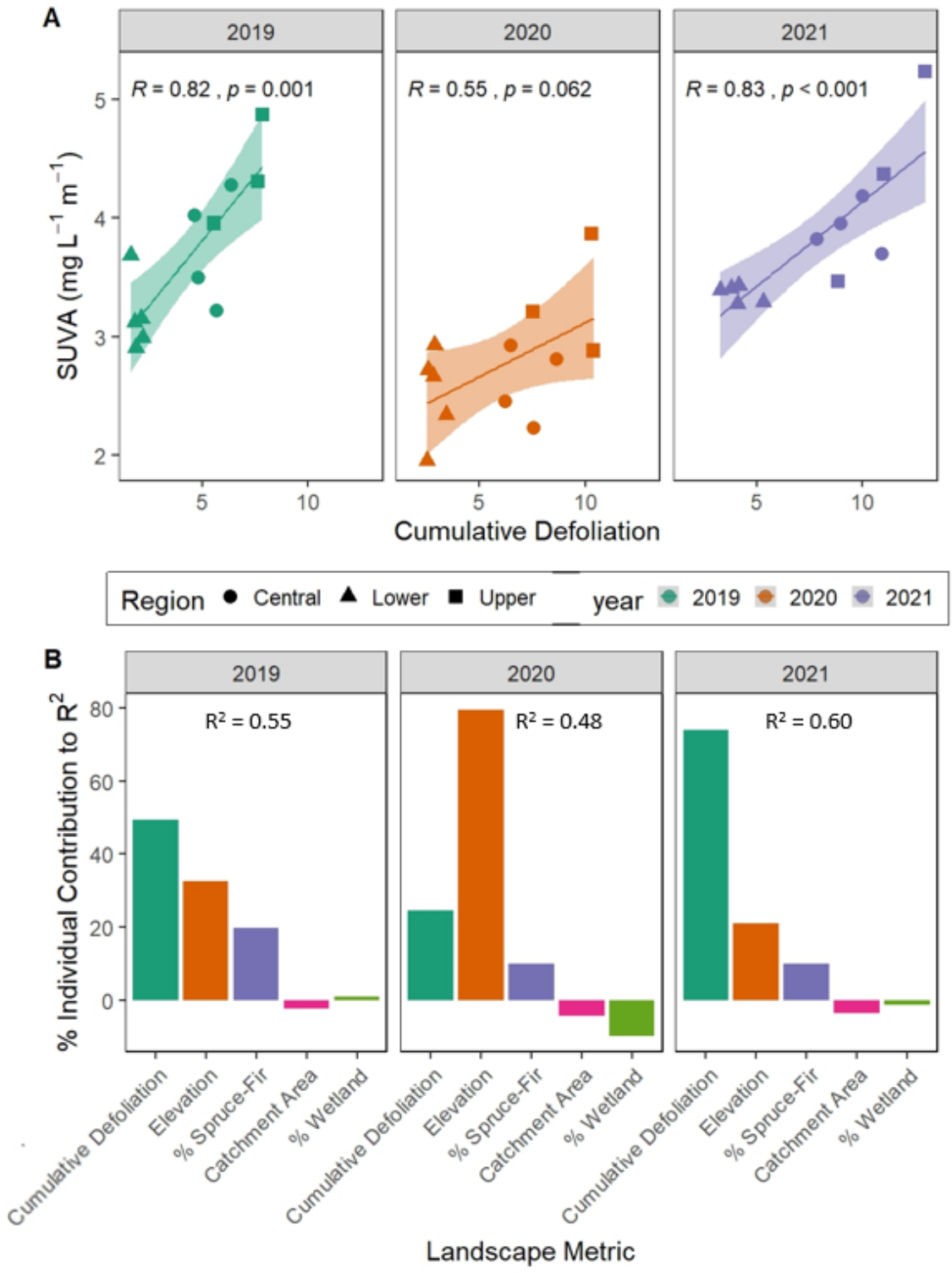

Figure 3. Mean SUVA concentrations (mg-$L^{-1}m^{-1}$) from streams in the Gaspésie Peninsula, QC, Canada in 2019 (n=8), 2020 (n=10), and 2021 (n=10) with **A)** Pearson correlations between SUVA and cumulative defoliation, and **B)** percentage of individual contributions of landscape metrics to the total R^2 from the hierarchical partitioning model for SUVA concentrations.

Table 4. Hierarchical partitioning model results for mean SUVA concentrations (mg-$L^{-1}m^{-1}$) from streams in the Gaspésie Peninsula, QC, Canada in 2019 (n=8), 2020 (n=10), and 2021 (n=10). Values represent the amount of variation explained by each landscape metric, with individual contributions representing the sum of the unique and shared contributions.

	Hierarchical partitioning contributions		
Variable	**Unique**	**Average shared**	**Individual**
2019			
Cumulative defoliation	-0.01	0.28	0.27
Elevation	-0.05	0.23	0.18
% spruce-fir	-0.05	0.16	0.11
Catchment area	-0.01	-0.01	-0.02
Wetland area	0.05	-0.04	0.01
Total variance explained (model R^2) = 0.55			
2020			
Cumulative defoliation	0.11	0.01	0.12
Elevation	0.41	-0.03	0.38
% spruce-fir	-0.02	0.07	0.05
Catchment area	0.06	-0.08	-0.02
Wetland area	-0.04	-0.01	-0.05
Total variance explained (model R^2) = 0.48			
2021			
Cumulative defoliation	0.37	0.08	0.45
Elevation	0.01	0.12	0.13
% spruce-fir	-0.04	0.10	0.06
Catchment area	0.07	-0.09	-0.02
Wetland area	0.05	-0.06	-0.01
Total variance explained (model R^2) = 0.60			

3.1.3 Stream Flow

Stream flow rates were similar across all years (0.04 – 0.3 m^3/s) and were positively related to cumulative defoliation in all years (Figure 4A). Hierarchical partitioning results suggest that elevation was the strongest individual driver of flow rates, followed by cumulative defoliation (Figure 4B). In 2019 and 2020, there was a large pool of shared variance between elevation and cumulative defoliation, while in 2021, most of the variance was unique to elevation (Table 5). Further, the total explained variation in the HP model in 2020 was lower (R^2= 0.41) relative to 2019 and 2020 (R^2 = 0.77 and 0.73 respectively).

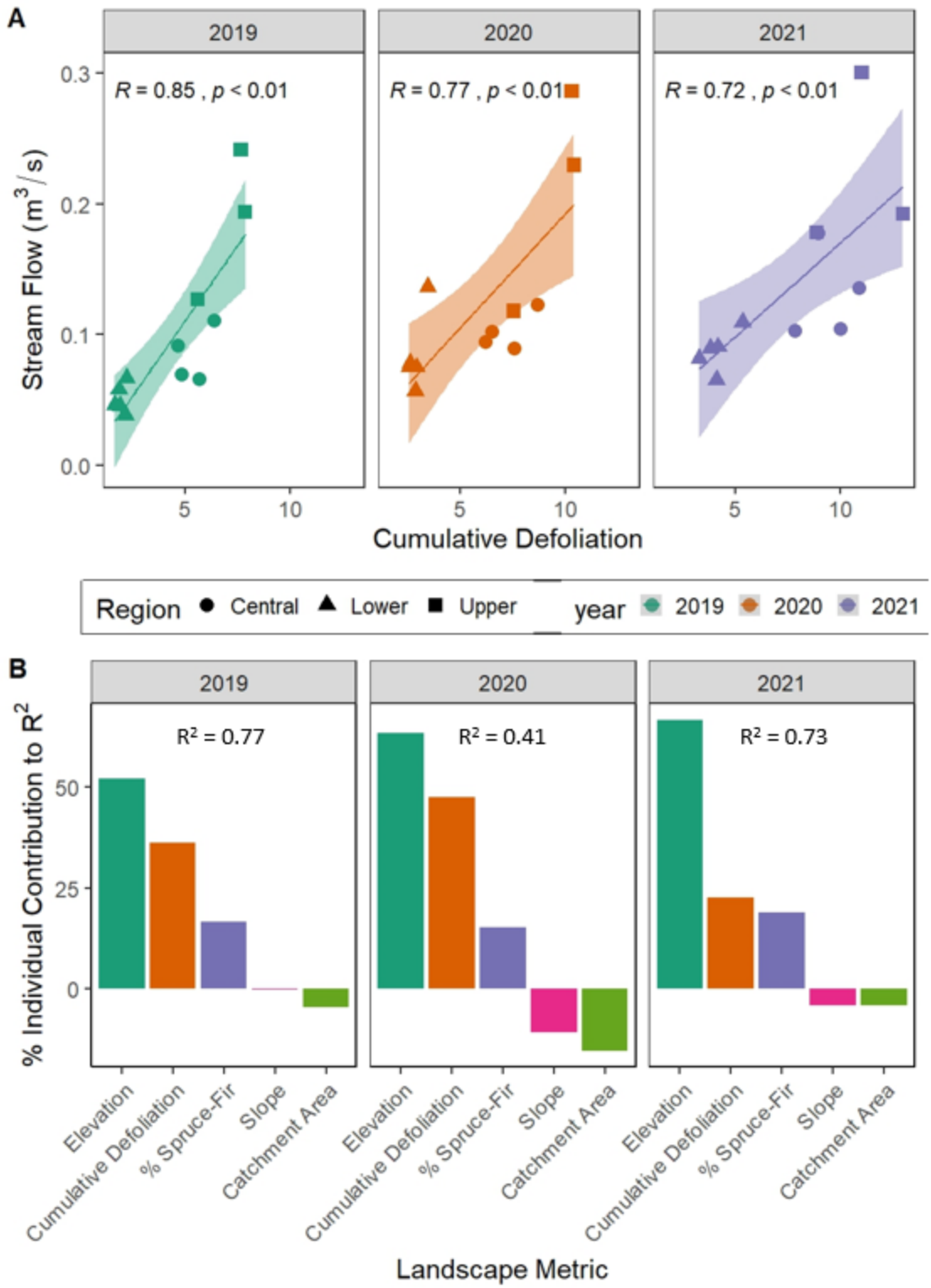

Figure 4. Mean flow rates (m^3/s) from streams in the Gaspésie Peninsula, QC, Canada in 2019 (n=8), 2020 (n=10), and 2021 (n=10) with **A)** Pearson correlations between flow rates and cumulative defoliation, and **B)** percentage of individual contributions of landscape metrics to the total R^2 from the hierarchical partitioning model for flow rates.

Table 5. Hierarchical partitioning model results for mean stream flow rates (m^3/s) from streams in the Gaspésie Peninsula, QC, Canada in 2019 (n=8), 2020 (n=10), and 2021 (n=10). Values represent the amount of variation explained by each landscape metric, with individual contributions representing the sum of the unique and shared contributions.

	Hierarchical partitioning contributions		
Variable	**Unique**	**Average shared**	**Individual**
2019			
Cumulative defoliation	-0.03	0.31	0.28
Elevation	0.13	0.27	0.40
% spruce-fir	-0.03	0.16	0.13
Catchment area	-0.02	-0.02	-0.04
Slope	0.01	-0.01	0
Total variance explained (model R^2) = 0.77			
2020			
Cumulative defoliation	-0.08	0.27	0.19
Elevation	0.02	0.24	0.26
% spruce-fir	-0.08	0.14	0.06
Catchment area	-0.06	0.00	-0.06
Slope	-0.06	0.02	-0.04
Total variance explained (model R^2) = 0.41			
2021			
Cumulative defoliation	-0.01	0.18	0.17
Elevation	0.32	0.17	0.49
% spruce-fir	-0.04	0.18	0.14
Catchment area	0.00	-0.03	-0.03
Slope	-0.03	0.00	-0.03
Total variance explained (model R^2) = 0.73			

3.1.4 Stream Temperature

Average stream temperatures during the leaf pack incubation period were similar in 2019 (6.1 – 9.3 °C) and 2020 (6.2 – 9.6 °C) and elevated by 1°C – 2°C in 2021 (7.1 – 10.6 °C). When analyzing all sites together, a strong negative correlation between cumulative defoliation and stream temperature was observed in all years (Figure 5A). However, this was masked by the among-site gradients in elevation/latitude and spruce-fir composition as the hierarchical partitioning models indicated that these were the strongest drivers of temperature in these sites (Figure 5B; Table 6). To account for these landscape gradients which are associated with

regions, data were also analyzed by region, with all years pooled (Figure 6). This indicated that there was a positive relationship between cumulative defoliation and temperature in the lower and central regions, but not in the upper region.

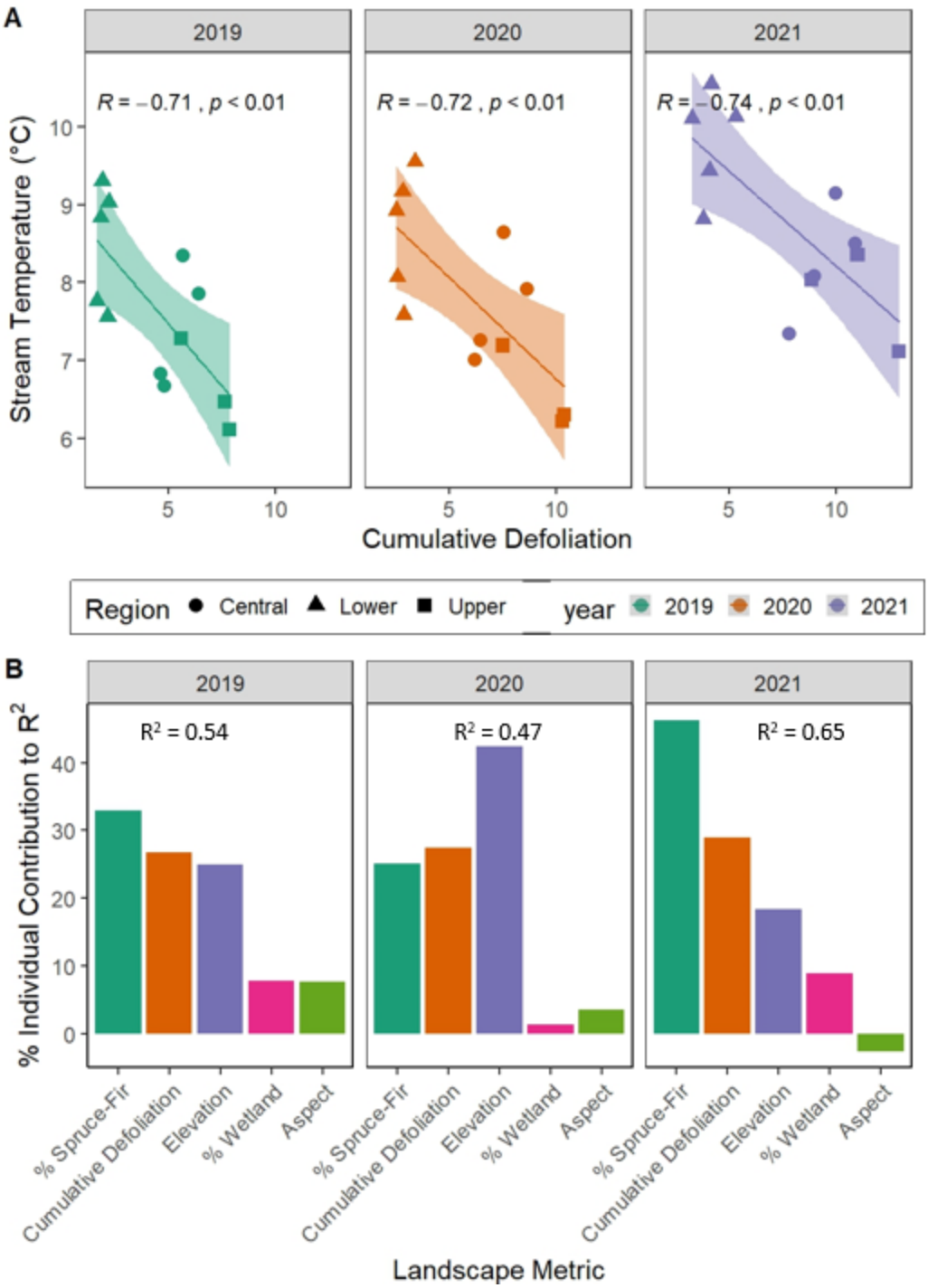

Figure 5. Mean summer stream temperatures (°C) from streams in the Gaspésie Peninsula, QC, Canada in 2019, 2020, and 2021 with **A)** Pearson correlations between stream temperatures and cumulative defoliation and **B)** percentage of individual contributions of landscape metrics to the total R^2 from the hierarchical partitioning model for stream temperatures. Temperature values represent the site average of data recorded every 10-min from 6 replicates per site.

Table 6. Hierarchical partitioning model results for mean summer stream temperatures (°C) (site average of data recorded every 10-min from 6 replicates per site per year) from streams in the Gaspésie Peninsula, QC, Canada in 2019, 2020, and 2021. Values represent the amount of variation explained by each landscape metric, with individual contributions representing the sum of the unique and shared contributions.

	Hierarchical partitioning contributions		
Variable	**Unique**	**Average shared**	**Individual**
2019			
Cumulative defoliation	0.02	0.13	0.15
Elevation	-0.05	0.19	0.14
% spruce-fir	-0.04	0.22	0.18
Aspect	-0.01	0.05	0.04
% wetland area	0.01	0.03	0.04
Total variance explained (model R^2) = 0.54			
2020			
Cumulative defoliation	-0.06	0.19	0.13
Elevation	-0.05	0.25	0.20
% spruce-fir	-0.07	0.19	0.12
Aspect	-0.07	0.09	0.02
% wetland area	-0.04	0.05	0.01
Total variance explained (model R^2) = 0.47			
2021			
Cumulative defoliation	0.05	0.15	0.19
Elevation	-0.03	0.15	0.12
% spruce-fir	0.06	0.24	0.30
Aspect	-0.05	0.03	-0.02
% wetland area	0.01	0.05	0.06
Total variance explained (model R^2) = 0.65			

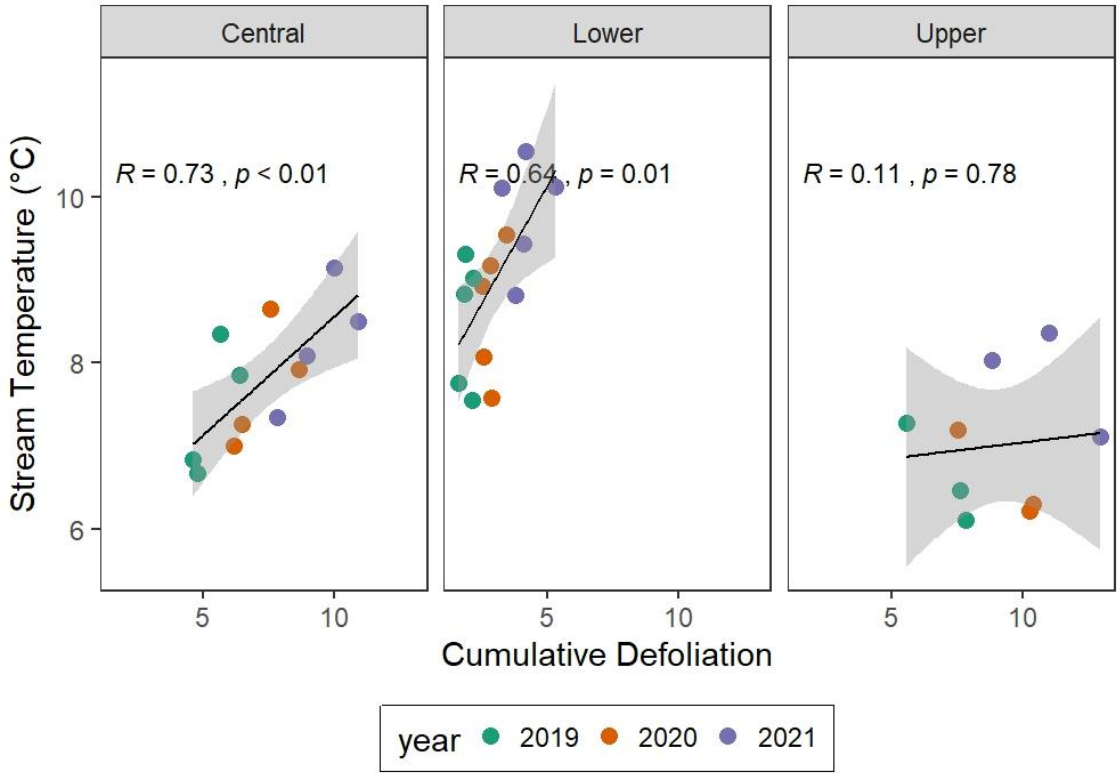

Figure 6. Pearson correlations between mean summer stream temperatures and cumulative defoliation in each study region (lower, central, and upper) in the Gaspésie Peninsula, QC, Canada with years (2019, 2020, and 2021) pooled together. Temperature values represent the site average of data recorded every 10-min from 6 replicates per site.

3.2 Stream Microbiome Structure

3.2.1 Microbiome Structure: Bacteria and Fungi Alpha Diversity

Bacteria ESV richness across all sites was similar in 2019 and 2020, and considerably lower in 2021, while Shannon diversity and evenness metrics were more similar across years (Table 7). In contrast, fungi ESV richness increased in 2021 relative to 2019 and 2020 (Table 7). All metrics for both bacteria and fungi were variable across sites within each year, however no significant relationships were observed between any of the diversity metrics and cumulative defoliation in any year (Figure 7), nor with any of the stream habitat variables that changed with cumulative defoliation (SUVA, flow, and/or temperature) (Figure A10).

Table 7. Ranges of bacteria diversity metrics (ESV richness, Shannon diversity, and evenness) and fungi ESV richness from leaf packs incubated in streams in the Gaspésie Peninsula, QC, Canada from August – September of 2019, 2020, and 2021. Ranges are based on the average of the diversity metric (ESV level) across replicates (n=6/site/year). One outlier site in 2019 removed from fungi ranges (site U03, mean richness = 463).

	2019	**2020**	**2021**
Bacteria			
ESV Richness	1336 – 2315	1620 – 2503	709 – 1534
Shannon Diversity	6.0 – 6.9	5.8 – 6.7	5.4 – 6.6
Evenness	0.06 – 0.16	0.05 – 0.11	0.05 – 0.20
Fungi			
ESV Richness	176 – 249	194 – 290	214 – 461

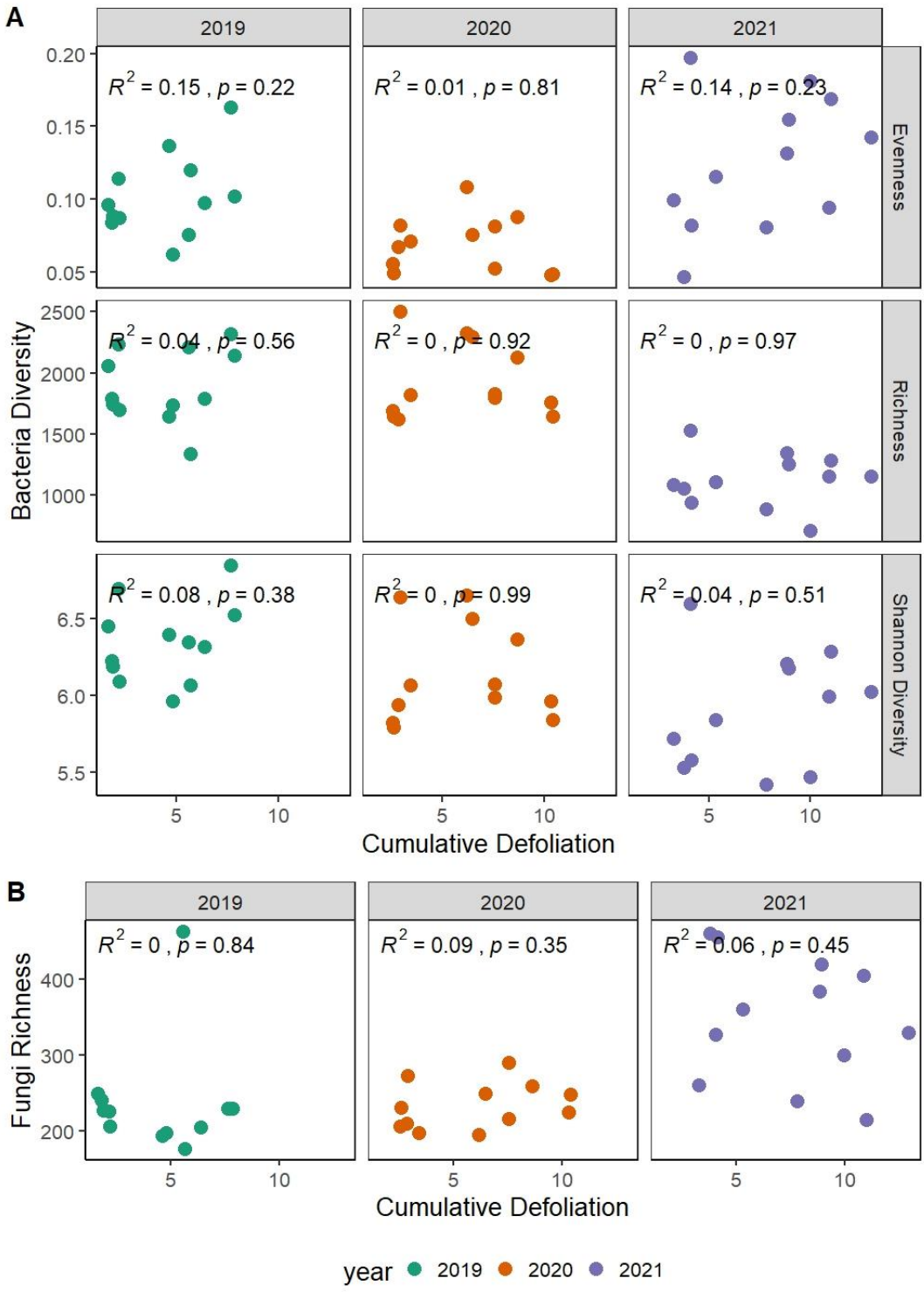

Figure 7. Pearson correlations between cumulative defoliation and A) bacteria diversity metrics (ESV richness, Shannon diversity, and evenness) and B) fungi ESV richness from leaf packs incubated in streams in the Gaspésie Peninsula, QC, Canada from August – September of 2019, 2020, and 2021. Each value represents the average diversity (ESV level) across replicates at each site (n=6/site/year) with the associated watershed cumulative defoliation intensity.

3.2.2 Microbiome Structure: Bacteria Community Composition

Bacteria community composition at the phylum level was relatively constant across sites and years and was dominated by Proteobacteria and Bacteroidetes (Figure 8A). Community composition at the class level was also relatively constant across sites and years, with the two most abundant classes being Alphaproteobacteria and Betaproteobacteria (Figure 8B). There were no apparent trends with the cumulative defoliation gradient for community composition at the phylum or class level. CoDA PCA ordinations suggest that at a lower taxonomic level (ESV), there were differences in bacteria community composition across years (PERMANOVA, R^2 = 0.17, $p < 0.001$) (Figure 9A). Years 2019 and 2021 separate out from one another more on PC1 (12% of variation), while 2020 separates out from the other years more on PC2 (9.2% of variation). Given this, subsequent ordinations were conducted for each year individually and we observed that the separation of communities at the ESV level became more distinct as cumulative defoliation progressed and intensified over time. In 2019, there was considerable overlap between low and high defoliated sites, with some separation between these groups on PC2 (9% of variation) (PERMANOVA, $R^2 = 0.05$, $p < 0.001$) (Figure 9B). In 2020, there was still considerable overlap between the high and low defoliated sites, with some separation between the groups on both PC1 (13% variation) and PC2 (8% variation) (PERMANOVA, R^2 = 0.04, $p < 0.001$) (Figure 9C). By 2021, however, there was clear separation between the low and high defoliated sites, with 28% variation explained in the first two PC axes (PERMANOVA, R^2 = 0.12, $p < 0.001$) (Figure 9D). The sites with tree top mortality in 2020 (U02) and 2021 (U01, U02, and C05) did not visually separate out from the other sites, suggesting that these early

stages of spruce/fir mortality did not have additional effects on bacteria community composition.

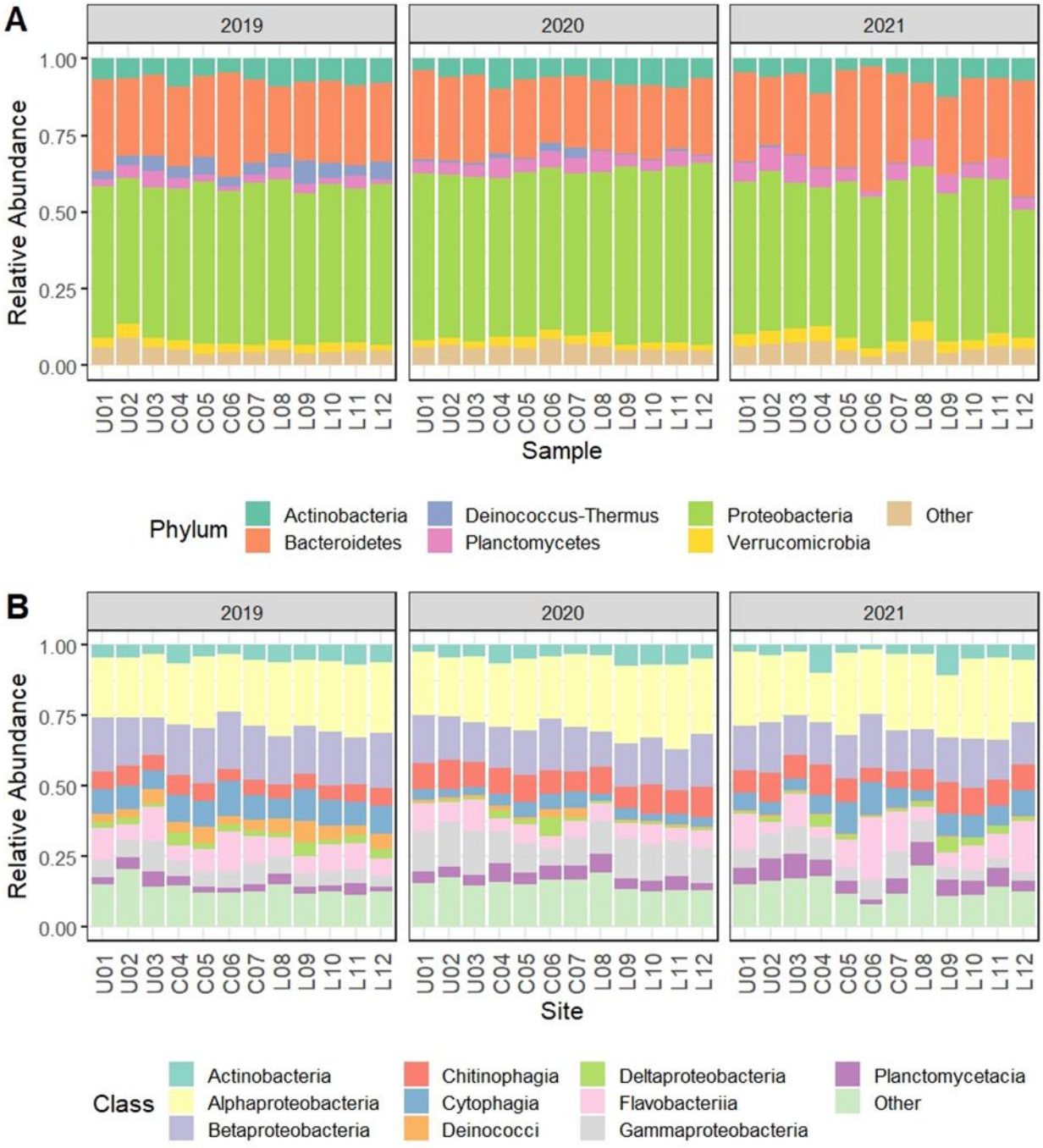

Figure 8. Relative abundance of the bacteria at the **A)** phyla and **B)** class levels from leaf packs incubated in streams in the Gaspésie Peninsula, QC, Canada from August – September of 2019, 2020, and 2021 (n=6 replicates/site/year). The top 6 phyla are shown as separate categories, with the remaining phlya (< 5% relative abundance) shown in the 'other' category. The top 10 classes are shown as separate categories, with the remaining classes (< 6 % relative abundance) shown in the 'other' category. All values represent the average across replicates (n=6) per site.

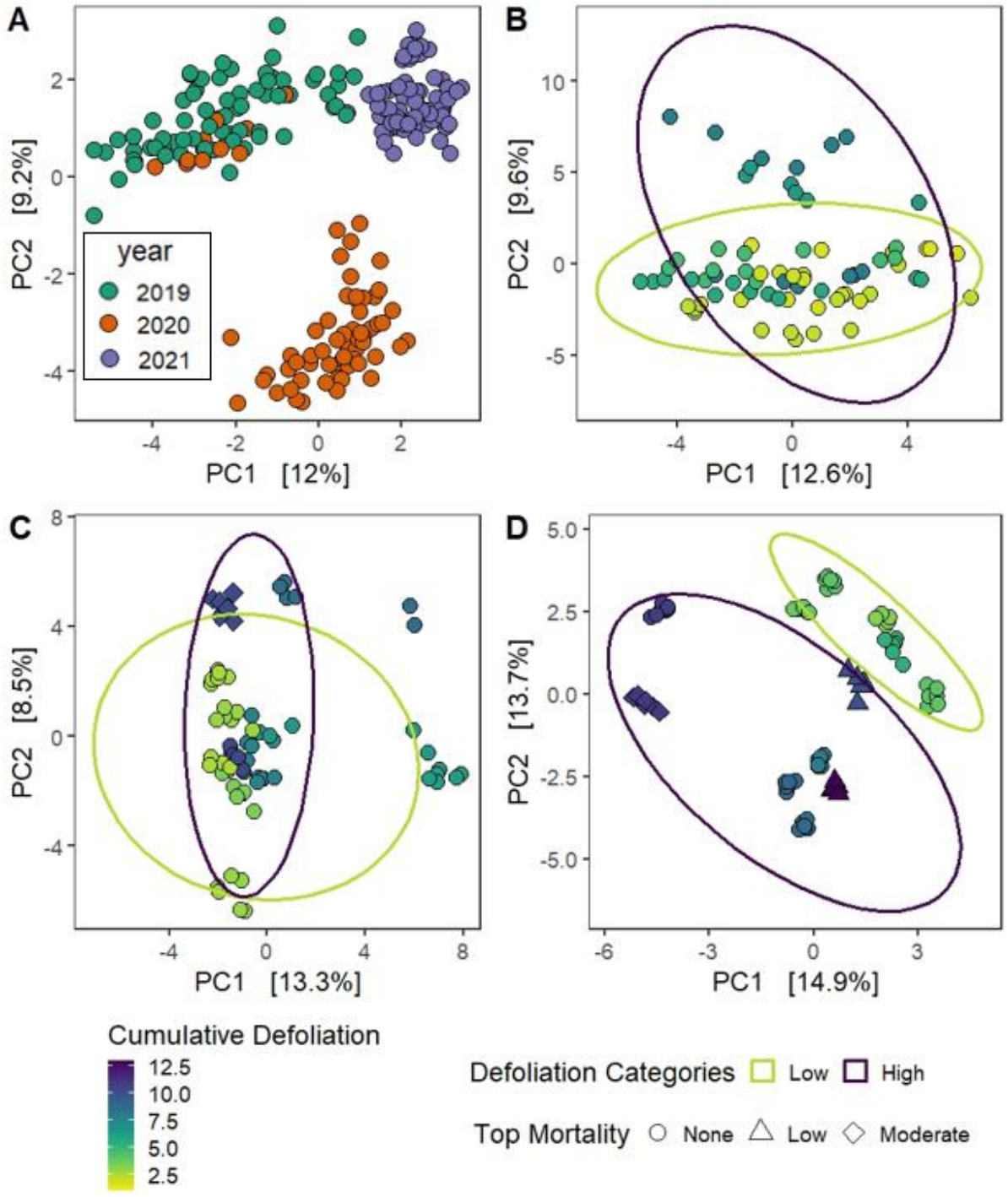

Figure 9. Compositional data analysis (CoDA) PCA ordinations for bacteria communities at the ESV level in **A)** all three sample years, **B)** 2019, **C)** 2020, and **D)** 2021. Each point represents a bacteria community from a leaf pack sample (n=6 replicates/site/year) incubated in streams in the Gaspésie Peninsula, QC, Canada from August – September of each year. Panel A is coloured by year. Panels A, B, and C are coloured by the cumulative defoliation gradient (increasing from yellow to blue), with shapes representing the amount of tree top mortality, and ellipses representing low (0 – 7.5) and high (7.5 – 15) cumulative defoliation categories.

The comparative RDA plots explained similar amounts of variation, which suggests that cumulative defoliation was altering bacteria community composition through changes to these stream habitat variables (SUVA, temperature, and flow) (Figure 10). Cumulative defoliation, temperature, and flow were positively associated with RDA2 (6% variation) and SUVA was positively associated with both RDA2 and RDA1 (23% variation). When each year was examined in a separate set of comparative RDA plots (Figure A12), the stream habitat variables explained 6% more variation on the first two axes than cumulative defoliation in 2019, 11% more in 2020, and 18% more in 2021.

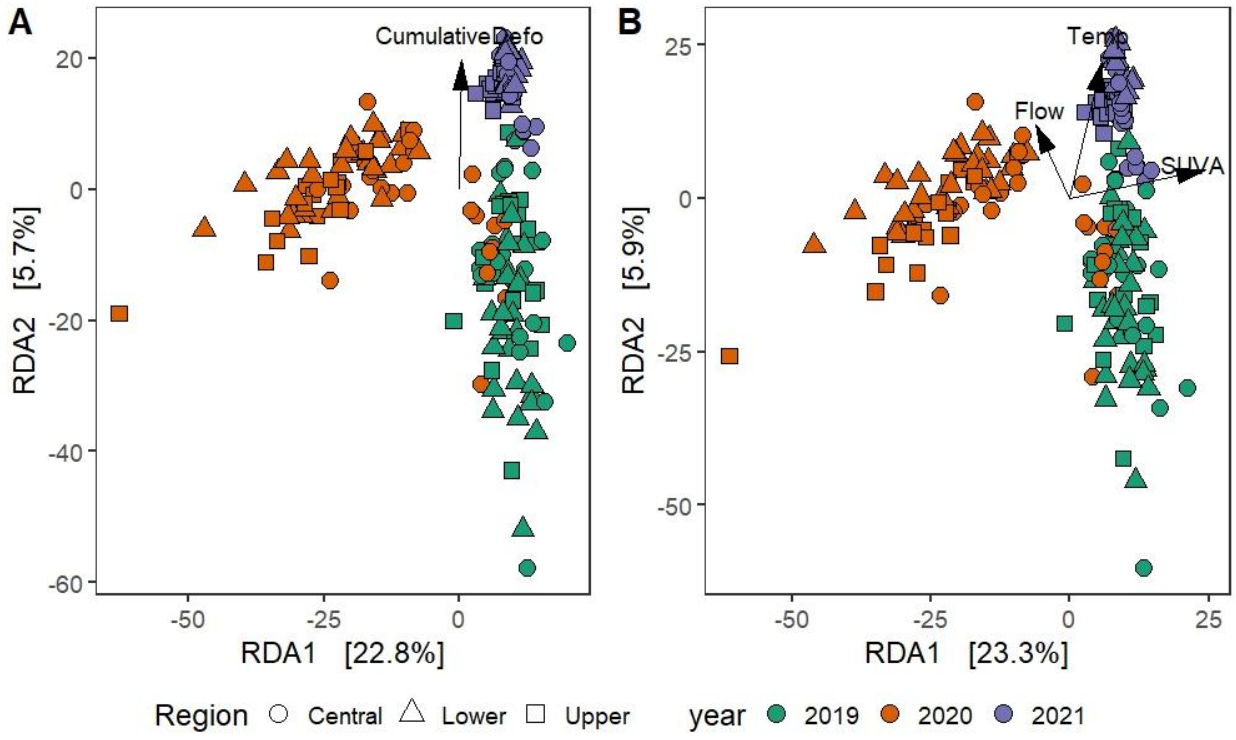

Figure 10. Comparison of bacteria community RDA plots constrained by **A)** cumulative defoliation and year and **B)** stream habitat variables (SUVA, temperature, and flow) and year. Each point represents a bacteria community from a leaf pack sample (n=6 replicates/site/year) incubated in streams in the Gaspésie Peninsula, QC, Canada from August – September of 2019, 2020, and 2021. Points are coloured by year with shapes representing geographic region.

Differential abundance analysis was conducted to assess if there were specific ESVs associated with the observed changes in overall community composition between low (0 – 7.5) and high (7.5 – 15) cumulative defoliation. These results indicated that a total of 65 unique ESVs were differentially abundant between the low and high cumulative defoliation categories ($p<0.05$, effect size >1), with 34 ESVs associated with the high group and 31 with the low group across all years. There were 25 ESVs in 2019, 3 in 2020, and 39 in 2021 with low overlap across years (there were 65 unique ESVs, with 2 overlapping between multiple years) (Figure 11). In each year, the Proteobacteria phylum had several different genera that were differentially abundant in high cumulative defoliation sites and many others that were abundant in the low defoliated sites. However, Novosphingobium is the only genus in the Proteobacteria phylum that was consistently differentially abundant in multiple years, as it was found in the low cumulative defoliation sites in both 2020 and 2021. The Fimbriiglobus genus of the Planctomycetes phylum had a mixed response across years, as it was more abundant in the high cumulative defoliation group in 2019 and more abundant in the low cumulative defoliation group in 2021. Overall, results indicate that while there are specific genera that were differentially abundant in the high and low cumulative defoliation categories, there were no consistent trends across years at the phylum level.

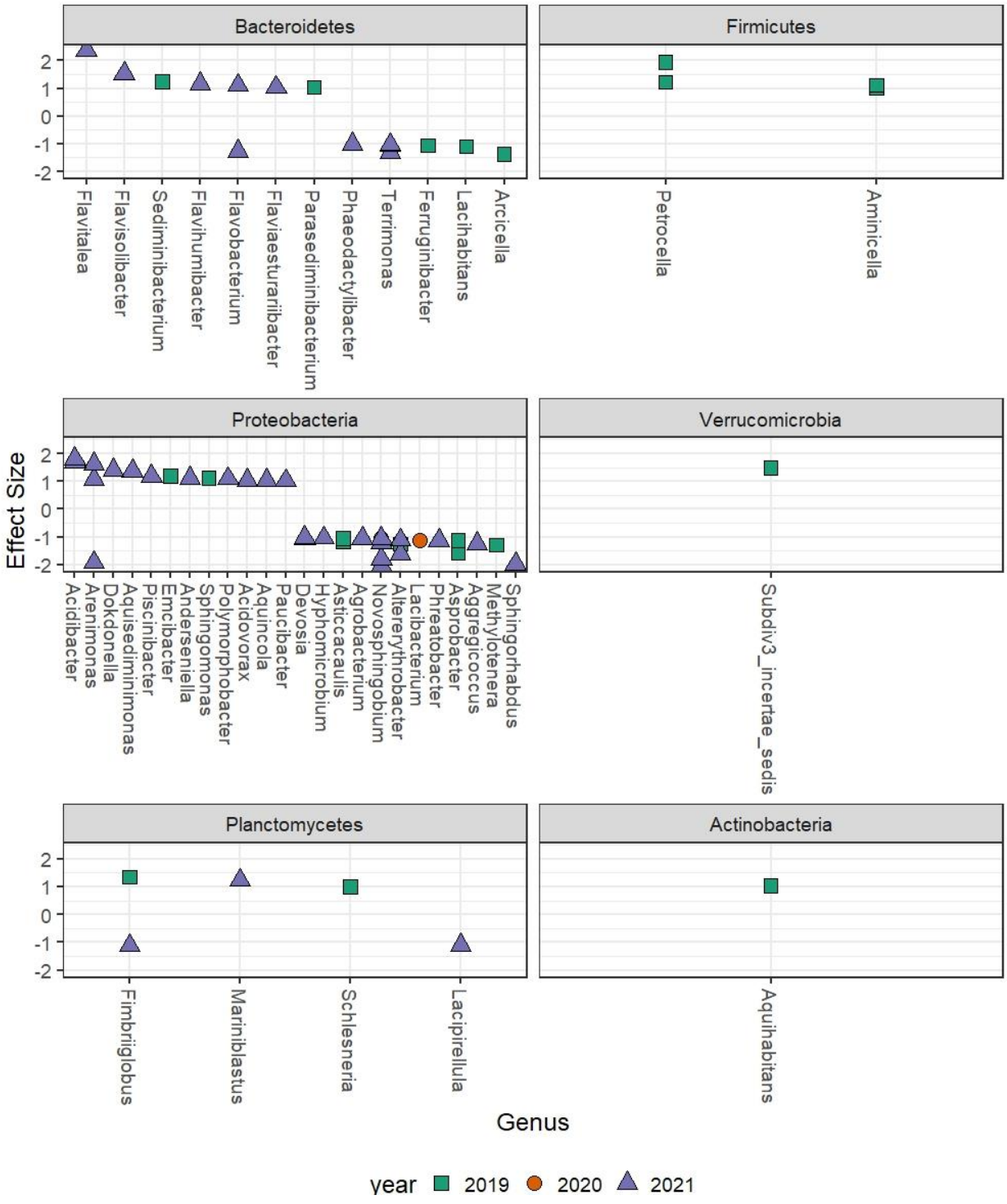

Figure 11. Differential abundance analysis (Aldex2) of bacteria ESVs from leaf pack samples (n=6 replicates/site/year) incubated in streams in the Gaspésie Peninsula, QC, Canada from August – September in 2019, 2020, and 2021. Bacteria ESVs that are associated with high (positive effect size) and low (negative effect size) cumulative defoliation sites are displayed with the genus shown on the x-axis and panels for each phylum. Values for all three years (2019, 2020 and 2021) are shown with different shapes and colours.

3.2.3 Microbiome Structure: Fungi Community Composition

CoDA PCA ordinations at the ESV level suggest that there were differences in fungi community composition across years (PERMANOVA, $R^2 = 0.25$, $p < 0.001$) (Figure 12A). Years 2019 and 2021 separated from one another more on PC1 (16% variation), while 2020 separated from the other years more on PC2 (12% variation). However, data dispersions between years were not homogenous, so results should be interpreted cautiously (permutation test, $p < 0.001$). Nevertheless, the PERMANOVA and visual inspections indicate that there are distinct yearly communities, and as such ordinations were also conducted for each year individually. In 2019, the variation explained in the first 2 PCA axes was low (14%) and there was no visually apparent trend with cumulative defoliation (Figure 12B). More variation was explained in 2020 (24%), but with limited separation along the cumulative defoliation gradient (Figure 12C). As was observed for the bacteria, although not as strongly, in the later year (2021) there was more separation between the high and low cumulative defoliation groups along PC1 (14 % variation) (Figure 12D). The low and high cumulative defoliation groups were significantly different in all 3 years (PERMANOVA $p < 0.001$ for each year) and although the amount of variation increased through time, it was consistently small across years ($R^2 = 0.03$ in 2019, $R^2 = 0.04$ in 2020, and $R^2 = 0.08$ in 2021). In addition, the assumption of equal dispersion between groups was violated in 2019 (permutation test, $p < 0.01$) indicating that PERMANOVA results in that year are not as reliable as in 2020 and 2021.

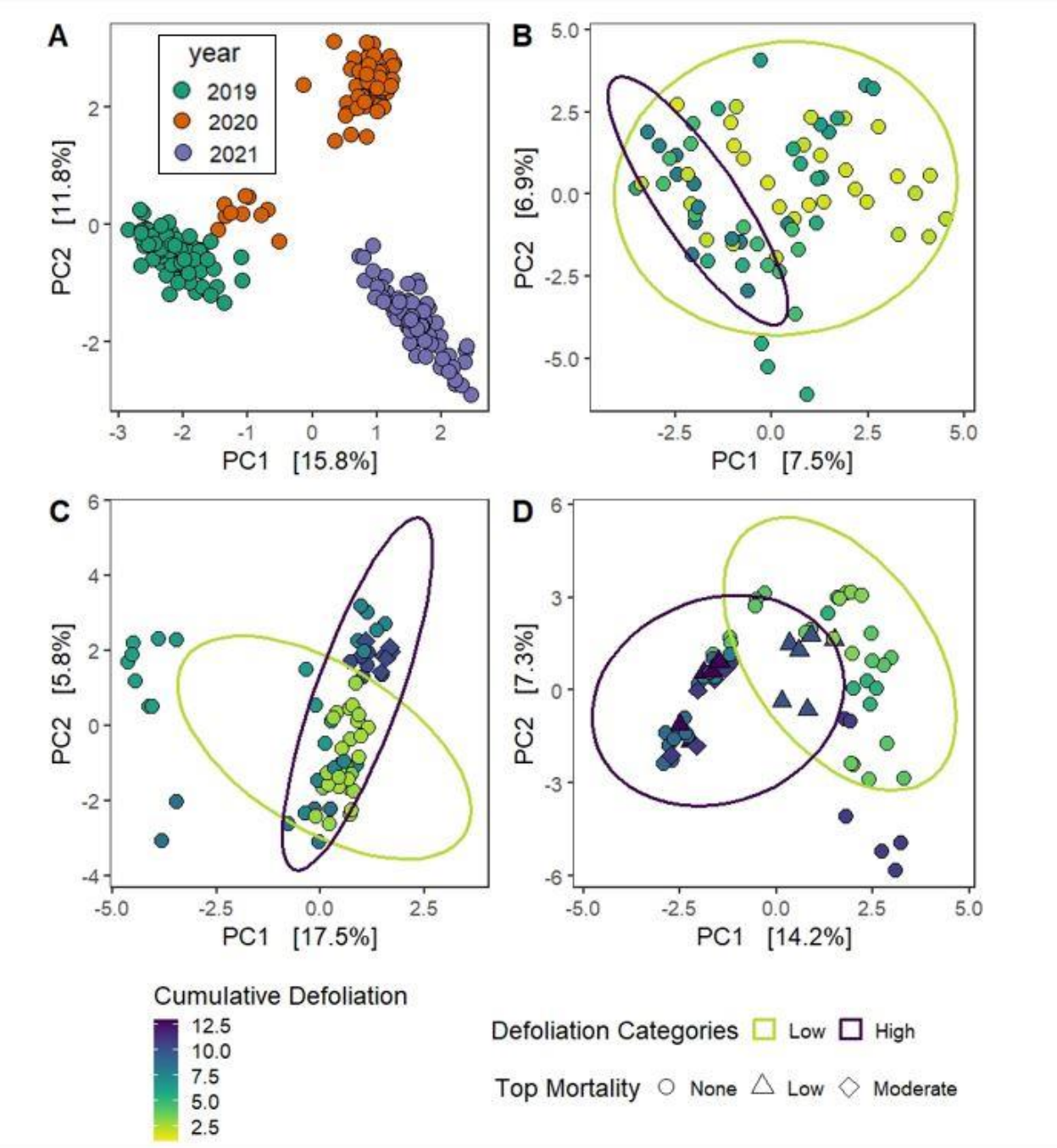

Figure 12. Compositional data analysis (CoDA) PCA ordinations for fungi communities at the ESV level in **A)** all three sample years, **B)** 2019, **C)** 2020, and **D)** 2021. Each point represents a fungi community from a leaf pack sample (n=6 replicates/site/year) incubated in streams in the Gaspésie Peninsula, QC, Canada from August – September of each year. Panel A is coloured by year. Panels A, B, and C are coloured by the cumulative defoliation gradient (increasing from yellow to blue), with shapes representing the amount of tree top mortality, and ellipses representing low (0 – 7.5) and high (7.5 – 15) cumulative defoliation categories.

As for bacteria, the comparative RDA plots indicate that the changes in fungi communities attributed to cumulative defoliation were likely mediated through its impacts on the three stream habitat variables of SUVA, flow, and temperature. The two RDAs explained similar amounts of variance in the first two RDA axes (~41%) (Figure 13). When data were analyzed with each year separately, the stream habitat variable RDAs explained more variation than the cumulative defoliation RDAs, with 2% more in 2019, 8% more in 2020, and 7% more in 2021 (Figure A13).

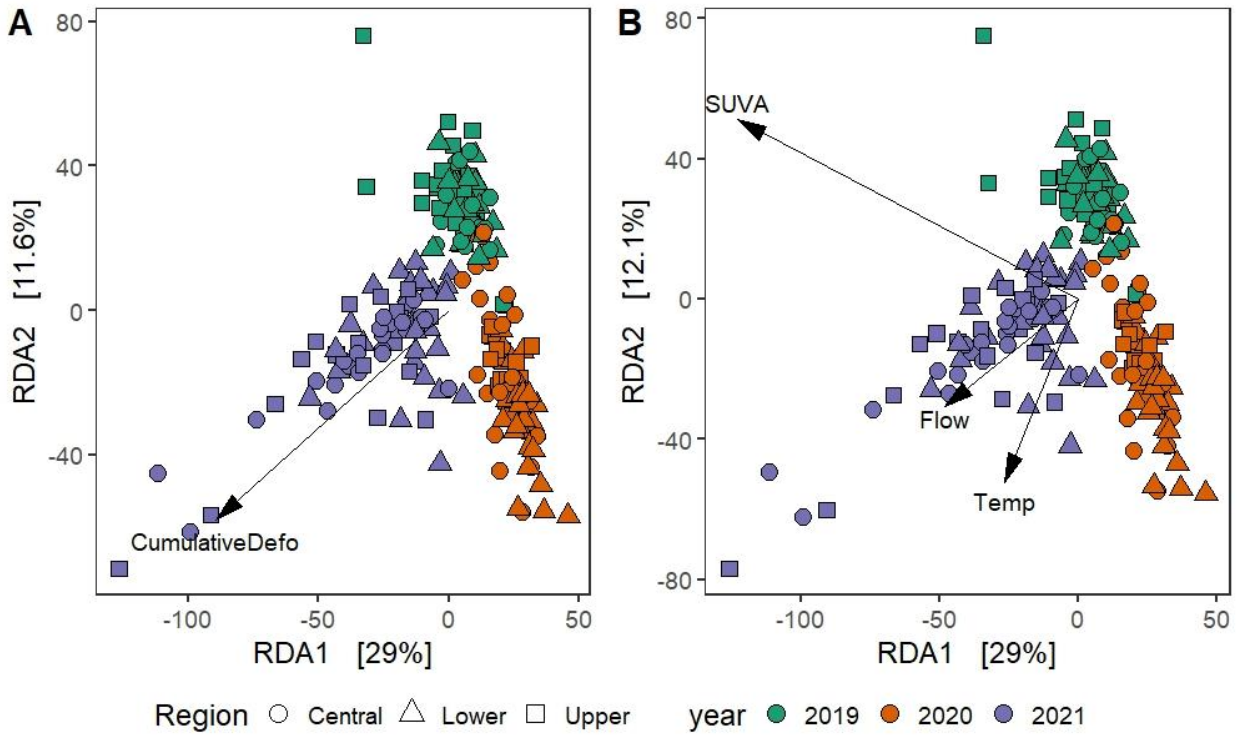

Figure 13. Comparison of fungi community RDA plots constrained by **A)** cumulative defoliation and year, and **B)** stream habitat variables (SUVA, temperature, and flow) and year. Each point represents a fungi community from a leaf pack sample (n=6 replicates/site/year) incubated in streams in the Gaspésie Peninsula, QC, Canada from August – September of 2019, 2020, and 2021. Points are coloured by year with shapes representing geographic region.

Differential abundance analysis was conducted to assess if there were specific ESVs associated with the observed changes in overall fungi community composition between low and high cumulative defoliation. There were no differentially abundant ESVs in 2019 or 2020, which

corresponds well with the limited community composition differences between low and high cumulative defoliation in those years. In 2021, there were 8 differentially abundant ESVs, all of which were associated with the low cumulative defoliation category. Of these ESVs, 7 belong to the Ascomycota phylum and 1 to the Basidiomycota phylum, with each in a different taxonomic order and family.

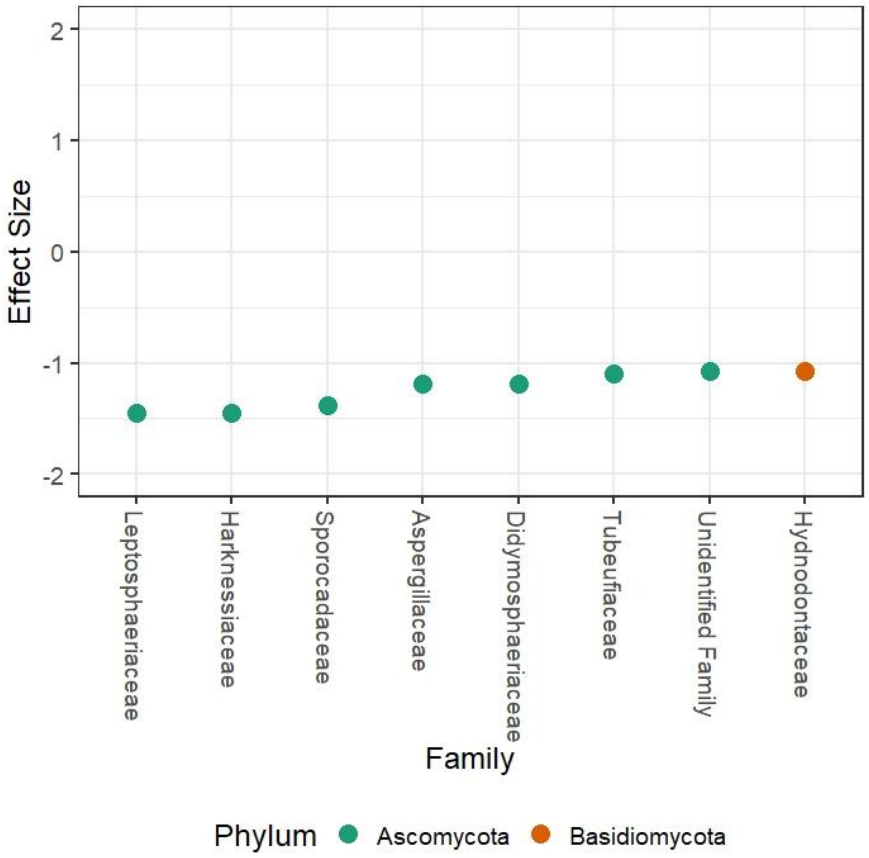

Figure 14. Differential abundance analysis (Aldex2) of the fungi ESVs from leaf pack samples incubated in streams in the Gaspésie Peninsula, QC, Canada from August – September in 2019, 2020, and 2021. Fungi ESVs that are associated with high (positive effect size) and low (negative effect size) cumulative defoliation sites in 2021 are displayed with the family shown on the x-axis and panels for each phylum. There were no differentially abundant fungi ESVs in 2019 or 2020.

3.2.4 Microbiome Structure: Algal Biomass

Total algal biomass was similar in both 2019 and 2021 (not measured in 2020) and was dominated by diatoms, followed by green algae and cyanobacteria. Total algae, green algae, and cyanobacteria biomass were all positively related to cumulative defoliation in both years, while diatom biomass was only positively related in 2019 (Figure 15). The HP models indicate that total algal biomass was well explained by SUVA, temperature, and flow in 2019 (R^2= 0.6) and was strongly driven by flow, but the stream habitat variables did not explain any variation in 2021 (R^2= -0.06) (Table 8). This could be due to the lack of relationship between diatoms and cumulative defoliation in 2021, as total algal biomass is a sum of the three other algal parameters. The green algae HP models explained large amounts of variance in both 2019 (R^2 = 0.63) and 2021 (R^2=0.51) but the most important variable differed between years, with flow in 2019 and SUVA in 2021. The cyanobacteria HP models were not as well explained by the stream habitat variables (R^2=0.29 in 2019 and R^2=0.16 in 2020), indicating that there are additional factors driving cyanobacteria that we did not account for in our model.

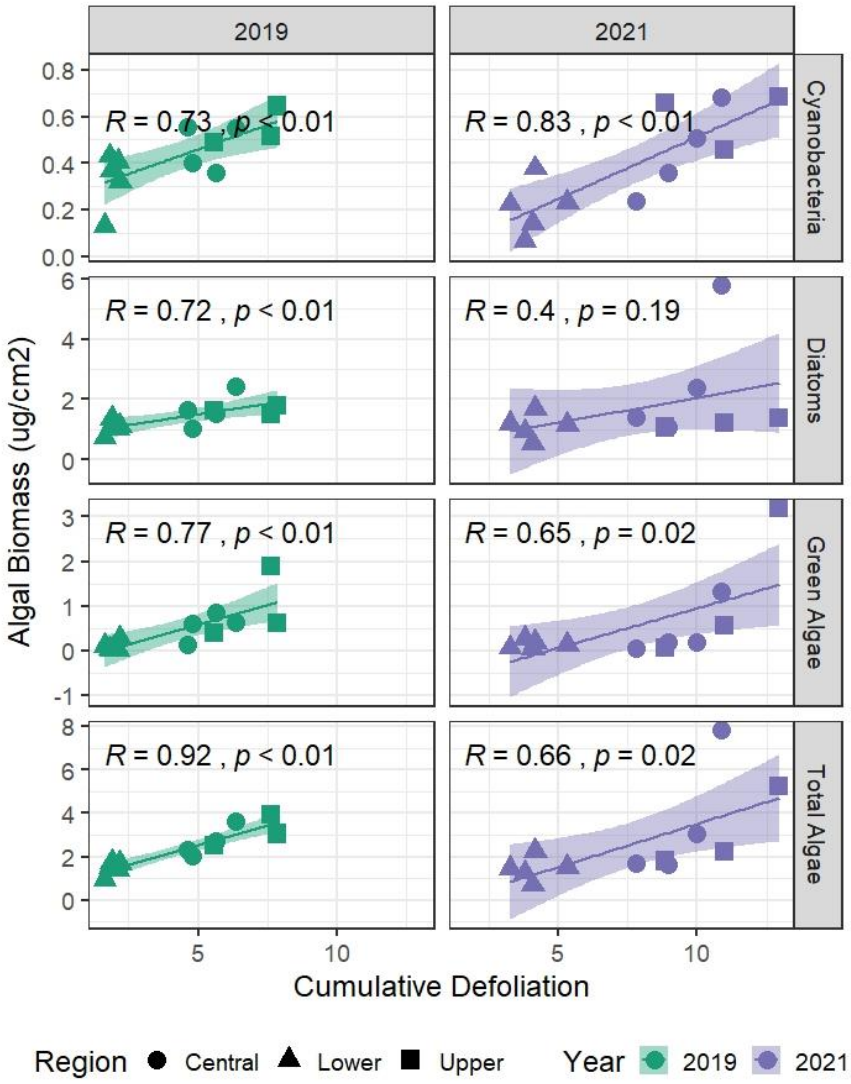

Figure 15. Pearson correlations between average algal biomass (cyanobacteria, diatoms, green algae, and total algae) in streams in the Gaspésie Peninsula, QC, Canada from August – September in 2019 (n=3) and 2021 (n=3) and watershed cumulative defoliation. Only 2019 and 2021 shown as algal biomass was not measured in 2020.

Table 8. Hierarchical partitioning model results for mean algal biomass (cyanobacteria, green algae, and total algae) from streams in the Gaspésie Peninsula, QC, Canada from August – September in 2019 (n=3) and 2021 (n=3). Values represent the amount of variation explained by each stream habitat metric (SUVA, temperature, and flow), with individual contributions representing the sum of the unique and shared contributions.

Hierarchical partitioning contributions						
	2019			2021		
Variable	**Unique**	**Average shared**	**Individual**	**Unique**	**Average shared**	**Individual**
Green Algae	Model R^2 = 0.63			Model R^2 = 0.51		
SUVA	0.06	0.01	0.07	0.40	0.07	0.47
Flow	0.53	0	0.53	-0.02	0.02	0
Temperature	-0.02	0.05	0.03	-0.05	0.09	0.04
Cyanobacteria	Model R^2 = 0.29			Model R^2 = 0.16		
SUVA	-0.04	0.17	0.13	-0.02	0.12	0.10
Flow	-0.03	0.16	0.13	-0.03	0.10	0.07
Temperature	-0.08	0.11	0.03	-0.09	0.08	-0.01
Total Algae	Model R^2 = 0.60			Model R^2 = -0.06		
SUVA	-0.02	0.19	0.17	0.03	0.05	0.08
Flow	0.20	0.19	0.39	-0.11	0.03	-0.08
Temperature	-0.01	0.05	0.04	-0.12	0.06	-0.06

3.3 Stream Microbiome Functions

3.3.1 Microbiome Functions: Extracellular Enzyme Assays and Decomposition Rates

Extracellular enzyme activity (across all sites and years) was highest for phosphatase (463 – 4874 nmol h^{-1} g), followed by N-acetyl-β-D-glucosaminidase (113 – 1748 nmol h^{-1} g), and xylosidase (35 – 752 nmol h^{-1} g). Activities for all three enzymes were variable across years, with the highest activity in 2020, and the lowest activity in 2021. There was variation across sites in 2019 and 2020, but limited variation in 2021, and no relationship with cumulative defoliation in any year (Figure 16). There was a significant relationship between phosphatase activity and SUVA in 2020 (r=0.62, p =0.032), however it was not a consistent relationship in other years (Figure 17). There were no significant trends between any of the extracellular enzyme activities and other stream habitat variables (temperature, flow, temperature, or nutrients) (Figure A14).

Leaf pack decomposition rates were generally low (0 – 1.3 % mass loss/day), with limited variability across sites and years. There were no relationships between decomposition rates and cumulative defoliation (Figure 18) or stream habitat variables (SUVA, flow, temperature, or nutrients) (Figure A14).

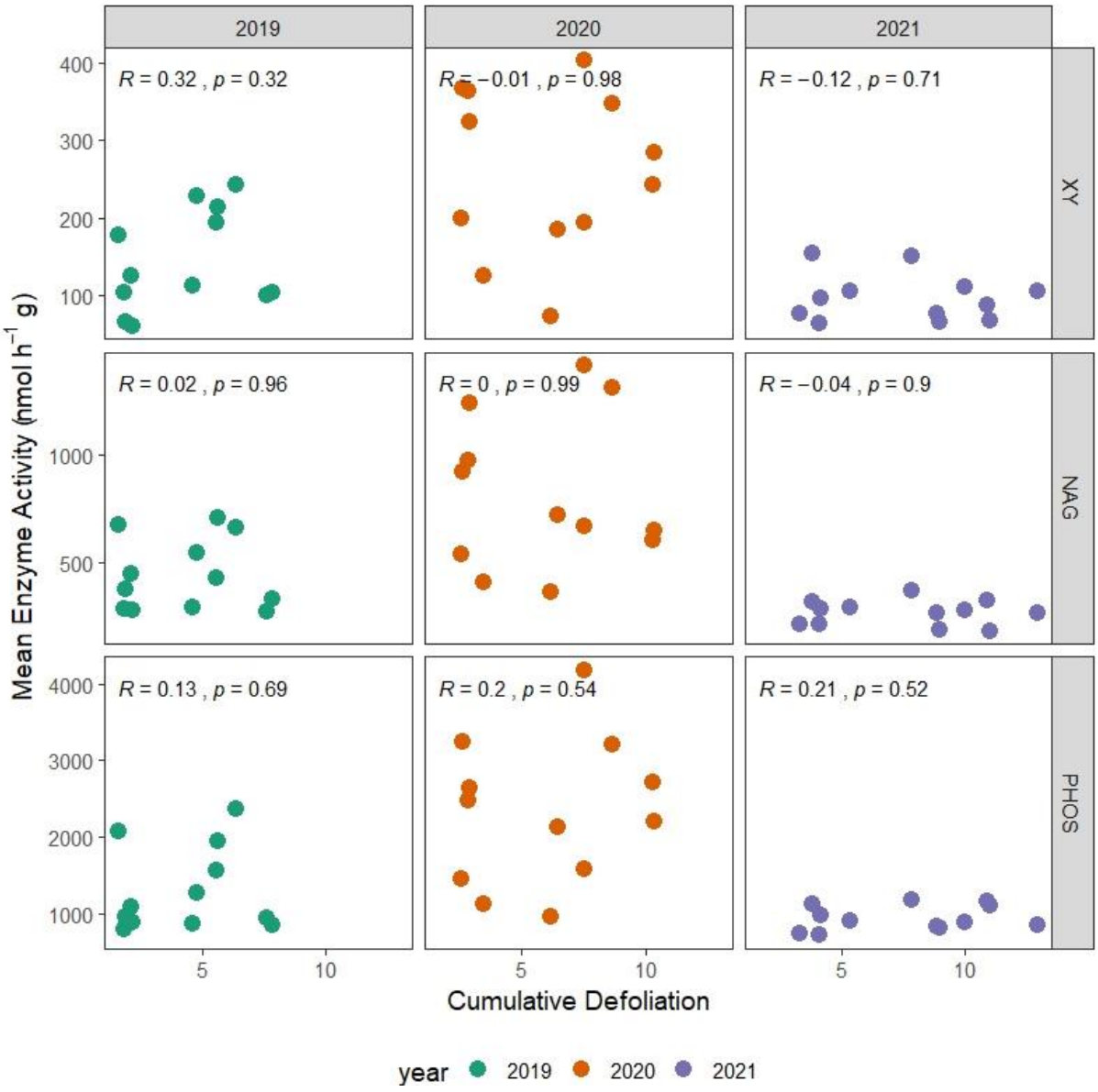

Figure 16. Pearson correlations between three extracellular enzyme (XY, NAG, and PHOS) activities (nmol h^{-1} g) and cumulative defoliation. Each point represents the average enzyme activity from leaf pack samples incubated in streams in the Gaspésie Peninsula, QC, Canada from August – September in 2019, 2020, and 2021 (n=6 replicates/site/year) and the associated cumulative defoliation intensity value in each watershed, with points coloured by year.

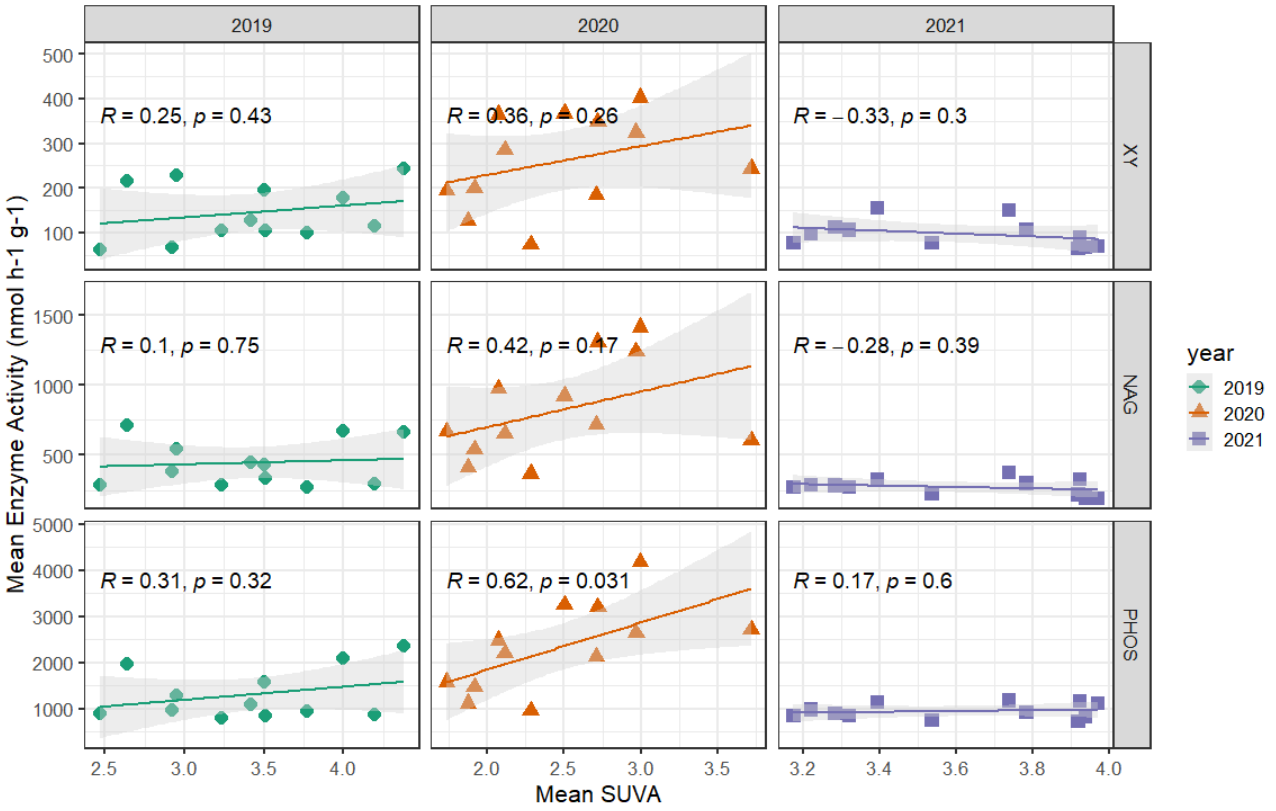

Figure 17. Pearson correlations between three extracellular enzyme (XY, NAG, and PHOS) activities (nmol h^{-1} g) and SUVA concentrations (mg-$L^{-1}m^{-1}$). Each point represents the average enzyme activity from leaf pack samples incubated in streams in the Gaspésie Peninsula, QC, Canada from August – September in 2019, 2020, and 2021 (n=6 replicates/site/year) and the average full season SUVA values in each stream (n=8 in 2019, n=10 in 2020, and n = 10 in 2021).

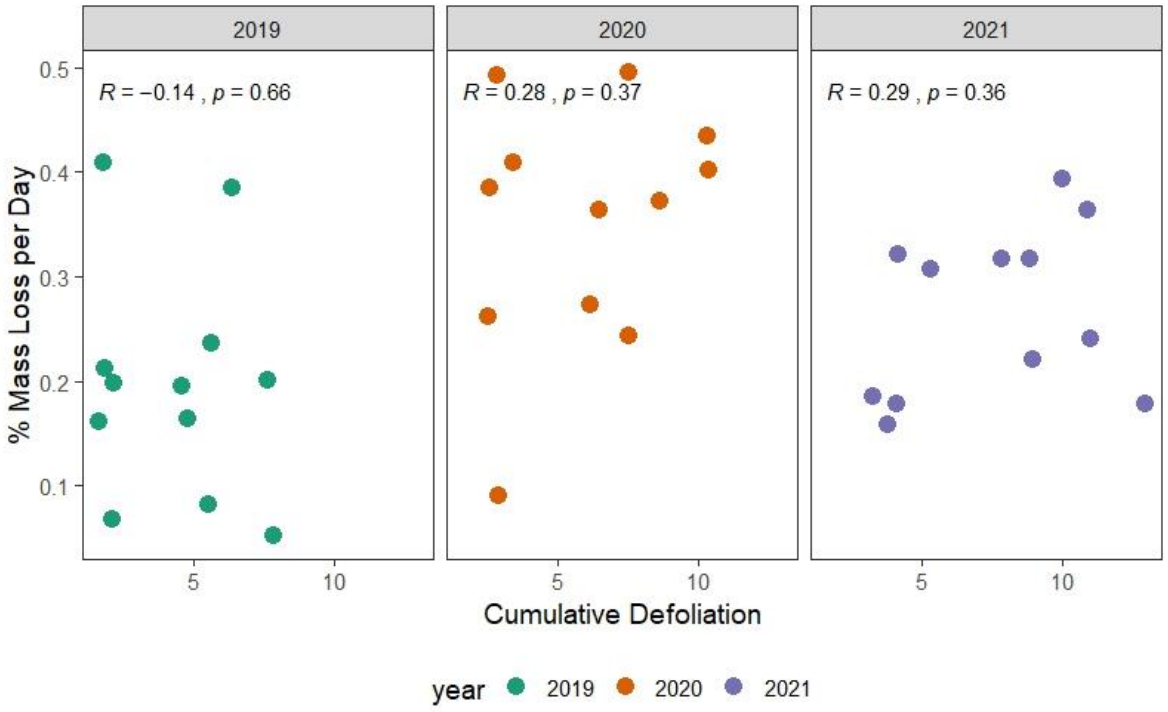

Figure 18. Pearson correlations between leaf pack decomposition rates (measured as % mass loss per day) and the associated cumulative defoliation intensity value in each watershed in 2019, 2020, and 2021. Each point represents the average % leaf mass loss per day from leaf pack samples incubated in streams in the Gaspésie Peninsula, QC, Canada from August – September in each year (n=6 replicates/site/year), with points coloured by year.

3.3.2 Microbiome Functions: Taxonomic Functional Assignments

Bacteria Community

Taxonomic functional assignments of the bacteria dataset identified 35 broad functional groups, with 12 involved in degradation and biosynthesis (Figure 19). Any functional groups with significant relationships to cumulative defoliation in all three years were investigated further. Two functional groups fit this criterion: the functional group for aromatic compound degradation had negative relationships and the carbohydrate biosynthesis group had positive relationships with cumulative defoliation in all three years (Figure 20).

Within these two functional groups, there were 66 pathways identified, with 42 in the aromatic compound degradation group and 24 in the carbohydrate biosynthesis group. Three of the aromatic compound degradation pathways belong to the sub-group vanillin degradation and each one was negatively related to cumulative defoliation in all three years (Figure 21). The vanillin degradation group only contains these three pathways, which are all variants of one another, meaning they perform the same biological function from the same starting material but do so with slightly different chemical reactions (BioCyc, 2023). Vanillin is an intermediate compound formed from the breakdown of lignin (an aromatic compound abundant in terrestrial vegetation) (Caspi et al., 2018; MetaCyc, 2023). There were an additional four aromatic compound degradation pathways negatively related to cumulative defoliation in two of the three years (2020 and 2021), and five with a negative relationship in 2020 and positive in 2021. There were 25 pathways that were only related to cumulative defoliation in one year, and they included 21 aromatic degradation pathways and 4 carbohydrate biosynthesis pathways.

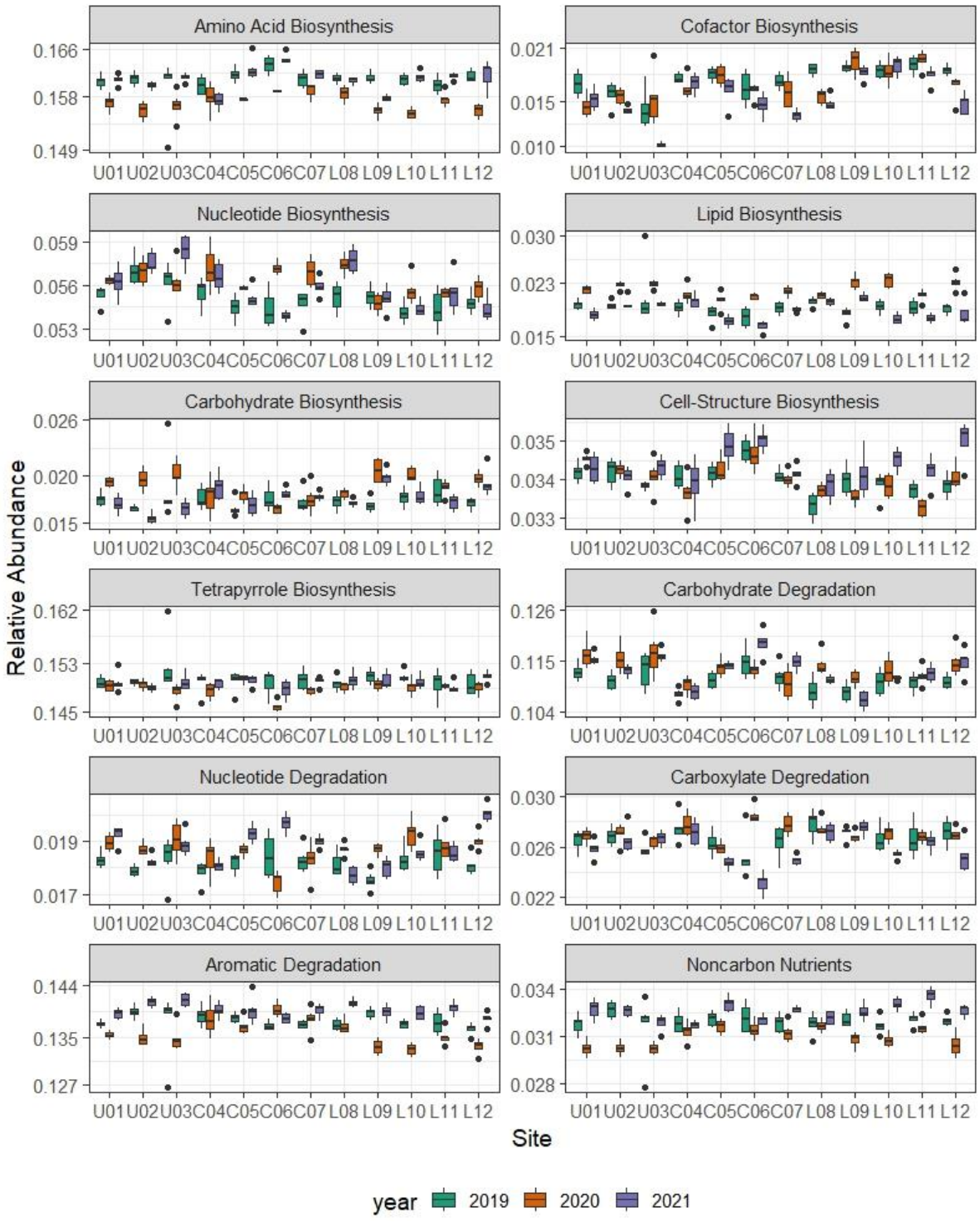

Figure 19. Boxplot of bacteria degradation and biosynthesis functional groups in each leaf pack sample (n=6/site/year) incubated in streams in the Gaspésie Peninsula, QC, Canada from August – September in 2019, 2020, and 2021. All functional pathways were identified with PiCRUT2 and sorted into functional groups based on the MetaCyc pathway type ontology. The relative abundances of all pathways within a functional group were summed and groups with a relative abundance of 2% or more are presented and coloured by year.

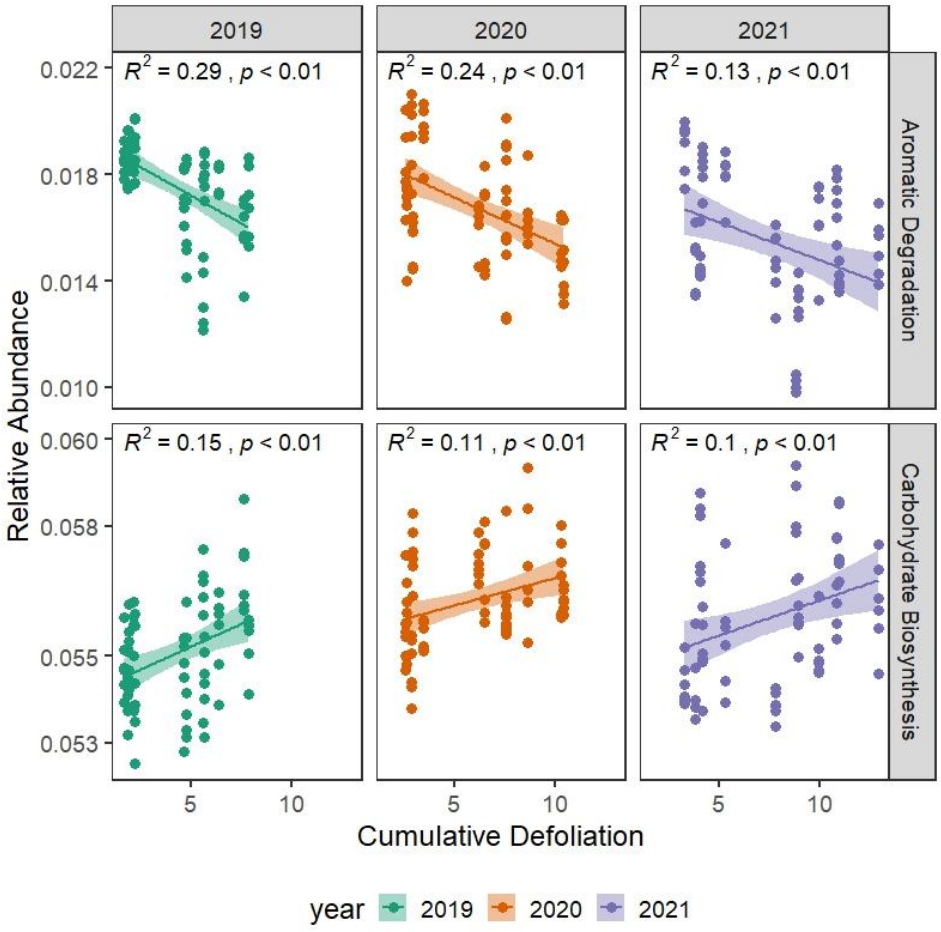

Figure 20. Linear models between bacteria functional groups (aromatic compound degradation and carbohydrate biosynthesis) significantly related to cumulative defoliation. Each point represents a leaf pack sample (n=6/site/year) incubated in streams in the Gaspésie Peninsula, QC, Canada from August – September in 2019, 2020, and 2021 and is coloured by sample year. The summed relative abundance of all functional pathways within the aromatic compound degradation (n=42 pathways) and carbohydrate biosynthesis (n= 24 pathways) functional groups are presented. Functional pathways were identified with PiCRUST2 and sorted into functional groups based on the MetaCyc pathway type ontology.

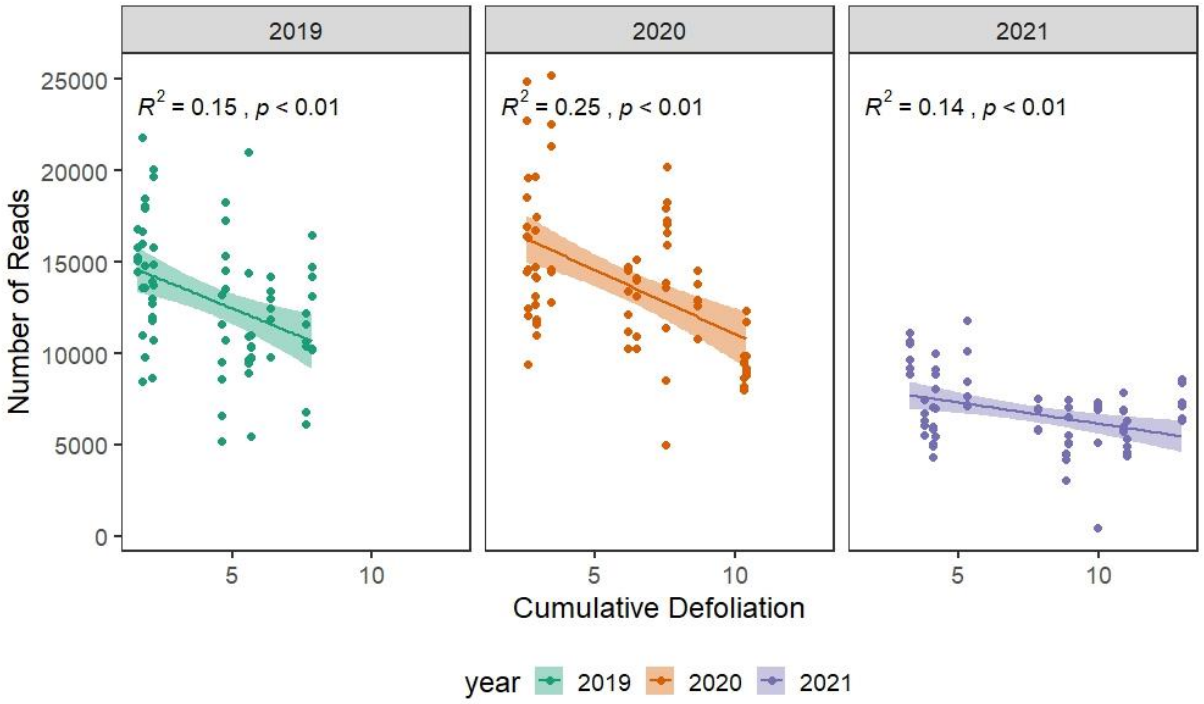

Figure 21. Linear models between the vanillin degradation functional group (sub-group of aromatic compound degradation) and cumulative defoliation. Each point represents a leaf pack sample (n=6/site/year) incubated in streams in the Gaspésie Peninsula, QC, Canada from August – September in 2019, 2020, and 2021 and is coloured by sample year. The number of reads represents the sum of reads from the three functional pathways that form the vanillin degradation subgroup. Functional pathways were identified with PiCRUSt2 and sorted into functional groups based on the MetaCyc pathway type ontology.

Fungi Community

Taxonomic functional assignments of the fungi dataset using FUNGuild identified 33 broad functional groups, with the plant pathogen, endophyte, and undefined saprotrophs as the most abundant groups (Figure 22). There was some variation in their relative abundances across sites and considerable interannual variability. There was 1 functional group related to cumulative defoliation in 2019 (algal parasite) and 1 in 2021 (epiphyte) (Figure 23). There were no consistent relationships between any functional groups and cumulative defoliation across multiple years.

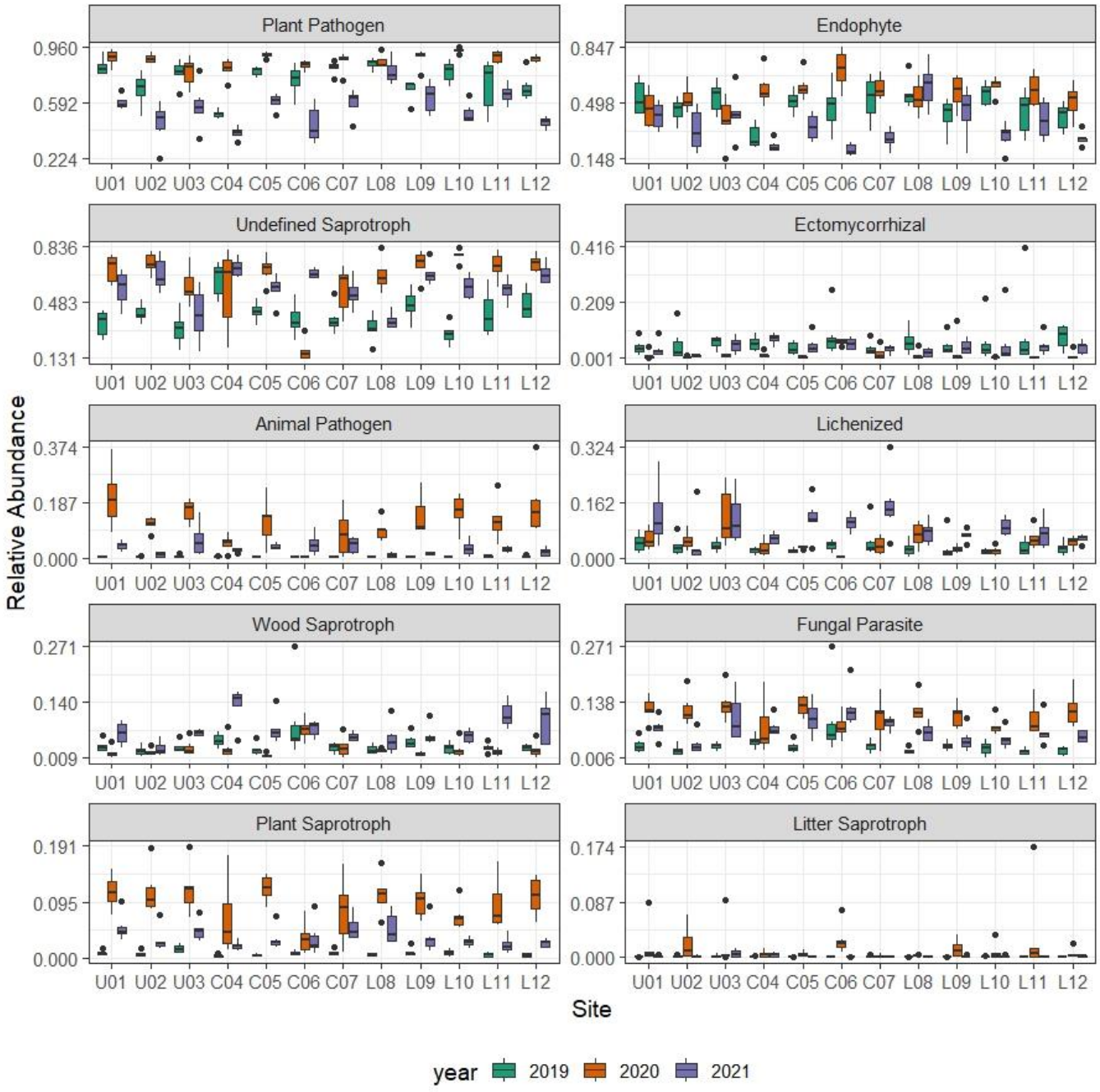

Figure 22. Boxplot of the fungi functional groups (guilds) in each leaf pack sample (n=6/site/year) incubated in streams in the Gaspésie Peninsula, QC, Canada from August – September in 2019, 2020, and 2021. Fungi ESVs in each sample were assigned functional groups with FUNGuild and assignments with a confidence level of highly probable and probable were retained (52% of all fungi ESVs in the dataset). Groups with a relative abundance of 7% or more are presented here and are coloured by year.

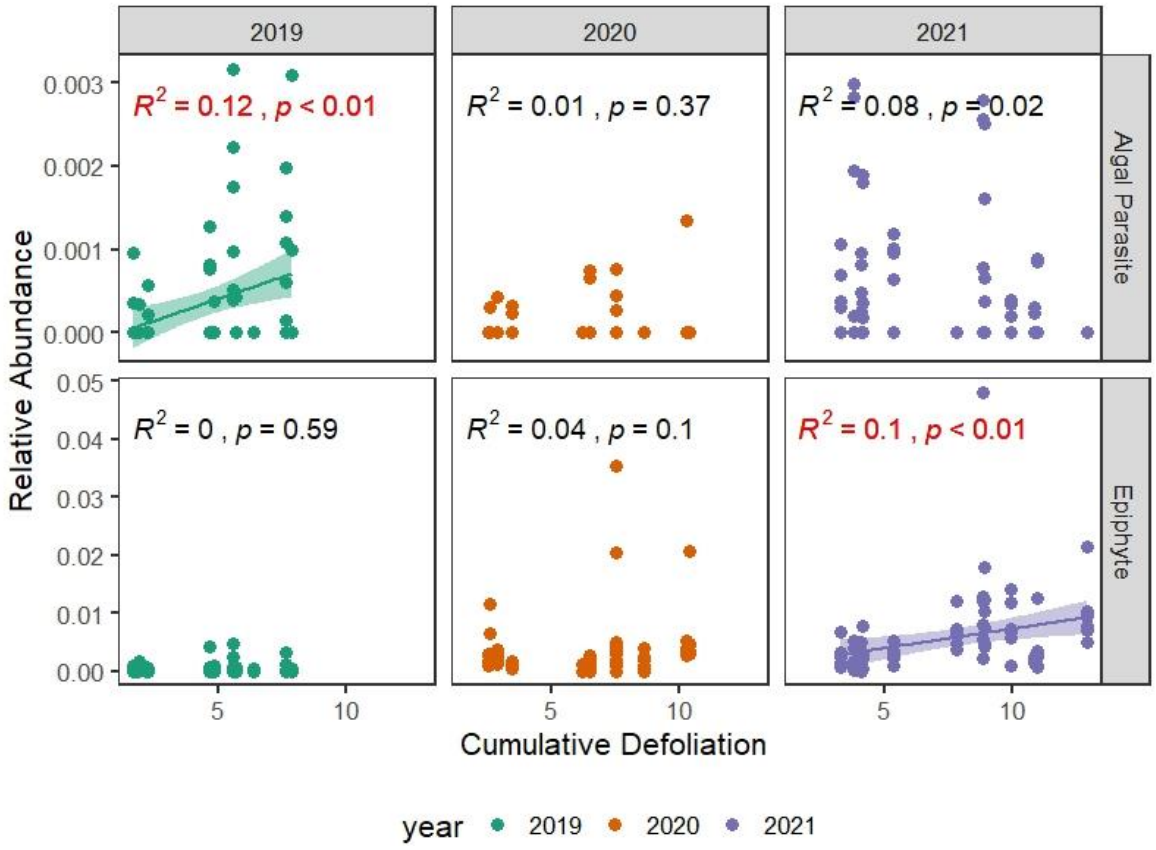

Figure 23. Linear models between fungi functional groups (algal parasite and epiphyte) significantly (p-values shown in red) related to cumulative defoliation. Each point represents a leaf pack sample (n=6/site/year) incubated in streams in the Gaspésie Peninsula, QC, Canada from August – September in 2019, 2020, and 2021 and is coloured by sample year. Fungi ESVs in leaf pack samples were assigned functional groups with FUNGuild and assignments with a confidence level of highly probable and probable (52% of all fungi ESVs in the dataset) were assessed for relationships with cumulative defoliation.

Functional Diversity

Bacteria and fungi functional diversity metrics (richness and Shannon diversity) were calculated based on the taxonomic functional assignment outputs (pathways for bacteria and guilds for fungi) and both metrics produced similar patterns within the two types of microorganisms. Bacteria functional diversity had limited variability across sites, but considerable interannual variability, with a decline in functional diversity across all sites in 2021 (Figure 24). In contrast, fungi functional diversity increased over time from 2019 to 2020 to 2021. There was no evidence of any trends between bacteria or fungi functional diversity and

cumulative defoliation (Figure 24) or with stream habitat variables (SUVA, flow, and temperature) (Figure A14).

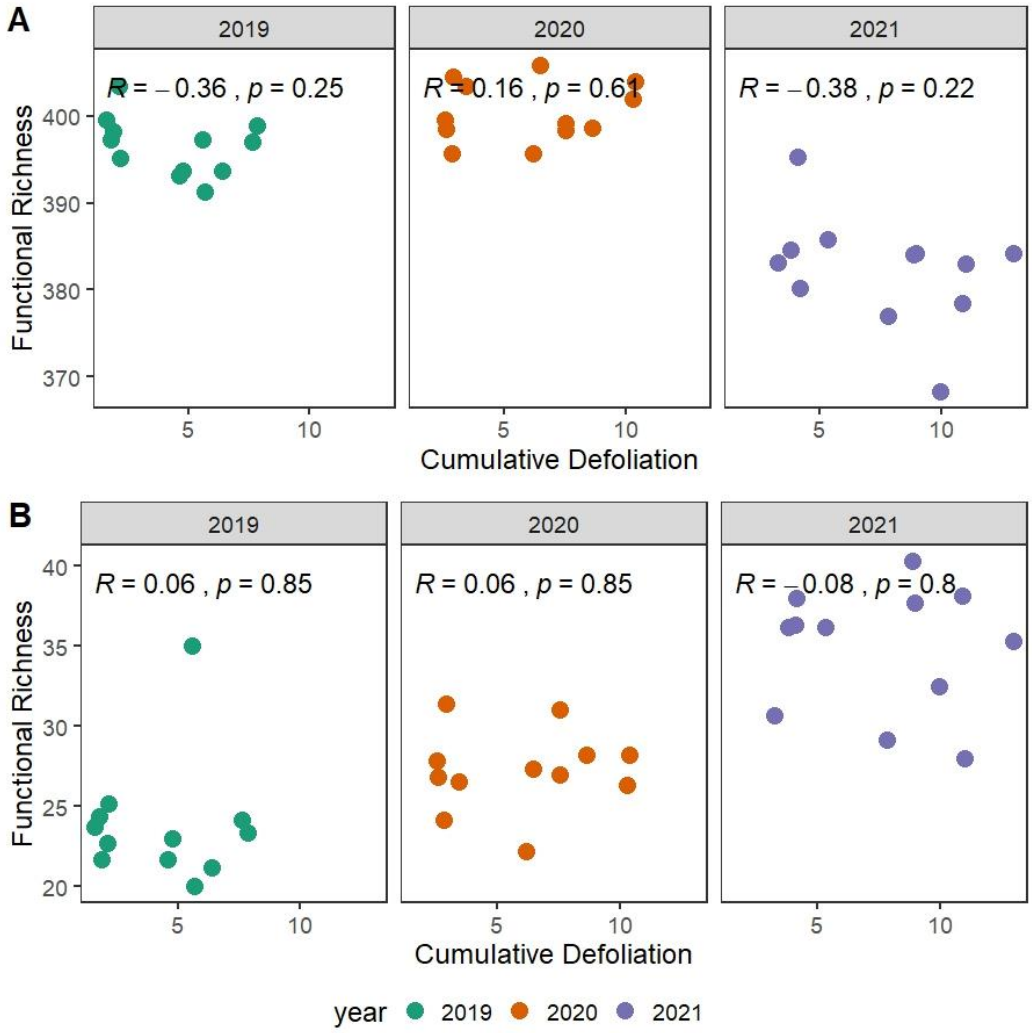

Figure 24. Pearson correlations between functional diversity (richness) of **A)** bacteria and **B)** fungi communities and cumulative defoliation. Average functional diversity from leaf pack samples (n=6/site/year) incubated in streams in the Gaspésie Peninsula, QC, Canada from August – September in 2019, 2020, and 2021, with points coloured by sample year. Bacteria functional richness represents the number of pathways identified using PICRUSt2, while fungi functional richness represents the number of guilds identified using FUNGuild.

4.0 Discussion

Spruce budworm defoliates spruce and fir trees and while the associated litter and frass inputs to forests alter terrestrial ecological processes (De Grandpré et al., 2022), less is known about their impact on aquatic ecosystems. We examined the influence of cumulative spruce budworm defoliation on stream ecosystems within 12 forested watersheds along a gradient of defoliation severity and there were three key outcomes. First, we found that cumulative defoliation altered stream habitat through changes to carbon quality (SUVA), temperature, and flow rates, but not nutrient concentrations or any other DOM quantity or quality metrics. Second, we observed changes to the structure of the microbiome, specifically increased algal biomass and changes to microbiome composition, but no change to overall microbial diversity. Finally, we found changes to bacterial functions associated with carbon cycling assessed through taxonomic assignments, but no changes to fungi taxonomic assignments or microbial functions measured through extracellular enzyme activities and leaf litter decomposition rates.

4.1 Microbiome Structure

Bacteria community composition in the Gaspésie streams varied among years and along the cumulative defoliation gradient within years. We found distinct yearly bacteria communities, which is consistent with the high temporal variability in stream bacteria community composition found in other studies (Portillo et al., 2012; Shade, Peter, et al., 2012; Zeglin, 2015). In the current study, a shift in bacteria community composition was observed between streams experiencing low and high cumulative defoliation, with the trend beginning in 2019 and strengthening each subsequent year. The strongest separation along the cumulative defoliation gradient occurred in 2021, suggesting that there is a cumulative defoliation intensity threshold of 7.5 or greater (on a scale of 0 – 15) along with a time threshold of 5 – 6 consecutive years of

defoliation. This suggests that cumulative defoliation has limited influence on stream bacterial community composition in the initial stages of a spruce budworm outbreak, but as the severity of the outbreak progresses and the effects of defoliation accumulate over time, it can influence community composition. Time lags in the response of microbiomes to disturbance are common, and with press disturbances (continuous disturbance over the long term) such as defoliation, it is difficult to determine when the threshold of maximum community change has been reached (Shade, Peter, et al., 2012). The observed lag effect in this study could also be due to the chronology of the outbreak across the study area. For example, defoliation was first observed in the upper watersheds in 2016, whereas it did not reach the central watersheds until 2017, and the lower watersheds until 2018. By 2021, all watersheds had 4 to 6 consecutive years of defoliation, with varying levels of severity. Additional years of field data in these watersheds would be beneficial to confirm the effects of the duration and severity of defoliation on stream microbiome composition.

Fungi community composition showed similar trends across years, but the shifts were not as strong as those observed in the bacteria community. This suggests that the fungi communities are more resistant to cumulative defoliation than the bacteria communities and that the initial stages of spruce budworm outbreaks will have less of an influence on fungi community composition. This is consistent with the response of soil microbial communities to environmental changes (e.g., mining, forest restoration, and drought) as fungi communities have been reported to be more resistant to environmental change than bacteria communities (Chen et al., 2020; De Vries et al., 2012; Sun et al., 2017). This is likely due to competitive differences in growth rates and resource use (De Vries et al., 2012; Shade, Peter, et al., 2012). Fungi have relatively slow growth rates, while bacteria have faster growth rates and can respond more quickly to

environmental changes (De Vries et al., 2012; Shade, Peter, et al., 2012; Sun et al., 2017). Further, fungi and bacteria often use different carbon substrates, for example, the breakdown of leaves is typically dominated by fungi, while sediments and fine particles are dominated by bacteria (Findlay, 2010; Sun et al., 2017). As such, fungi communities in this study are likely less responsive to the observed changes in DOM inputs to streams than bacteria communities. These differences in substrate use also provide a plausible explanation for the observed interannual differences in microbial diversity, with a decline in bacteria species richness alongside an increase in fungi species richness in 2021. This year had higher sedimentation rates relative to the previous two years (Figure A11), which may have a stronger negative influence on the bacteria communities that dominate the decomposition of fine particles, while the reduced competitive pressures with bacteria may subsequently allow fungi richness to increase.

As predicted, these changes in community composition along the cumulative defoliation gradient appear to be driven by alterations to stream habitat conditions related to defoliation (SUVA, temperature, and flow). This is in agreement with the literature as these three parameters are commonly reported to influence microbial community structure (Besemer, 2016; Zeglin, 2015). Elevated stream flow rates can increase the dispersal of microbial taxa from upstream, as well as increase the transfer of nutrients and carbon, which can shift microbial composition for resources (Besemer, 2016; Besemer et al., 2009; Woodcock et al., 2013). Similarly, increased SUVA levels can result in an increase in specialized microbial taxa that are able to process aromatic compounds (Fasching et al., 2020). Microbial taxa also have different optimal temperatures for growth which allows different groups to dominate at different temperatures and results in shifts in microbiome community composition (Adams et al., 2010). Additionally, the yearly comparative RDA plots in the current study show that considerably more variance is

explained by the stream habitat variables than the cumulative defoliation gradient. This is likely because the stream habitat variables represent the fine scale conditions that the bacteria and fungi communities are experiencing, whereas cumulative defoliation is a coarse measure of broad watershed condition.

While we observed shifts in bacteria and fungi community composition with increased cumulative defoliation and changes to stream habitat, there were no changes to alpha diversity. This suggests that there is species turnover occurring, but there is no associated decline in diversity. This pattern is consistent with other studies of land use gradients (e.g., urbanization, logging, industry, and forest fires) and stream microbial communities (Emilson et al., 2016; Hosen et al., 2017; Roberto et al., 2018; Simonin et al., 2019). In urban systems, this pattern has been attributed to the introduction of novel taxa from sewage and storm water inputs which offset the loss of sensitive taxa (Hosen et al., 2017; Simonin et al., 2019). In the current study, the increased inputs of litter and frass associated with defoliation could be introducing new microbial taxa, while taxa sensitive to the changing stream conditions are lost. Alternatively, this pattern could be because the small shifts we observed in the community composition (that were specific to changes in the organic matter source) were not large enough to cause shifts in overall microbial diversity. To improve the understanding of the underlying mechanism in this study, frass and litter samples could have been collected and microbiomes sequenced to compare the microbiome composition of frass, litter, and streams.

4.2 Shifts in Stream Carbon Quality and Bacteria Carbon Cycling Functions

With increased cumulative defoliation, we observed changes in the microbiome communities that were related to changes in carbon inputs and processing. We observed an increase in both SUVA and algal biomass, which would change carbon availability to microorganisms in two

ways. Higher SUVA indicates an increase in aromatic carbon compounds dissolved in the stream water (Weishaar et al., 2003), while higher algal biomass provides an increase in the availability of carbohydrates to microbial decomposers (glucose as a product of photosynthesis) in the streams (Wetzel, 2001). The changes in bacterial functional groups – to those with less aromatic degradation pathways and more carbohydrate biosynthesis pathways – suggests that the bacteria community responded to these changes in carbon quality by preferentially selecting carbohydrates as an energy source rather than the more complex, aromatic carbon source (SUVA), despite an increased availability of both sources. Bacteria commonly select carbon compounds that are the easiest to use as they allow for faster growth rates and thus a competitive advantage over other bacteria (Gorke & Stulke, 2008). The preference specifically for glucose has been observed in many bacteria species and it is known as a regulatory process called carbon catabolite regression (CCR) (Magasanik, 1961). When there is an abundance of a preferred carbon source the functions related to the use of other carbon sources decline, and their associated genes are not expressed (Gorke & Stulke, 2008). As such, the changes in SUVA co-occurring alongside likely changes in carbohydrates and the preferential selection by bacteria provide a likely explanation as to why the increased SUVA was not associated with an increase in functions associated with the processing of aromatic compounds as previously reported (e.g., Fasching et al., 2020).

The observed increase in SUVA associated with cumulative defoliation is likely mediated through two main pathways. Firstly, increased litter deposition to the forest floor from spruce budworm consuming and destroying foliage likely led to increased leaching of aromatic DOM in runoff as terrestrial vegetation is abundant in aromatic compounds (e.g., lignin and tannins) (Allan et al., 2021; Preston & Trofymow, 2000). Secondly, spruce budworm outbreaks have been

associated with increased soil temperature (De Grandpré et al., 2022) and water content (Balducci et al., 2020), which increases organic matter decomposition rates and would further increase the humic content and aromaticity of DOM runoff (Bertolet et al., 2018; Conant et al., 2011). This may be more a result of changes to soil moisture, as SUVA in soil leachate has been shown to be more sensitive to soil moisture levels than temperature, with SUVA lower in lakes during drought conditions (Bertolet et al., 2018). Measures of terrestrial processes such as leaf litter deposition rates and soil moisture levels in future studies would help delineate the factors that led to increased SUVA in streams in the current study.

Most of the variability in SUVA was driven by cumulative defoliation and elevation/latitude, but this differed among years, with defoliation explaining the most variability in 2019 and 2021 and elevation the most in 2020. This is likely due to differences in annual precipitation patterns, which can increase the hydrologic connectivity of organic soils and downstream waters under wet conditions, resulting in higher SUVA in streams and lakes with increased precipitation and soil moisture (Bertolet et al., 2018; Hood et al., 2006; Jane et al., 2017). This aligns with the lower SUVA observed in 2020 in this study, as there was lower cumulative precipitation in that year (Figure A9). A small amount of variance was also explained by forest composition, which can be attributed to the differences in the organic composition of leaf litter across tree species (Preston & Trofymow, 2000). This is consistent with other studies that found small differences in SUVA in throughfall, litter leachate, and soil between coniferous and deciduous forests (Cepáková et al., 2016; Thieme et al., 2019). Wetland area is typically a strong driver of SUVA in streams and rivers (Burns et al., 2013; Hanley et al., 2013) but was not an important predictor in our study. This could be attributed to the overall low wetland cover in the study area and limited range of variation across watersheds (0 – 2.5 % wetland cover).

Algal production is typically driven by light availability, temperature, and nutrients (Wetzel, 2001), however we did not see a strong influence of temperature or nutrients on algal biomass in these streams. As such, increased light availability is the most likely mechanism for the increased algal biomass, although we did not measure light availability directly in this study. Increased stream light availability due to loss of foliage has been observed in other pest outbreaks, for example, spongy moth (*Lymantria dispar dispar*) (Addy et al., 2018) and hemlock woody adelgid (*Adelges tsugae* Annand) (Siderhurst et al., 2010). Future work should investigate this mechanism directly for spruce budworm outbreaks by measuring both light availability and algal biomass across a gradient of defoliation intensity.

We also observed interannual variability in the relationships between algal biomass parameters and cumulative defoliation. In 2019, all parameters (cyanobacteria, diatoms, green algae, and total algae) displayed strong positive relationships with cumulative defoliation, while in 2021, the relationships weakened for diatoms, green algae, and total algae. Cyanobacteria was the exception and displayed strong relationships in both years. These yearly differences could be due to elevated sediment deposition rates in several stream sites in 2021 (Figure A11), as increased suspended sediment loads are known to reduce algal growth (Izagirre et al., 2009; Jones et al., 2012). Green algae have been found to be more sensitive to increased sedimentation than cyanobacteria and diatoms (Izagirre et al., 2009), however in the current study, both green algae and diatoms appeared to be sensitive to sedimentation.

4.3 Microbiome Functions and Stream Nutrients

Despite the changes in bacteria carbon cycling observed with the taxonomic functional assignments, leaf litter decomposition rates by microorganisms and their extracellular enzyme activities did not show any changes with cumulative defoliation. The lack of change in leaf litter

decomposition rates aligns with the limited changes to fungi community structure, as decomposition is typically dominated by fungi communities rather than bacteria (Findlay, 2010). Enzymes are produced by microbes to obtain nutrients from organic matter and are typically closely tied to stream nutrient levels, with the enzymes assessed in this study corresponding to phosphorus (PHOS), nitrogen (NAG), and carbon (XY) availability (Cunha et al., 2010; Luo et al., 2017). As such, the lack of relationship between enzyme activities and cumulative defoliation aligns well with the lack of response of nutrient levels (DOC, N, and P) to cumulative defoliation observed across sites. While we found no changes in the NAG enzyme or stream nitrogen levels associated with cumulative defoliation, we observed significantly higher concentrations of inorganic nitrogen (NO_2-NO_3) and total nitrogen (TN) in the watershed with substantial tree top mortality, though we did not observe any corresponding changes to enzyme activities. Spruce budworm defoliation has been found to result in a four-to-five-fold increase in nitrogen and phosphorus inputs to the boreal forest floor, though most of these nutrients are quickly taken up by surviving trees (De Grandpré et al., 2022). After five years of heavy defoliation tree mortality can occur (MacLean, 1984), which reduces nitrogen capture by trees and increases inorganic nitrogen pools in the soil (De Grandpré et al., 2022). This increased soil nitrogen associated with tree mortality likely resulted in excess nitrogen reaching the streams through runoff. Increased inorganic nitrogen in soils has been observed in response to tree mortality caused by bark beetles, but the response did not always translate to elevated nitrogen concentrations in streams, which may be attributed to differences in hydrological flow paths (Bearup et al., 2014; Clow et al., 2011; Mikkelson, Bearup, et al., 2013; Zimmermann et al., 2000). In contrast, there were no relationships between stream phosphorus concentrations or the PHOS enzyme and cumulative defoliation or tree mortality which could be attributed to relatively low levels of phosphorus in

litter and frass inputs from spruce budworm (De Grandpré et al., 2022). Spruce and fir foliage is nitrogen rich and nitrogen inputs from spruce budworm are 10 times higher than phosphorus (De Grandpré et al., 2022).

The lack of relationships between enzyme activities and cumulative defoliation aligns well with the observed increase in algal biomass and increase in bacteria carbohydrate biosynthesis functions which suggest an abundance of easily accessible carbon in the streams. Microbes only produce enzymes to obtain nutrients from organic matter when they do not have an adequate simple source of organic carbon (Cunha et al., 2010). Furthermore, we observed interannual variability in enzyme activities, with the lowest activity rates observed in 2021. This could be attributable to higher stream flow and sedimentation rates in this year (Table A2; Figure A11), as they can impede biofilm establishment and lead to reduced microbial functioning (Besemer, 2016).

4.4 Physical Stream Habitat Changes

We also observed changes in physical stream habitat characteristics (stream flow and temperature) associated with higher cumulative defoliation. Higher stream flow rates associated with increased cumulative defoliation intensity are likely due to the reduced evapotranspiration rates from foliage loss causing a decline in water storage potential in the catchment (Bearup et al., 2014; Sidhu et al., in prep; Sørensen et al., 2009). Hierarchical partitioning models indicate that elevation was a more important driver of stream flow than cumulative defoliation, however there is substantial shared variation between cumulative defoliation and elevation in 2019 and 2020. The large contribution of elevation to the models is likely driven by the considerable variability in snowpack levels associated with the elevation gradient across the study area (M. Stastny, personal communication, February 13, 2023). The lower importance of cumulative

defoliation in 2021 could be attributed to interannual climatic variability (Schäfer et al., 2014), spatiotemporal distribution of defoliation across the study area (Robert et al., 2012), and the influence of spray treatments on some watersheds (Sidhu et al., in prep). By 2021, half of the watersheds had received two years of spray treatments, which has the potential to reduce the impacts of previous years of defoliation and alter the relationship between flow and cumulative defoliation (Sidhu et al., in prep).

The positive association between stream temperatures and cumulative defoliation observed in this study is likely due to increased soil temperatures from a reduction in foliage (De Grandpré et al., 2022). Increased light levels in the streams could also have an effect on stream temperatures (Addy et al., 2018), however this can only be speculated as light levels were not measured in this study. Further, previous studies assessing the influence of increased light levels from defoliation on stream temperatures have found mixed responses. For example, spongy moth defoliation corresponded to increased light levels and stream temperatures (Addy et al., 2018), while hemlock woody adelgid defoliation led to increased light levels but no accompanying increase in stream temperatures (Siderhurst et al., 2010). This is possibly due to varying proportions of groundwater inputs to streams, as streams with greater groundwater inputs (and less hydrologic flow through warming surface soils) likely do not result in increased stream temperatures (Siderhurst et al., 2010). In this study, the observed increase in stream temperatures cannot be attributed to cumulative defoliation alone, as hierarchical partitioning models suggest that the variance explained by defoliation is shared with other landscape parameters (elevation, latitude, and spruce-fir composition). These parameters are interconnected on the landscape and the increased temperatures we observed were likely driven by the combined influence of all metrics rather than one individual metric. The observed changes in physical stream characteristics

(temperature and flow), combined with the changes in carbon quality, appear to have contributed to the alterations of bacteria and fungi community composition that were observed along the cumulative defoliation gradient.

4.5 Limitations

While functional inference and trait assignment tools provide valuable insights about potential microbial functions, they also come with several limitations that are important to consider. Functional inference tools (i.e., PICRUSt2 used in this study) have three main limitations. First, they assume that phylogenetic traits are conserved and don't account for gene gain or loss associated with horizontal gene transfer (Djemiel et al., 2022; Taberlet et al., 2018). Second, they only provide insight on functional *potential*, as a gene present in a sample may not be expressed under all environmental conditions. Finally, the accuracy of PICRUSt2 functional predictions depends on the quality of the reference genome database (Djemiel et al., 2022; Taberlet et al., 2018). We used PICRUSt2 for 16S data as the number of sequenced genomes present in the 16S reference database is sufficient to make predictions (Douglas et al., 2020). In contrast, we did not use PICRUSt2 for the ITS data as the number of sequenced genomes present in the ITS reference database is much lower, making the predictions only slightly better than random and much less accurate than 16S (Djemiel et al., 2022; Douglas et al., 2020).

The functional trait assignment tool (FUNGuild) used to predict ITS functions provides more general assignments and is a more accurate approach for predicting fungi functions (Djemiel et al., 2022). There are two main limitations with this tool. First, it only assigns traits to organisms found in the reference database rather than relying on the assumption of phylogenetic relatedness like PiCRUSt2 (Djemiel et al., 2022). While this has the benefit of improved accuracy of assignments, it also has the drawback of many sequences in the dataset without any

functional assignment (i.e., in our study, 40% of the ITS sequences were unassigned). Second, this method is limited by the taxonomic resolution of the sequences. Many of the functional traits are assigned at the genus level rather than species level, and one genus can be assigned multiple functional traits, which limits the precision of the prediction (Djemiel et al., 2022).

4.6 Broader Implications and Future Directions

The shifts in carbon cycling functions observed in this study require further investigation, particularly with the potential implications related to climate change. There are currently global efforts to accurately quantify carbon sinks and sources across different ecosystem types (e.g., wetlands, forests, and streams) to inform management strategies that enhance carbon capture or reduce carbon emissions under forest change and disturbance scenarios (Casas-Ruiz et al., 2023). It is well recognized that carbon is transferred from terrestrial ecosystems to aquatic ecosystems, however it is still highly uncertain how much of this transferred carbon is stored in aquatic sediments or released back to the atmosphere, challenging the ability to assess impacts of forest change (Casas-Ruiz et al., 2023). Furthermore, spruce budworm management interventions (e.g., aerial spray with Btk) have been found to reduce carbon losses and maintain carbon storage in boreal forests (Z. Liu et al., 2020). Given that forest pest defoliation is the most widespread disturbance type in Canadian forests, understanding the fate of the associated carbon transfer from defoliated forests to freshwater ecosystems and to the atmosphere is critical for accurate carbon budget assessments. Future work should implement the framework proposed by (Casas-Ruiz et al., 2023) and link terrestrial and aquatic carbon transfer to obtain accurate estimates of carbon transfer within defoliated watersheds.

The influence of spruce budworm outbreaks on stream microbiomes should be explored further in future years as defoliation in the study area separates from natural gradients on the

landscape and tree mortality increases. As defoliation continues to intensify in the lower and central watersheds, collinearity between cumulative defoliation, elevation, and forest composition will be reduced. Further, while we found no evidence of an influence of tree mortality on microbial community structure or function, we did find increased NO_2-NO_3 and TN concentrations in streams associated with tree mortality. Elevated nutrient levels can influence stream microbial community composition, diversity, and function (Besemer, 2016; Fernandes et al., 2014). Tree mortality is expected to increase in the study area as the spruce budworm outbreak continues, and future work should investigate the potential implications for stream microbiomes.

Finally, as forests in the study area recover from the spruce budworm outbreak, the resilience of the stream microbial communities should be examined. Several short-term studies (< 1 year) of microbial communities in freshwater ecosystems have reported that communities are resilient to pulse disturbances and return to the pre-disturbance state (Eckert et al., 2019; Shade et al., 2011; Shade, Read, et al., 2012; Walker et al., 2022). In contrast, press disturbances (like spruce budworm defoliation) are not well studied in freshwater ecosystems and are more likely to cause microbial communities to shift to an alternative stable state post-disturbance (Beattie et al., 2020; Shade, Peter, et al., 2012).

5.0 Conclusion

Canada's boreal forests are increasingly threatened by natural disturbances including forest pest outbreaks (Natural Resources Canada, 2022). This study evaluated the influence of cumulative spruce budworm defoliation on stream ecosystems within forested watersheds and there were three key outcomes. First, we demonstrated that cumulative defoliation altered stream habitat through increases in SUVA (DOM aromaticity), temperature, and flow rates, but not nutrient concentrations or any other DOM quantity or quality metrics. We also observed early indications of defoliation induced tree mortality increasing stream nitrogen levels. Second, we observed changes to stream microbiome structure, with increased algal biomass and changes to microbial community composition, but we did not observe any changes to overall microbial diversity. Finally, cumulative defoliation was associated with changes to bacterial functions involved in carbon cycling, but no changes were observed to fungi functions or overall microbial functions measured through extracellular enzyme activities and leaf litter decomposition rates. Overall, the observed alterations to dissolved organic matter quality and the bacteria communities associated with carbon cycling provide key insights into how forest disturbances can influence stream carbon processing.

Proactive forest management interventions like the Early Intervention Strategy (EIS) drastically reduce economic costs, forest carbon emissions, and impacts to forest resources (Johns et al., 2019) and the findings of this study suggest that the benefits could also extend to carbon processing in stream ecosystems. However, more research is needed to explore if these changes in within stream carbon cycling are altering the rates of carbon transfer from the streams to the atmosphere. This is particularly important given the current climate crisis, as there are

global efforts to manage ecosystems in ways that can enhance carbon capture or reduce carbon emissions to mitigate climate change (Casas-Ruiz et al., 2023).

This study evaluated the influence of cumulative defoliation during the first six years of a spruce budworm outbreak and found alterations to stream habitat and microbial community structure and function, but the influence of defoliation should continue to be explored as the outbreak progresses over time. Tree mortality typically begins after the fifth year of intense defoliation (MacLean, 1984), and many of the watersheds in this region have not yet reached this level of defoliation. It will be important to evaluate the influence of tree mortality on stream ecosystems as it is likely to affect stream hydrology and biogeochemical cycling (Mikkelson, Bearup, et al., 2013; Mikkelson, Dickenson, et al., 2013; Reed et al., 2018; Sidhu et al., in prep; Zimmermann et al., 2000) which could have further implications for stream microbial community structure and function.

References

Abarenkov, K., Zirk, A., Piirmann, T., Pöhönen, R., Ivanov, F., Nilsson, R. H., & Kõljalg, U. (2021). *Full UNITE+INSD dataset for eukaryotes*. https://doi.org/https://dx.doi.org/10.15156/BIO/1281567

Adams, H. E., Crump, B. C., & Kling, G. W. (2010). Temperature controls on aquatic bacterial production and community dynamics in arctic lakes and streams. *Environmental Microbiology*, *12*(5), 1319–1333. https://doi.org/10.1111/j.1462-2920.2010.02176.x

Addy, K., Gold, A. J., Loffredo, J. A., Schroth, A. W., Inamdar, S. P., Bowden, W. B., Kellogg, D. Q., & Birgand, F. (2018). Stream response to an extreme drought-induced defoliation event. *Biogeochemistry*, *140*(2), 199–215. https://doi.org/10.1007/s10533-018-0485-3

Allan, J. D., Castillo, M. N., & Kapps, K. A. (2021). Stream Microbial Ecology. In *Stream Ecology*. Springer, Cham. https://doi.org/10.1007/978-3-030-61286-3_8

Balducci, L., Fierravanti, A., Rossi, S., Delzon, S., De Grandpré, L., Kneeshaw, D. D., & Deslauriers, A. (2020). The paradox of defoliation: Declining tree water status with increasing soil water content. *Agricultural and Forest Meteorology*, *290*(April), 108025. https://doi.org/10.1016/j.agrformet.2020.108025

Bearup, L. A., Maxwell, R. M., Clow, D. W., & McCray, J. E. (2014). Hydrological effects of forest transpiration loss in bark beetle-impacted watersheds. *Nature Climate Change*, *4*(6), 481–486. https://doi.org/10.1038/nclimate2198

Beattie, R. E., Bandla, A., Swarup, S., & Hristova, K. R. (2020). Freshwater Sediment Microbial Communities Are Not Resilient to Disturbance From Agricultural Land Runoff. *Frontiers in Microbiology*, *11*(October), 1–14. https://doi.org/10.3389/fmicb.2020.539921

Bengtsson-Palme, J., Ryberg, M., Hartmann, M., Branco, S., Wang, Z., Godhe, A., De Wit, P., Sánchez-García, M., Ebersberger, I., de Sousa, F., Amend, A., Jumpponen, A., Unterseher, M., Kristiansson, E., Abarenkov, K., Bertrand, Y. J. K., Sanli, K., Eriksson, K. M., Vik, U., … Nilsson, R. H. (2013). Improved software detection and extraction of ITS1 and ITS2 from ribosomal ITS sequences of fungi and other eukaryotes for analysis of environmental sequencing data. *Methods in Ecology and Evolution*, *4*(10), 914–919. https://doi.org/10.1111/2041-210X.12073

Berger, J. ., & Blouin, J. (2004). *Guide de reconnaissance des types écologiques des régions écologiques 4g – Côte de la baie des Chaleur et 4h – Côte gaspésienne*.

Berger, J. ., & Blouin, J. (2006). *Guide de reconnaissance des types écologiques des régions écologiques 5h - Massif gaspésien et 5i - Haut massif gaspésien*.

Bertolet, B. L., Corman, J. R., Casson, N. J., Sebestyen, S. D., Kolka, R. K., & Stanley, E. H. (2018). Influence of soil temperature and moisture on the dissolved carbon, nitrogen, and phosphorus in organic matter entering lake ecosystems. *Biogeochemistry*, *139*(3), 293–305.

https://doi.org/10.1007/s10533-018-0469-3

Besemer, K. (2016). Biodiversity , community structure and function of biofilms in stream ecosystems. *Research in Microbiology*, *166*(10), 774–781. https://doi.org/10.1016/j.resmic.2015.05.006.Biodiversity

Besemer, K., Singer, G., Hödl, I., & Battin, T. J. (2009). Bacterial community composition of stream biofilms in spatially variable-flow environments. *Applied and Environmental Microbiology*, *75*(22), 7189–7195. https://doi.org/10.1128/AEM.01284-09

BioCyc. (2023). *PATHWAY/GENOME DATABASE CONCEPTS GUIDE*. https://biocyc.org/PGDBConceptsGuide.shtml

Brandt, J. P. (2009). The extent of the North American boreal zone. *Environmental Reviews*, *17*, 101–161. https://doi.org/10.1139/A09-004

Burdon, F. J., Bai, Y., Reyes, M., Tamminen, M., Staudacher, P., Mangold, S., Singer, H., Räsänen, K., Joss, A., Tiegs, S. D., Jokela, J., Eggen, R. I. L., & Stamm, C. (2020). Stream microbial communities and ecosystem functioning show complex responses to multiple stressors in wastewater. *Global Change Biology*, *26*(11), 6363–6382. https://doi.org/10.1111/gcb.15302

Burns, D. A., Aiken, G. R., Bradley, P. M., Journey, C. A., & Schelker, J. (2013). Specific ultra-violet absorbance as an indicator of mercury sources in an Adirondack River basin. *Biogeochemistry*, *113*(1–3), 451–466. https://doi.org/10.1007/s10533-012-9773-5

Candau, J. N., & Fleming, R. A. (2011). Forecasting the response of spruce budworm defoliation to climate change in Ontario. *Canadian Journal of Forest Research*, *41*(10), 1948–1960. https://doi.org/10.1139/x11-134

Casas-Ruiz, J. P., Bodmer, P., Bona, K. A., Butman, D., Couturier, M., Emilson, E. J. S., Finlay, K., Genet, H., Hayes, D., Karlsson, J., Paré, D., Peng, C., Striegl, R., Webb, J., Wei, X., Ziegler, S. E., & Del Giorgio, P. A. (2023). Integrating terrestrial and aquatic ecosystems to constrain estimates of land-atmosphere carbon exchange. *Nature Communications*, *14*(1), 1571. https://doi.org/10.1038/s41467-023-37232-2

Caspi, R., Billington, R., Fulcher, C. A., Keseler, I. M., Kothari, A., Krummenacker, M., Latendresse, M., Midford, P. E., Ong, Q., Ong, W. K., Paley, S., Subhraveti, P., & Karp, P. D. (2018). The MetaCyc database of metabolic pathways and enzymes. *Nucleic Acids Research*, *46*(D1), D633–D639. https://doi.org/10.1093/nar/gkx935

Cepáková, Š., Tošner, Z., & Frouz, J. (2016). The effect of tree species on seasonal fluctuations in water-soluble and hot water-extractable organic matter at post-mining sites. *Geoderma*, *275*, 19–27. https://doi.org/10.1016/j.geoderma.2016.04.006

Chen, J., Nan, J., Xu, D., Mo, L., Zheng, Y., Chao, L., Qu, H., Guo, Y., Li, F., & Bao, Y. (2020). Response differences between soil fungal and bacterial communities under opencast coal mining disturbance conditions. *Catena*, *194*(January).

https://doi.org/10.1016/j.catena.2020.104779

Clow, D. W., Rhoades, C., Briggs, J., Caldwell, M., & Lewis, W. M. (2011). Responses of soil and water chemistry to mountain pine beetle induced tree mortality in Grand County, Colorado, USA. *Applied Geochemistry*, *26*(SUPPL.), S174–S178. https://doi.org/10.1016/j.apgeochem.2011.03.096

Conant, R. T., Ryan, M. G., Ågren, G. I., Birge, H. E., Davidson, E. A., Eliasson, P. E., Evans, S. E., Frey, S. D., Giardina, C. P., Hopkins, F. M., Hyvönen, R., Kirschbaum, M. U. F., Lavallee, J. M., Leifeld, J., Parton, W. J., Megan Steinweg, J., Wallenstein, M. D., Martin Wetterstedt, J. Å., & Bradford, M. A. (2011). Temperature and soil organic matter decomposition rates - synthesis of current knowledge and a way forward. *Global Change Biology*, *17*(11), 3392–3404. https://doi.org/10.1111/j.1365-2486.2011.02496.x

Cunha, A., Almeida, A., Coelho, F. J. R. C., Gomes, N. C. M., Oliveira, V., & Santos, A. L. (2010). Bacterial Extracellular Enzymatic Activity in Globally Changing Aquatic Ecosystems. *Current Research, Technology and Education Topics in Applied Microbiology and Microbial Biotechnology*, *1*, 124–135.

De Grandpré, L., Marchand, M., Kneeshaw, D. D., Paré, D., Boucher, D., Bourassa, S., Gervais, D., Simard, M., Griffin, J. M., & Pureswaran, D. S. (2022). Defoliation-induced changes in foliage quality may trigger broad-scale insect outbreaks. *Communications Biology*, *5*(1), 1–10. https://doi.org/10.1038/s42003-022-03407-8

De Vries, F. T., Liiri, M. E., Bjørnlund, L., Bowker, M. A., Christensen, S., Setälä, H. M., & Bardgett, R. D. (2012). Land use alters the resistance and resilience of soil food webs to drought. *Nature Climate Change*, *2*(4), 276–280. https://doi.org/10.1038/nclimate1368

Djemiel, C., Maron, P. A., Terrat, S., Dequiedt, S., Cottin, A., & Ranjard, L. (2022). Inferring microbiota functions from taxonomic genes: a review. *GigaScience*, *11*, 1–30. https://doi.org/10.1093/gigascience/giab090

Douglas, G. M., Maffei, V. J., Zaneveld, J. R., Yurgel, S. N., Brown, J. R., Taylor, C. M., & Huttenhower, C. (2020). PICRUSt2 for prediction of metagenome functions. *Nature Biotechnology*, *38*(6), 685–688. https://doi.org/10.1038/s41587-020-0548-6

Dudgeon, D., Arthington, A. H., Gessner, M. O., Kawabata, Z. I., Knowler, D. J., Lévêque, C., Naiman, R. J., Prieur-Richard, A. H., Soto, D., Stiassny, M. L. J., & Sullivan, C. A. (2006). Freshwater biodiversity: Importance, threats, status and conservation challenges. *Biological Reviews of the Cambridge Philosophical Society*, *81*(2), 163–182. https://doi.org/10.1017/S1464793105006950

ECCC. (2022). *Environment and Climate Change Canada Historical Climate Data*. https://climate.weather.gc.ca/index_e.html

Eckert, E. M., Quero, G. M., Di Cesare, A., Manfredini, G., Mapelli, F., Borin, S., Fontaneto, D., Luna, G. M., & Corno, G. (2019). Antibiotic disturbance affects aquatic microbial community composition and food web interactions but not community resilience. *Molecular*

Ecology, *28*(5), 1170–1182. https://doi.org/10.1111/mec.15033

Edgar, R. C. (2016a). UCHIME2: improved chimera prediction for amplicon sequencing. *BioRxiv*, 074252. https://www.biorxiv.org/content/10.1101/074252v1%0Ahttps://www.biorxiv.org/content/10.1101/074252v1.abstract

Edgar, R. C. (2016b). UNOISE2: improved error-correction for Illumina 16S and ITS amplicon sequencing. *BioRxiv*, 081257. https://www.biorxiv.org/content/10.1101/081257v1%0Ahttps://www.biorxiv.org/content/10.1101/081257v1.abstract

Emilson, C. E., Kreutzweiser, D. P., Gunn, J. M., & Mykytczuk, N. C. S. (2016). Effects of land use on the structure and function of leaf-litter microbial communities in boreal streams. *Freshwater Biology*, *61*(7), 1049–1061. https://doi.org/10.1111/fwb.12765

Erdozain, M., Kidd, K., Kreutzweiser, D., & Sibley, P. (2018). Linking stream ecosystem integrity to catchment and reach conditions in an intensively managed forest landscape. *Ecosphere*, *9*(5). https://doi.org/10.1002/ecs2.2278

Fasching, C., Akotoye, C., Bižić, M., Fonvielle, J., Ionescu, D., Mathavarajah, S., Zoccarato, L., Walsh, D. A., Grossart, H. P., & Xenopoulos, M. A. (2020). Linking stream microbial community functional genes to dissolved organic matter and inorganic nutrients. *Limnology and Oceanography*, *65*(S1), S71–S87. https://doi.org/10.1002/lno.11356

Fernandes, I., Seena, S., Pascoal, C., & Cássio, F. (2014). Elevated temperature may intensify the positive effects of nutrients on microbial decomposition in streams. *Freshwater Biology*, *59*(11), 2390–2399. https://doi.org/10.1111/fwb.12445

Findlay, S. (2010). Stream microbial ecology. *Journal of the North American Benthological Society*, *29*(1), 170–181. https://doi.org/10.1899/09-023.1

Gorke, B., & Stulke, J. (2008). Carbon catabolite repression in bacteria: many ways to make the most out of nutrients. *Nature Reviews Microbiology*, *6*, 613–624. https://doi.org/https://doi.org/10.1038/nrmicro1932

Gray, D. R., & MacKinnon, W. E. (2006). Outbreak patterns of the spruce budworm and their impacts in Canada. *Forestry Chronicle*, *82*(4), 550–561. https://doi.org/10.5558/tfc82550-4

Gray, David R. (2008). The relationship between climate and outbreak characteristics of the spruce budworm in eastern Canada. *Climatic Change*, *87*(3–4), 361–383. https://doi.org/10.1007/s10584-007-9317-5

Grossart, H. P., Massana, R., McMahon, K. D., & Walsh, D. A. (2020). Linking metagenomics to aquatic microbial ecology and biogeochemical cycles. *Limnology and Oceanography*, *65*(S1), S2–S20. https://doi.org/10.1002/lno.11382

Hanley, K. W., Wollheim, W. M., Salisbury, J., Huntington, T., & Aiken, G. (2013). Controls on

dissolved organic carbon quantity and chemical character in temperate rivers of North America. *Global Biogeochemical Cycles*, *27*(2), 492–504. https://doi.org/10.1002/gbc.20044

Hazlett, P., Broad, K., Gordon, A., Sibley, P., Buttle, J., & Larmer, D. (2008). The importance of catchment slope to soil water N and C concentrations in riparian zones: Implications for riparian buffer width. *Canadian Journal of Forest Research*, *38*(1), 16–30. https://doi.org/10.1139/X07-146

Hood, E., Gooseff, M. N., & Johnson, S. L. (2006). Changes in the character of stream water dissolved organic carbon during flushing in three small watersheds, Oregon. *Journal of Geophysical Research: Biogeosciences*, *111*(1), 1–8. https://doi.org/10.1029/2005JG000082

Hosen, J. D., Febria, C. M., Crump, B. C., & Palmer, M. A. (2017). Watershed urbanization linked to differences in stream bacterial community composition. *Frontiers in Microbiology*, *8*(AUG), 1–17. https://doi.org/10.3389/fmicb.2017.01452

Huguet, A., Vacher, L., Relexans, S., Saubusse, S., Froidefond, J. M., & Parlanti, E. (2009). Properties of fluorescent dissolved organic matter in the Gironde Estuary. *Organic Geochemistry*, *40*(6), 706–719. https://doi.org/10.1016/j.orggeochem.2009.03.002

Izagirre, O., Serra, A., Guasch, H., & Elosegi, A. (2009). Effects of sediment deposition on periphytic biomass, photosynthetic activity and algal community structure. *Science of the Total Environment*, *407*(21), 5694–5700. https://doi.org/10.1016/j.scitotenv.2009.06.049

Jane, S. F., Winslow, L. A., Remucal, C. K., & Rose, K. C. (2017). Long-term trends and synchrony in dissolved organic matter characteristics in Wisconsin, USA, lakes: Quality, not quantity, is highly sensitive to climate. *Journal of Geophysical Research: Biogeosciences*, *122*, 546–561. https://doi.org/10.1002/2016JG003630.Received

Jenicek, M., Pevna, H., & Matejka, O. (2018). Canopy structure and topography effects on snow distribution at a catchment scale: Application of multivariate approaches. *Journal of Hydrology and Hydromechanics*, *66*(1), 43–54. https://doi.org/10.1515/johh-2017-0027

Johns, R. C., Bowden, J. J., Carleton, D. R., Cooke, B. J., Edwards, S., Emilson, E. J. S., James, P. M. A., Kneeshaw, D., MacLean, D. A., Martel, V., Moise, E. R. D., Mott, G. D., Norfolk, C. J., Owens, E., Pureswaran, D. S., Quiring, D. T., Régnière, J., Richard, B., & Stastny, M. (2019). A conceptual framework for the spruce budworm Early Intervention Strategy: Can outbreaks be stopped? *Forests*, *10*(10), 1–19. https://doi.org/10.3390/f10100910

Jones, J. I., Murphy, J. F., Collins, A. L., Sear, D. A., Naden, P. S., & Armitage, P. . (2012). THE IMPACT OF FINE SEDIMENT ON MACRO-INVERTEBRATES. *River Research and Applications*, *28*, 1055–1071. https://doi.org/10.1002/rra.1516

Karp, P. D., Paley, S., Krieger, C. J., & Zhang, P. (2004). An Evidence Ontology for Use in Pathway/Genome Databases. *Pacific Symposium on Biocomputing*, *9*, 190–201.

Kielstra, B. W., Mackereth, R. W., Melles, S. J., & Emilson, E. J. S. (2021). *hydroweight:*

Inverse distance-weighted rasters and landscape attributes (R package version 1.2.0). https://doi.org/https://doi.org/10.5281/zenodo.4728558

Kreutzweiser, D. P., Gringorten, J. L., Thomas, D. R., & Butcher, J. T. (1996). Functional effects of the bacterial insecticide Bacillus thuringiensis var. kurstaki on aquatic microbial communities. *Ecotoxicology and Environmental Safety*, *33*(3), 271–280. https://doi.org/10.1006/eesa.1996.0035

Kreutzweiser, D. P., Hazlett, P. W., & Gunn, J. M. (2008). Logging impacts on the biogeochemistry of boreal forest soils and nutrient export to aquatic systems: A review. *Environmental Reviews*, *16*, 157–179. https://doi.org/10.1139/A08-006

Lai, J., Zou, Y., Zhang, J., & Peres-Neto, P. R. (2022). Generalizing hierarchical and variation partitioning in multiple regression and canonical analyses using the rdacca.hp R package. *Methods in Ecology and Evolution*, *13*(4), 782–788. https://doi.org/10.1111/2041-210X.13800

Laperriere, S. M., Hilderbrand, R. H., Keller, S. R., Trott, R., & Santoro, A. E. (2020). Headwater stream microbial diversity and function across agricultural and urban land use gradients. *Applied and Environmental Microbiology*, *86*(11). https://doi.org/10.1128/AEM.00018-20

Lau, K. E. M., Washington, V. J., Fan, V., Neale, M. W., Lear, G., Curran, J., & Lewis, G. D. (2015). A novel bacterial community index to assess stream ecological health. *Freshwater Biology*, *60*(10), 1988–2002. https://doi.org/10.1111/fwb.12625

Liu, E. Y., Lantz, V. A., MacLean, D. A., & Hennigar, C. (2019). Economics of early intervention to suppress a potential spruce budworm outbreak on crown land in New Brunswick, Canada. *Forests*, *10*(6). https://doi.org/10.3390/f10060481

Liu, Z., Peng, C., De Grandpré, L., Candau, J. N., Work, T., Zhou, X., & Kneeshaw, D. (2020). Aerial spraying of bacterial insecticides to control spruce budworm defoliation leads to reduced carbon losses. *Ecosphere*, *11*(1). https://doi.org/10.1002/ecs2.2988

Lofgren, L. A., Uehling, J. K., Branco, S., Bruns, T. D., Martin, F., & Kennedy, P. G. (2019). Genome-based estimates of fungal rDNA copy number variation across phylogenetic scales and ecological lifestyles. *Molecular Ecology*, *28*(4), 721–730. https://doi.org/10.1111/mec.14995

Luo, L., Meng, H., & Gu, J. D. (2017). Microbial extracellular enzymes in biogeochemical cycling of ecosystems. *Journal of Environmental Management*, *197*, 539–549. https://doi.org/10.1016/j.jenvman.2017.04.023

MacLean, D. A. (1984). Effects of Spruce Budworm Outbreaks on the Productivity and Stability of Balsam Fir Forests. *The Forestry Chronicle*, *60*(5), 273–279. https://doi.org/10.5558/tfc60273-5

MacLean, D. A., & MacKinnon, W. E. (1996). Accuracy of aerial sketch-mapping estimates of

spruce budworm defoliation in New Brunswick. *Canadian Journal of Forest Research*, *26*(12), 2099–2108. https://doi.org/10.1139/x26-238

Magasanik, B. (1961). Catabolite Repression. *Cold Spring Harbor Symposium on Quantitative Biiology*, *26*, 249–256. https://doi.org/10.1101/sqb.1961.026.01.031.

Martin, M. (2011). Cutadapt removes adapter sequences from high -throughput sequencing reads. *EMBnet.Journal*, 10–12.

MetaCyc. (2023). *MetaCyc Pathway: superpathway of vanillin and vanillate degradation*. https://metacyc.org/META/NEW-IMAGE?type=PATHWAY&object=PWY-6338

Mikkelson, K. M., Bearup, L. A., Maxwell, R. M., Stednick, J. D., McCray, J. E., & Sharp, J. O. (2013). Bark beetle infestation impacts on nutrient cycling, water quality and interdependent hydrological effects. *Biogeochemistry*, *115*(1–3), 1–21. https://doi.org/10.1007/s10533-013-9875-8

Mikkelson, K. M., Dickenson, E. R. V., Maxwell, R. M., Mccray, J. E., & Sharp, J. O. (2013). Water-quality impacts from climate-induced forest die-off. *Nature Climate Change*, *3*(3), 218–222. https://doi.org/10.1038/nclimate1724

Ministère des Ressources naturelles et des Forêts. (2022). *Aires infestées par la tordeuse des bourgeons de l ' épinette au Québec en 2022*. https://mffp.gouv.qc.ca/documents/forets/RA_Aires_infesteesTBE_2022_MRNF.pdf

Muto, E., & Emilson, C. (2018). *Hydrolase Enzyme Assay Protocol - Leaf Litter Samples*. Natural Resources Canada.

Natural Resources Canada. (2018). *Spruce budworm: Research at the Laurentian Forestry Centre of Natural Resources Canada*. https://cfs.nrcan.gc.ca/publications?id=39413

Natural Resources Canada. (2022). *The State of Canada's Forests: Annual Report 2022*. https://natural-resources.canada.ca/sites/nrcan/files/forest/sof2022/SoF_Annual2022_EN_access.pdf

Nguyen, N. H., Song, Z., Bates, S. T., Branco, S., Tedersoo, L., Menke, J., Schilling, J. S., & Kennedy, P. G. (2016). FUNGuild: An open annotation tool for parsing fungal community datasets by ecological guild. *Fungal Ecology*, *20*, 241–248. https://doi.org/10.1016/j.funeco.2015.06.006

Ohno, T. (2002). Fluorescence inner-filtering correction for determining the humification index of dissolved organic matter. *Environmental Science and Technology*, *36*(4), 742–746. https://doi.org/10.1021/es0155276

Paul, M. J., LeDuc, S. D., Lassiter, M. G., Moorhead, L. C., Noyes, P. D., & Leibowitz, S. G. (2022). Wildfire Induces Changes in Receiving Waters: A Review With Considerations for Water Quality Management. *Water Resources Research*, *58*(9). https://doi.org/10.1029/2021WR030699

Peterson, E. E., Sheldon, F., Darnell, R., Bunn, S. E., & Harch, B. D. (2011). A comparison of spatially explicit landscape representation methods and their relationship to stream condition. *Freshwater Biology*, *56*(3), 590–610. https://doi.org/10.1111/j.1365-2427.2010.02507.x

Porter, T. M. (2020). *MetaWorks: A Multi-Marker Metabarcode Pipeline (Version v1.10.0)*. Zenodo. https://doi.org/doi:10.5281/zenodo.4741407

Porter, T. M. (2021). *terrimporter/UNITE_ITSClassifier: UNITE v2.0*. Zenodo. https://doi.org/https://doi.org/10.5281/zenodo.5565208

Porter, T. M., & Hajibabaei, M. (2022). METAWORKS: A flexible, scalable bioinformatic pipeline for multi-marker biodiversity assessments. *PLoS ONE*, *17*(9). https://doi.org/10.1371/journal.pone.0274260

Portillo, M. C., Anderson, S. P., & Fierer, N. (2012). Temporal variability in the diversity and composition of stream bacterioplankton communities. *Environmental Microbiology*, *14*(9), 2417–2428. https://doi.org/10.1111/j.1462-2920.2012.02785.x

Preston, C. M., & Trofymow, J. A. (2000). Variability in litter quality and its relationship to litter decay in Canadian forests. *Canadian Journal of Botany*, *78*(10), 1269–1287. https://doi.org/10.1139/cjb-78-10-1269

Qiagen. (2017). *DNeasy PowerSoil Kit Handbook*. https://www.qiagen.com/ca/resources/resourcedetail?id=5a0517a7-711d-4085-8a28-2bb25fab828a&lang=en

Reed, D. E., Ewers, B. E., Pendall, E., Frank, J., & Kelly, R. (2018). Bark beetle-induced tree mortality alters stand energy budgets due to water budget changes. *Theoretical and Applied Climatology*, *131*(1–2), 153–165. https://doi.org/10.1007/s00704-016-1965-9

Reid, A. J., Carlson, A. K., Creed, I. F., Eliason, E. J., Gell, P. A., Johnson, P. T. J., Kidd, K. A., MacCormack, T. J., Olden, J. D., Ormerod, S. J., Smol, J. P., Taylor, W. W., Tockner, K., Vermaire, J. C., Dudgeon, D., & Cooke, S. J. (2019). Emerging threats and persistent conservation challenges for freshwater biodiversity. *Biological Reviews*, *94*(3), 849–873. https://doi.org/10.1111/brv.12480

Robert, L. E., Kneeshaw, D., & Sturtevant, B. R. (2012). Effects of forest management legacies on spruce budworm (Choristoneura fumiferana) outbreaks. *Canadian Journal of Forest Research*, *42*(3), 463–475. https://doi.org/10.1139/X2012-005

Roberto, A. A., Van Gray, J. B., & Leff, L. G. (2018). Sediment bacteria in an urban stream: Spatiotemporal patterns in community composition. *Water Research*, *134*, 353–369. https://doi.org/10.1016/j.watres.2018.01.045

Rognes, T., Flouri, T., Nichols, B., Quince, C., & Mahé, F. (2016). VSEARCH: A versatile open source tool for metagenomics. *PeerJ*, *10*, 1–22. https://doi.org/10.7717/peerj.2584

Schäfer, K. V. R., Renninger, H. J., Clark, K. L., & Medvigy, D. (2014). Hydrological responses to defoliation and drought of an upland oak/pine forest. *Hydrological Processes*, *28*(25), 6113–6123. https://doi.org/10.1002/hyp.10104

Schowalter, T. D. (2012). Insect Herbivore Effects on Forest Ecosystem Services. *Journal of Sustainable Forestry*, *31*(6), 518–536. https://doi.org/10.1080/10549811.2011.636225

Shade, A., Peter, H., Allison, S. D., Baho, D. L., Berga, M., Bürgmann, H., Huber, D. H., Langenheder, S., Lennon, J. T., Martiny, J. B. H., Matulich, K. L., Schmidt, T. M., & Handelsman, J. (2012). Fundamentals of microbial community resistance and resilience. *Frontiers in Microbiology*, *3*(DEC), 1–19. https://doi.org/10.3389/fmicb.2012.00417

Shade, A., Read, J. S., Welkie, D. G., Kratz, T. K., Wu, C. H., & McMahon, K. D. (2011). Resistance, resilience and recovery: Aquatic bacterial dynamics after water column disturbance. *Environmental Microbiology*, *13*(10), 2752–2767. https://doi.org/10.1111/j.1462-2920.2011.02546.x

Shade, A., Read, J. S., Youngblut, N. D., Fierer, N., Knight, R., Kratz, T. K., Lottig, N. R., Roden, E. E., Stanley, E. H., Stombaugh, J., Whitaker, R. J., Wu, C. H., & McMahon, K. D. (2012). Lake microbial communities are resilient after a whole-ecosystem disturbance. *ISME Journal*, *6*(12), 2153–2167. https://doi.org/10.1038/ismej.2012.56

Siderhurst, L. A., Griscom, H. P., Hudy, M., & Bortolot, Z. J. (2010). Changes in light levels and stream temperatures with loss of eastern hemlock (Tsuga canadensis) at a southern Appalachian stream: Implications for brook trout. *Forest Ecology and Management*, *260*(10), 1677–1688. https://doi.org/10.1016/j.foreco.2010.08.007

Sidhu, H., Kidd, K., Emilson, E., Stastny, M., Venier, L., Keilstra, B., & McCarter, C. (n.d.). *Spruce budworm defoliation increases catchment runoff in conifer forests*.

Simonin, M., Voss, K. A., Hassett, B. A., Rocca, J. D., Wang, S. Y., Bier, R. L., Violin, C. R., Wright, J. P., & Bernhardt, E. S. (2019). In search of microbial indicator taxa: shifts in stream bacterial communities along an urbanization gradient. *Environmental Microbiology*, *21*(10), 3653–3668. https://doi.org/10.1111/1462-2920.14694

Sørensen, R., Ring, E., Meili, M., Högbom, L., Seibert, J., Grabs, T., Laudon, H., & Bishop, K. (2009). Forest harvest increases runoff most during low flows in two boreal streams. *Ambio*, *38*(7), 357–363. https://doi.org/10.1579/0044-7447-38.7.357

St. John, J. (2016). *SeqPrep*. https://github.com/jstjohn/SeqPrep/releases

Sun, S., Li, S., Avera, B. N., Strahm, B. D., & Badgley, B. D. (2017). Soil bacterial and fungal communities show distinct recovery patterns during forest ecosystem restoration. *Applied and Environmental Microbiology*, *83*(14). https://doi.org/10.1128/AEM.00966-17

Taberlet, P., Bonin, A., Zinger, L., & Coissac, E. (2018). *Environmental DNA for Biodiversity Research and Monitoring*. Oxford University Press. https://doi.org/10.1093/oso/9780198767220.001.0001

Thieme, L., Graeber, D., Hofmann, D., Bischoff, S., Schwarz, M. T., Steffen, B., Meyer, U. N., Kaupenjohann, M., Wilcke, W., Michalzik, B., & Siemens, J. (2019). Dissolved organic matter characteristics of deciduous and coniferous forests with variable management: Different at the source, aligned in the soil. *Biogeosciences*, *16*(7), 1411–1432. https://doi.org/10.5194/bg-16-1411-2019

Walker, J. R., Woods, A. C., Pierce, M. K., Steichen, J. L., Quigg, A., Kaiser, K., & Labonté, J. M. (2022). Functionally diverse microbial communities show resilience in response to a record-breaking rain event. *ISME Communications*, *2*(1). https://doi.org/10.1038/s43705-022-00162-z

Wang, Q., Garrity, G. M., Tiedje, J. M., & Cole, J. R. (2007). Naïve Bayesian classifier for rapid assignment of rRNA sequences into the new bacterial taxonomy. *Applied and Environmental Microbiology*, *73*(16), 5261–5267. https://doi.org/10.1128/AEM.00062-07

Warren, D. R., Keeton, W. S., Kiffney, P. M., Kaylor, M. J., Bechtold, H. A., & Magee, J. (2016). Changing forests-changing streams: Riparian forest stand development and ecosystem function in temperate headwaters. *Ecosphere*, *7*(8). https://doi.org/10.1002/ecs2.1435

Weishaar, J. L., Aiken, G. R., Bergamaschi, B. A., Fram, M. S., Fujii, R., & Mopper, K. (2003). Evaluation of specific ultraviolet absorbance as an indicator of the chemical composition and reactivity of dissolved organic carbon. *Environmental Science and Technology*, *37*(20), 4702–4708. https://doi.org/10.1021/es030360x

Wetzel, R. G. (2001). *Limnology: Lake and River Ecosystems* (Third edit). Academic Press.

Woodcock, S., Besemer, K., Battin, T. J., Curtis, T. P., & Sloan, W. T. (2013). Modelling the effects of dispersal mechanisms and hydrodynamic regimes upon the structure of microbial communities within fluvial biofilms. *Environmental Microbiology*, *15*(4), 1216–1225. https://doi.org/10.1111/1462-2920.12055

Zeglin, L. H. (2015). Stream microbial diversity in response to environmental changes: Review and synthesis of existing research. *Frontiers in Microbiology*, *6*(MAY), 1–15. https://doi.org/10.3389/fmicb.2015.00454

Zimmermann, L., Moritz, K., Kennel, M., & Bittersohl, J. (2000). Influence of bark beetle infestation on water quantity and quality in the Grosse Ohe catchment (Bavarian Forest National Park). *Silva Gabreta*, *4*, 51–62.

Appendix A: Supplemental Stream Habitat Tables and Figures

Table A1. Abbreviations and detection limits for stream water chemistry parameters measured in streams in the Gaspésie Peninsula, QC, Canada from May – October in 2019, 2020, and 2021. Parameters with less than 60% of measurements above detection limits were removed from analyses and are displayed in bold. A total of 336 measurements were taken across all 12 sites (96 in 2019, 120 in 2020, and 120 in 2021).

Parameter	Abbreviation	Detection limit (mg/L)	% of values above detection limit
Calcium	Ca	0.01	100
Potassium	K	0.01	100
Sodium	Na	0.01	100
Magnesium	Mg	0.005	100
Sulfate	SO_4	0.2	100
Chloride	Cl	0.2	100
Silica dioxide	SiO_2	.25	100
Total nitrogen	TN	0.05	98
Nitrite/Nitrate	NO_2 -NO_3	0.04	85
Ammonia	**NH_4**	**0.01**	**19**
Dissolved organic carbon	DOC	0.4	100
Dissolved inorganic carbon	DIC	0.5	100
Soluble reactive phosphorus	**SRP**	**0.001**	**32**
Total phosphorus	TP	0.001	92
Zinc	Zn	0.001	91
Aluminum	**Al**	**0.005**	**43**
Iron	**Fe**	**0.005**	**59**
Manganese	**Mn**	**0.0005**	**26**
Cadmium	**Cd**	**0.0005**	**0**
Copper	Cu	0.0005	96
Nickel	**Ni**	**0.0005**	**19**
Lead	**Pb**	**0.0005**	**0**

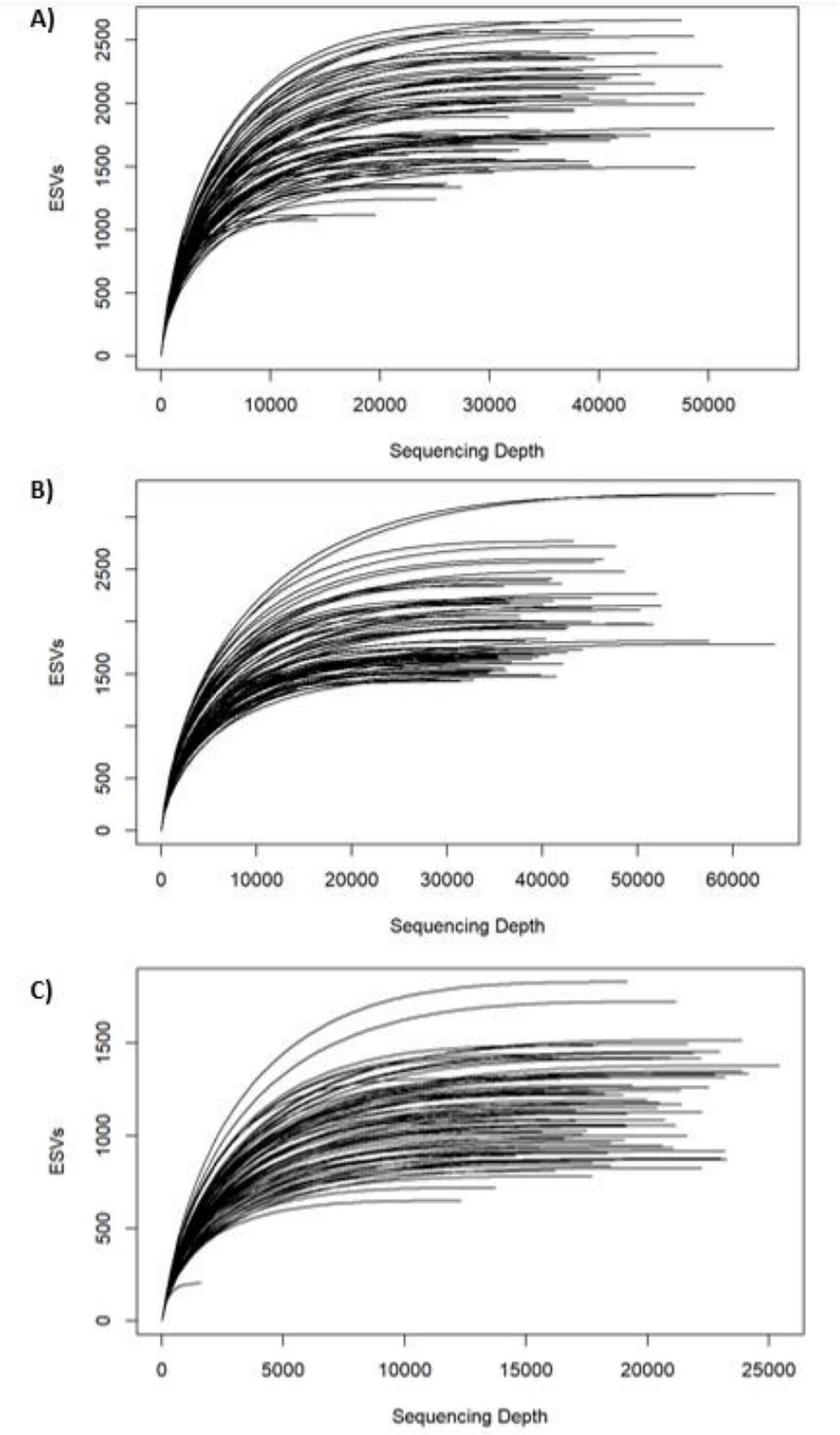

Figure A1. Rarefaction curves for 16S sequencing data from leaf packs in 12 streams in the Gaspésie Peninsula, QC, Canada in **A)** 2019, **B)** 2020, and **C)** 2021. Each line represents a leaf pack replicate (n=6/site).

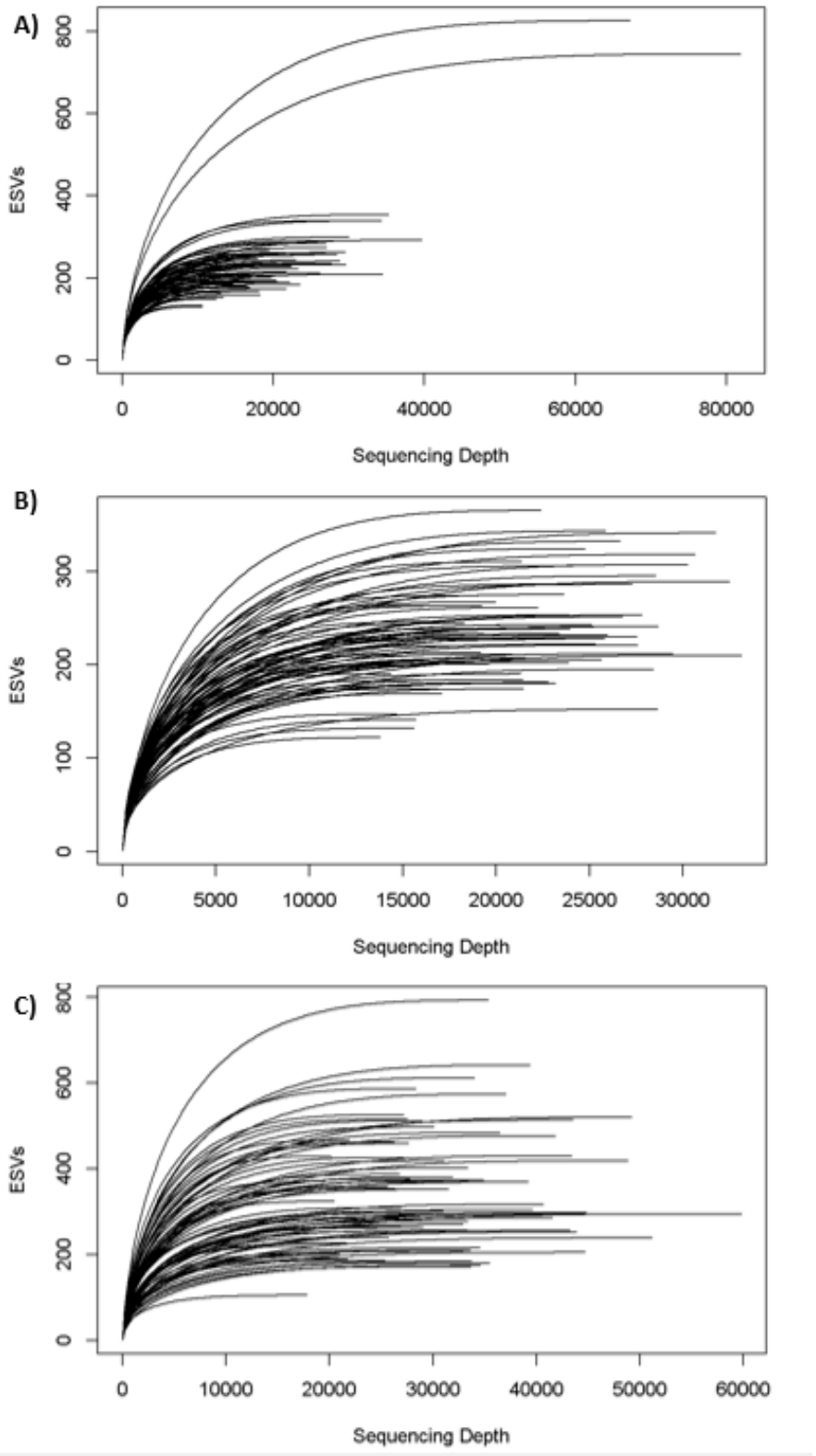

Figure A2. Rarefaction curves for ITS sequencing data from leaf packs in 12 streams in the Gaspésie Peninsula, QC, Canada in **A)** 2019, **B)** 2020, and **C)** 2021. Each line represents a leaf pack replicate (n=6/site).

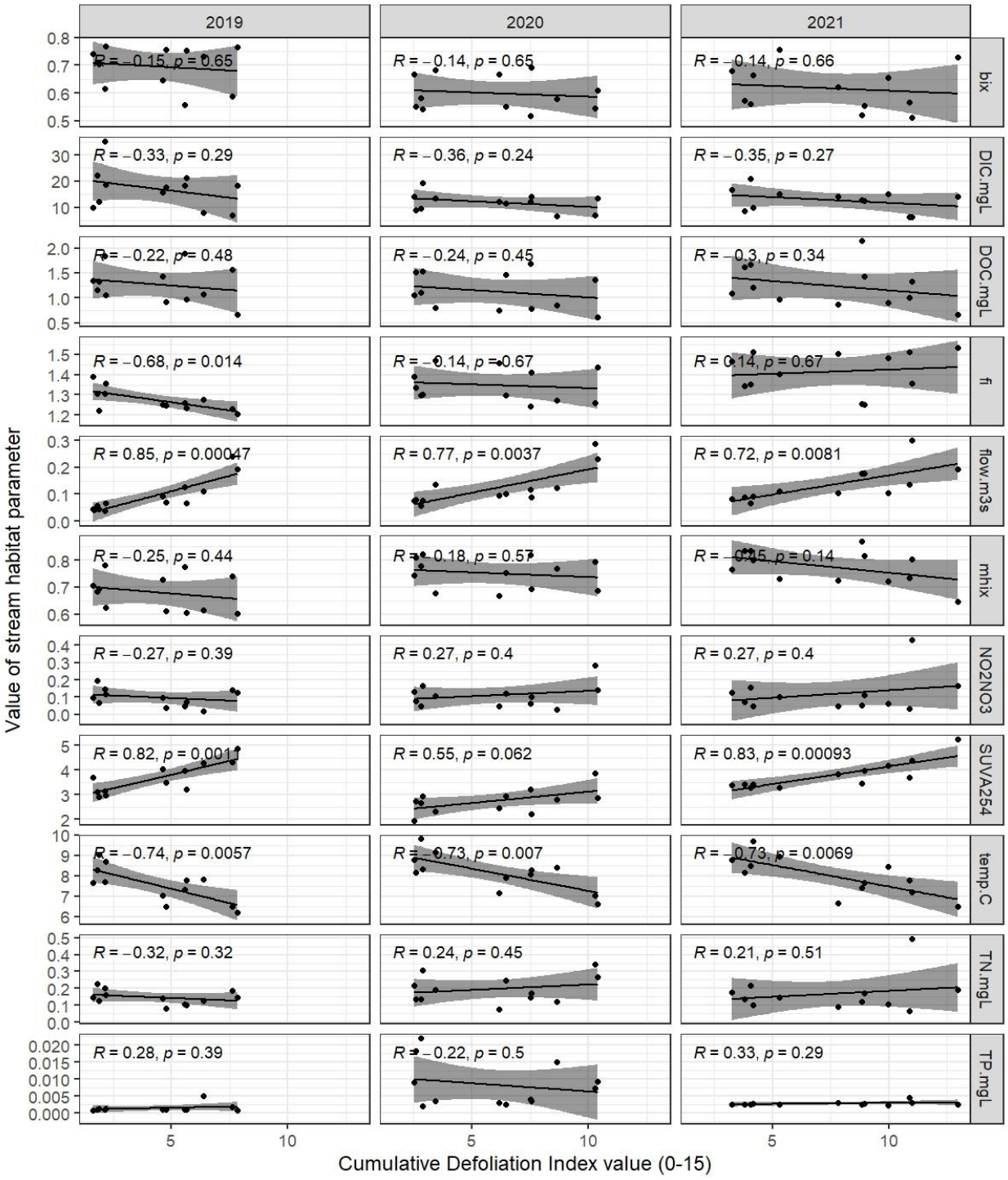

Figure A3. Pearson correlations between full season (May – October) stream habitat parameters and cumulative defoliation across all 12 sites in the Gaspésie Peninsula, QC, Canada. Average stream habitat values were used in analysis (n=8/site in 2019, n= 10/ site in 2020, and n=10/site in 2021).

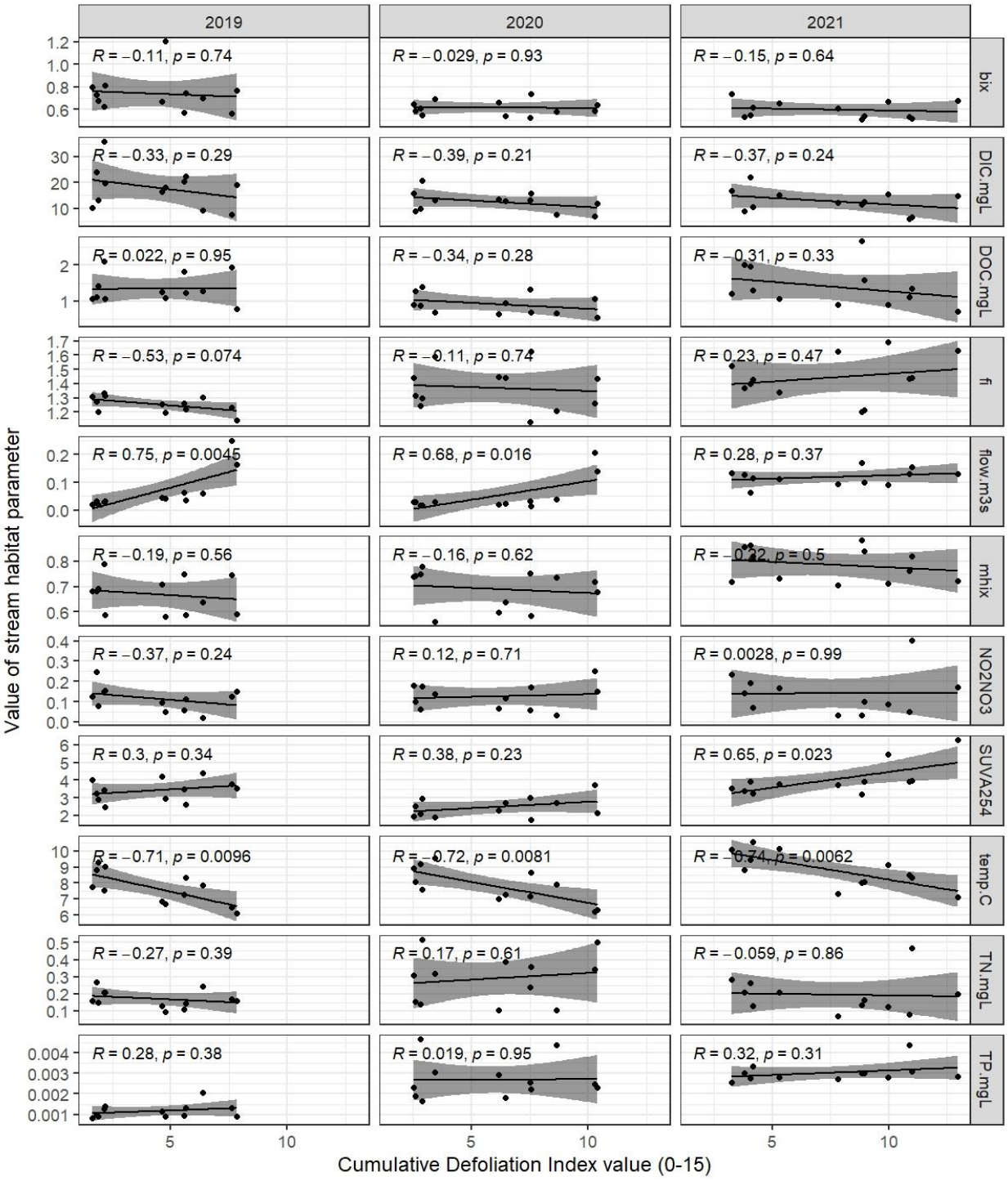

Figure A4. Pearson correlations between stream habitat parameters during leaf pack incubation (August- September) and cumulative defoliation across all 12 sites in the Gaspésie Peninsula, QC, Canada in 2019, 2020, and 2021. Average stream habitat values were used in analysis (n=3/site in each year).

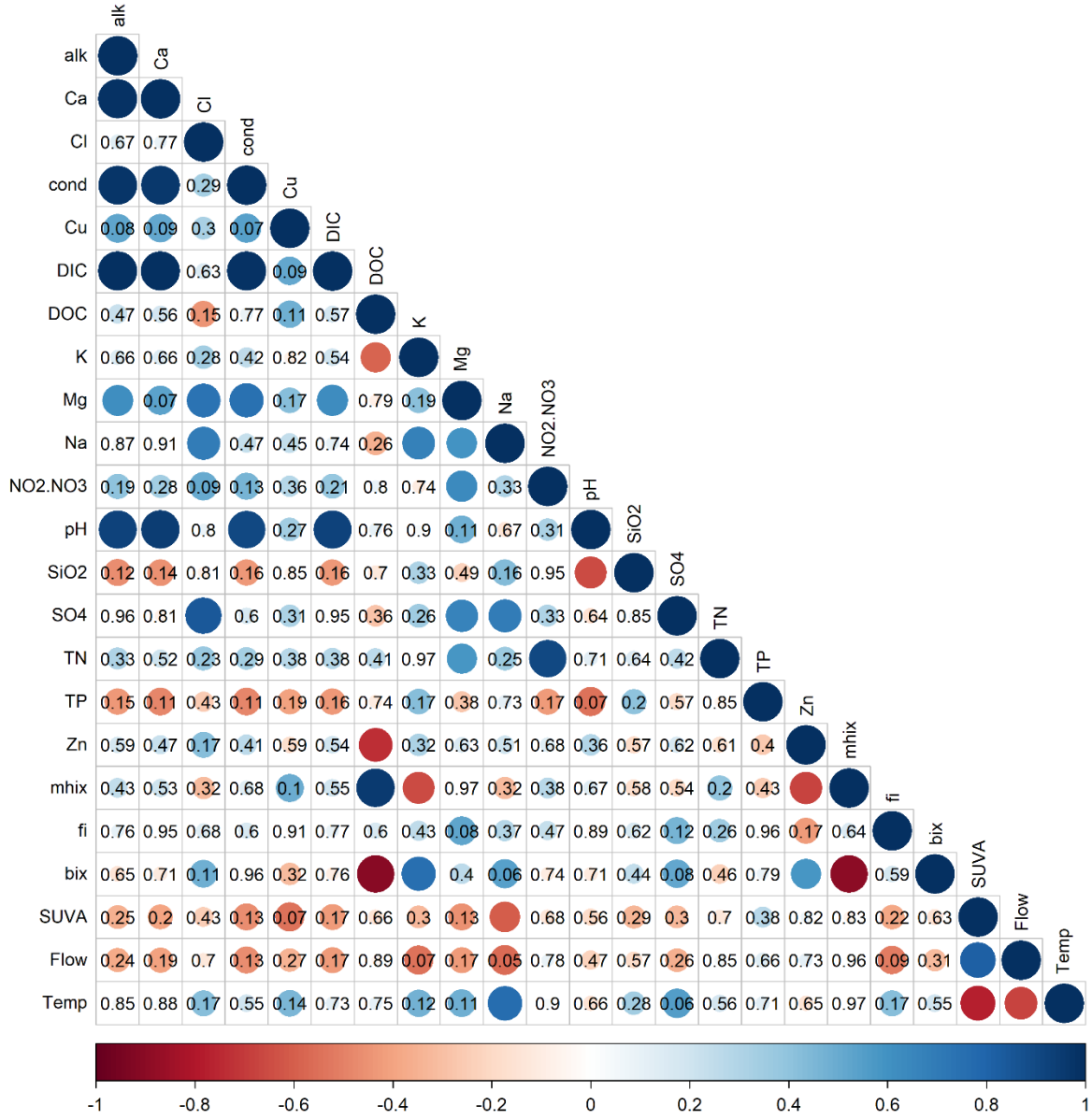

Figure A5. Pearson correlations between average full season (May – October) stream habitat metrics across all 12 stream sites the Gaspésie Peninsula, QC, Canada in 2019 (n=8 bi-weekly measurements/site). Blue circles represent a positive correlation and red circles represent a negative correlation, with darker shades and larger circles representing stronger correlations. P-values are displayed in the circle for all non-significant relationships and are not shown for significant relationships.

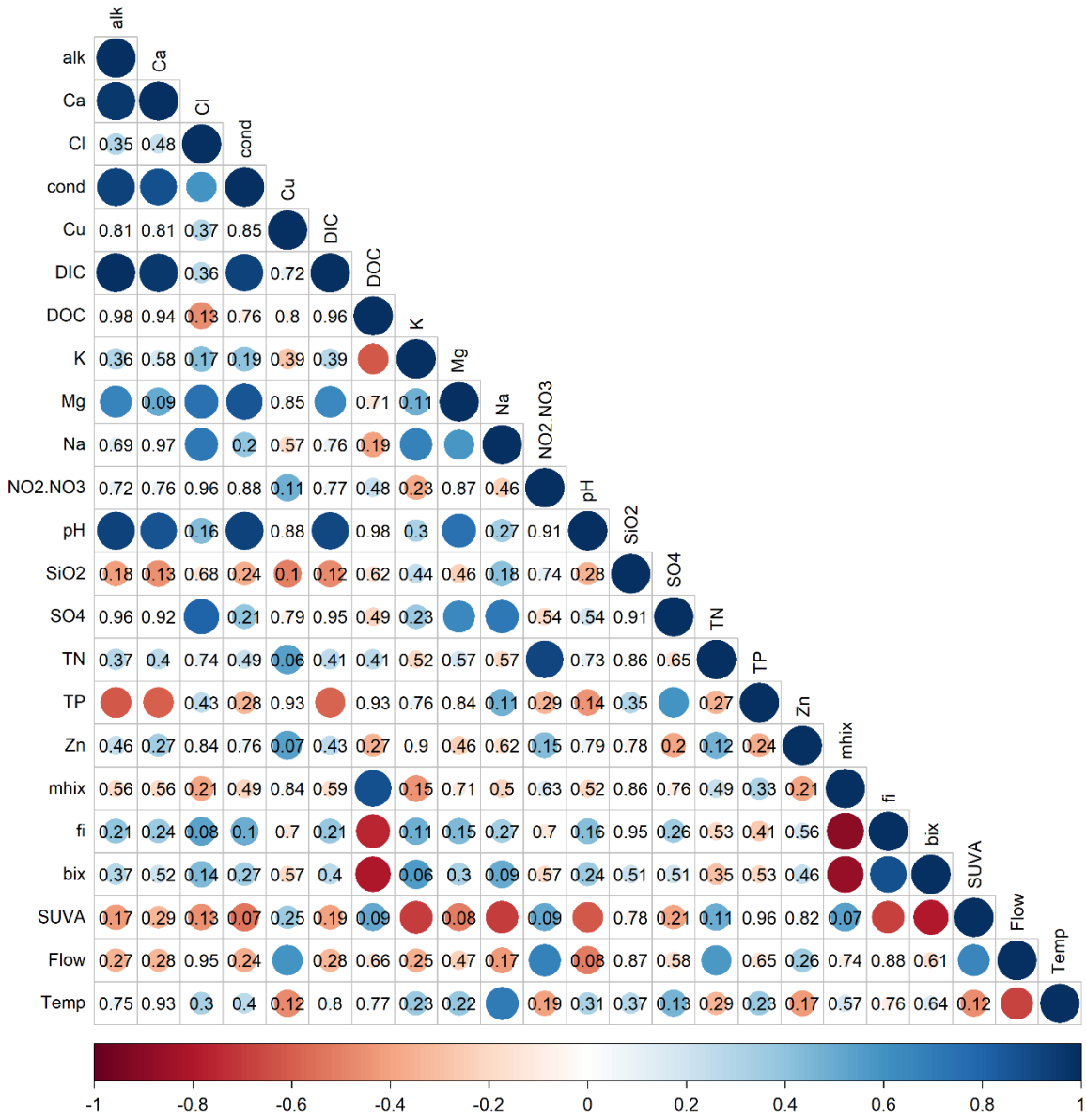

Figure A6. Pearson correlations between average full season (May – October) stream habitat metrics across all 12 stream sites in the Gaspésie Peninsula, QC, Canada in 2020 (n=10 bi-weekly measurements/site). Blue circles represent a positive correlation and red circles represent a negative correlation, with darker shades and larger circles representing stronger correlations. P-values are displayed in the circle for all non-significant relationships and are not shown for significant relationships.

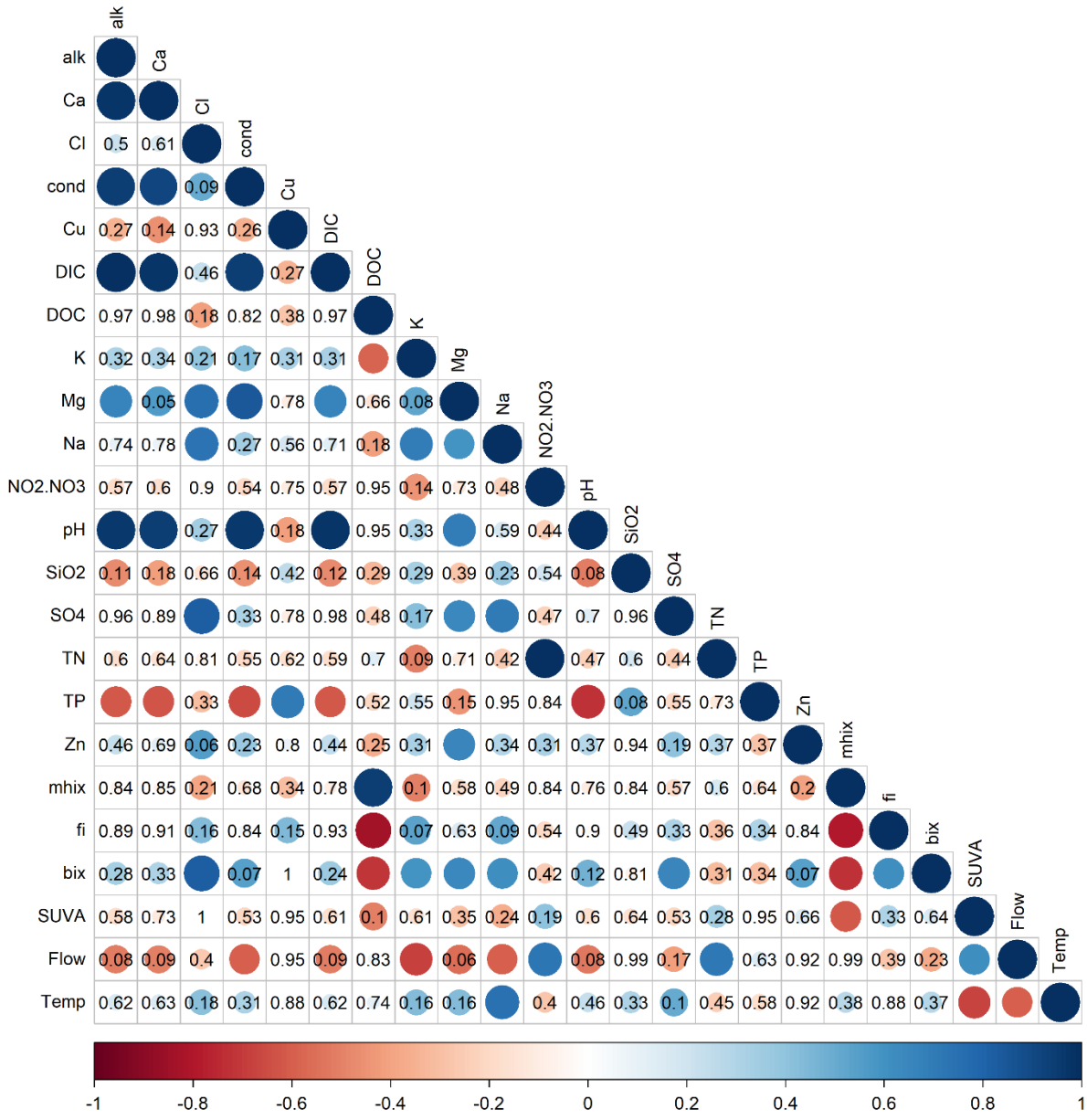

Figure A7. Pearson correlations between average full season (May – October) stream habitat metrics across all 12 stream sites in the Gaspésie Peninsula, QC, Canada in 2021 (n=10 bi-weekly measurements/site). Blue circles represent a positive correlation and red circles represent a negative correlation, with darker shades and larger circles representing stronger correlations. P-values are displayed in the circle for all non-significant relationships and are not shown for significant relationships.

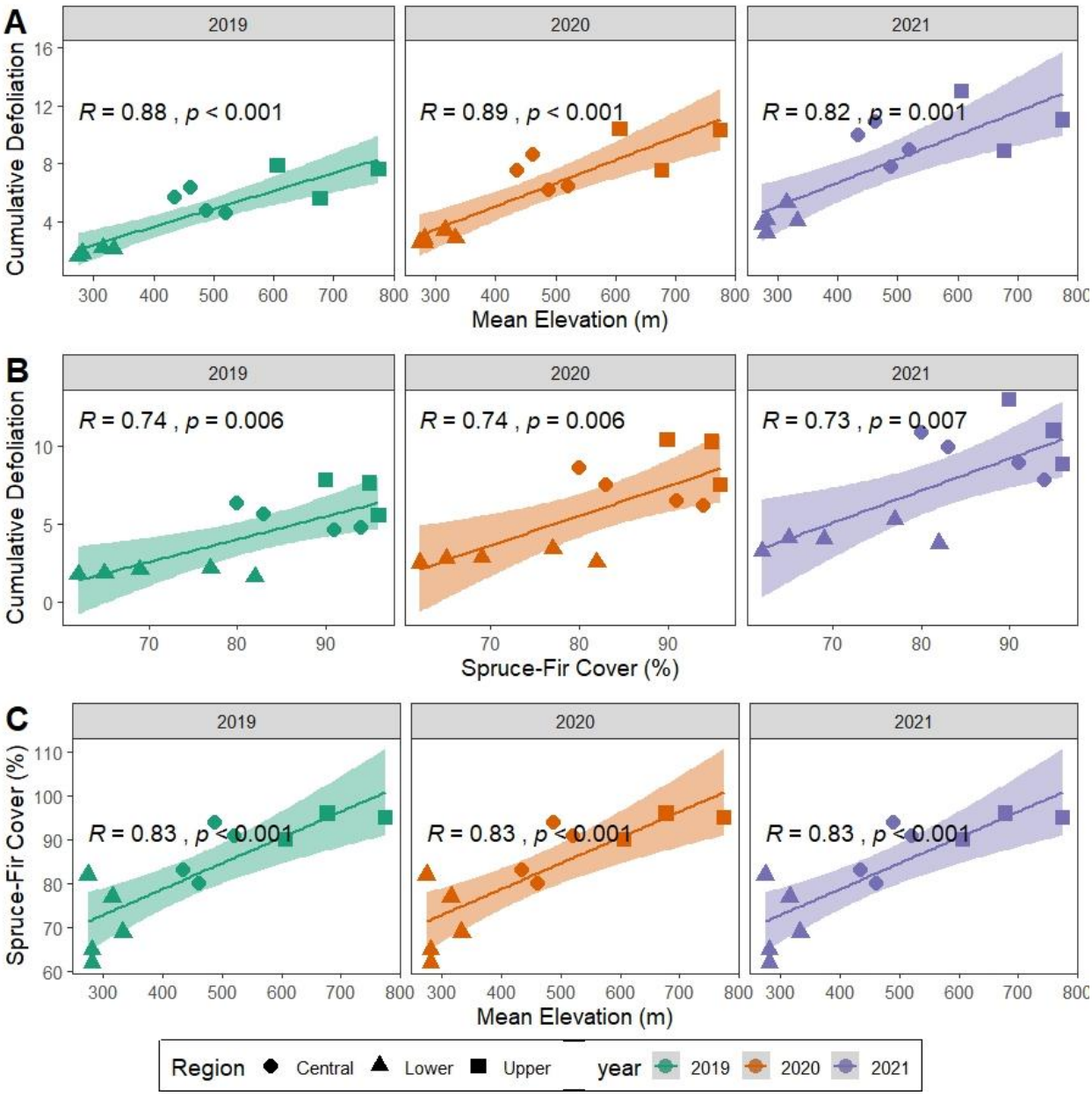

Figure A8. Pearson correlations between landscape parameters in watersheds in the Gaspésie Peninsula, QC, Canada in 2019, 2020, and 2021, with **A)** cumulative defoliation and mean elevation (m), **B)** cumulative defoliation and spruce-fir land cover (%), and **C)** mean elevation and spruce-fir land cover. Cumulative defoliation values for each year are used, while the same values for spruce-fir and elevation are used for all three years.

Table A2. Average stream habitat parameters per site per year from streams in the Gaspésie Peninsula, QC, Canada. SUVA, TN, NO2-NO3, TP, DOC, and flow are averages of biweekly measurements from May – October in 2019 (n=8/site), 2020 (n=10/site), and 2021 (n=10/site). Temperature averages (n=6 replicates/site, measured at 10-min intervals) are from data collected from mid-August-end of September each year.

Site	SUVA (L/mg-C m)	mhix	bix	fi	TN (mg/L)	NO_2-NO_3 (mg/L)	TP (mg/L)	DOC (mg/L)	Flow (m^3/s)	Temp (°C)
2019										
U01	4.87	0.60	0.77	1.21	0.14	0.13	0.0009	0.66	0.19	6.10
U02	4.31	0.74	0.59	1.23	0.19	0.14	0.0017	1.57	0.24	6.46
U03	3.96	0.78	0.56	1.26	0.11	0.05	0.0010	1.88	0.13	7.28
C04	4.28	0.61	0.73	1.28	0.13	0.02	0.0050	1.07	0.11	7.86
C05	3.22	0.61	0.75	1.23	0.10	0.07	0.0010	0.98	0.07	8.35
C06	3.50	0.61	0.76	1.25	0.08	0.04	0.0011	0.92	0.07	6.67
C07	4.03	0.73	0.65	1.25	0.14	0.10	0.0011	1.44	0.09	6.83
L08	3.15	0.78	0.62	1.31	0.20	0.15	0.0012	1.83	0.04	7.56
L09	2.90	0.69	0.71	1.22	0.13	0.07	0.0014	1.33	0.05	9.31
L10	3.12	0.69	0.71	1.31	0.23	0.20	0.0011	1.16	0.06	8.84
L11	2.99	0.62	0.77	1.35	0.16	0.12	0.0014	1.05	0.07	9.03
L12	3.69	0.71	0.74	1.39	0.15	0.10	0.0009	1.34	0.05	7.76
2020										
U01	2.88	0.69	0.61	1.44	0.27	0.14	0.0092	0.61	0.23	6.30
U02	3.87	0.79	0.54	1.26	0.34	0.29	0.0074	1.37	0.29	6.22
U03	3.21	0.82	0.52	1.24	0.15	0.06	0.0042	1.69	0.12	7.19
C04	2.81	0.77	0.58	1.27	0.12	0.03	0.0150	0.86	0.12	7.92
C05	2.23	0.69	0.69	1.41	0.17	0.10	0.0035	0.78	0.09	8.65
C06	2.45	0.67	0.67	1.46	0.08	0.05	0.0032	0.74	0.09	7.01
C07	2.92	0.75	0.55	1.30	0.25	0.12	0.0026	1.47	0.10	7.26
L08	2.93	0.82	0.54	1.30	0.31	0.17	0.0020	1.53	0.07	7.58
L09	2.67	0.78	0.58	1.30	0.14	0.05	0.0220	1.10	0.06	9.17
L10	1.95	0.74	0.67	1.39	0.21	0.13	0.0090	1.05	0.08	8.93
L11	2.34	0.68	0.68	1.47	0.19	0.11	0.0037	0.81	0.14	9.55
L12	2.72	0.81	0.55	1.34	0.14	0.08	0.0183	1.51	0.08	8.07
2021										
U01	5.24	0.65	0.73	1.53	0.19	0.16	0.0027	0.66	0.19	7.12
U02	4.37	0.80	0.51	1.36	0.49	0.43	0.0031	1.33	0.30	8.36
U03	3.47	0.87	0.52	1.26	0.12	0.05	0.0025	2.14	0.18	8.03
C04	3.70	0.74	0.57	1.51	0.07	0.03	0.0047	1.00	0.14	8.51
C05	4.19	0.72	0.66	1.48	0.10	0.06	0.0023	0.91	0.10	9.15
C06	3.83	0.72	0.62	1.50	0.09	0.05	0.0031	0.86	0.10	7.34
C07	3.95	0.82	0.55	1.25	0.17	0.11	0.0029	1.42	0.18	8.08
L08	3.28	0.83	0.56	1.35	0.22	0.16	0.0026	1.66	0.07	9.44
L09	3.43	0.80	0.66	1.51	0.10	0.05	0.0029	1.20	0.09	10.55

L10	3.39	0.76	0.68	1.47	0.18	0.13	0.0025	1.08	0.08	10.11
L11	3.29	0.73	0.76	1.40	0.14	0.10	0.0025	0.97	0.11	10.13
L12	3.41	0.84	0.57	1.34	0.14	0.07	0.0027	1.62	0.09	8.82

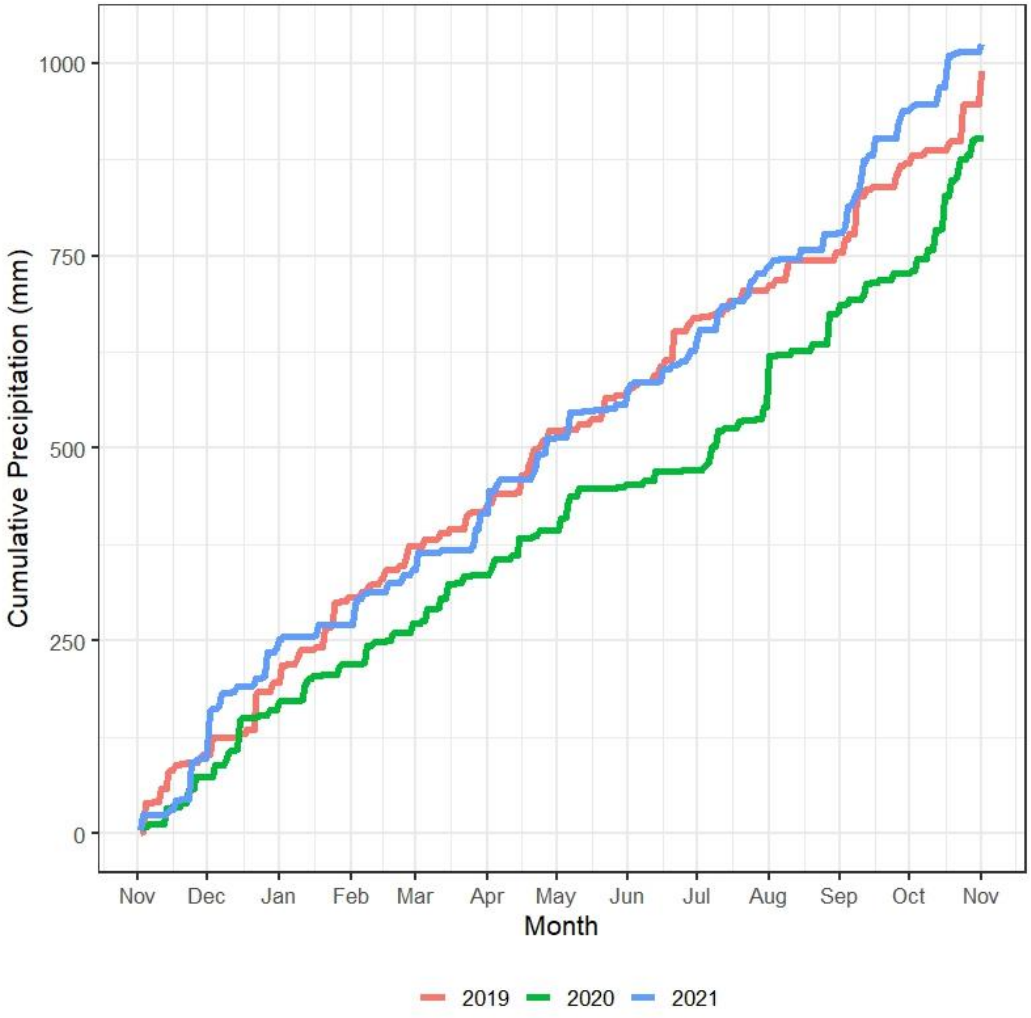

Figure A9. Cumulative precipitation (mm) measured at the New Richmond, QC Environment Canada Weather Station in 2019, 2020, 2021. Measurements start on Nov 1st of the previous year and end on Oct 31st of that year (i.e., 2019 = Nov 1st, 2018, to Oct 31st, 2019) to incorporate winter snowpack amounts.

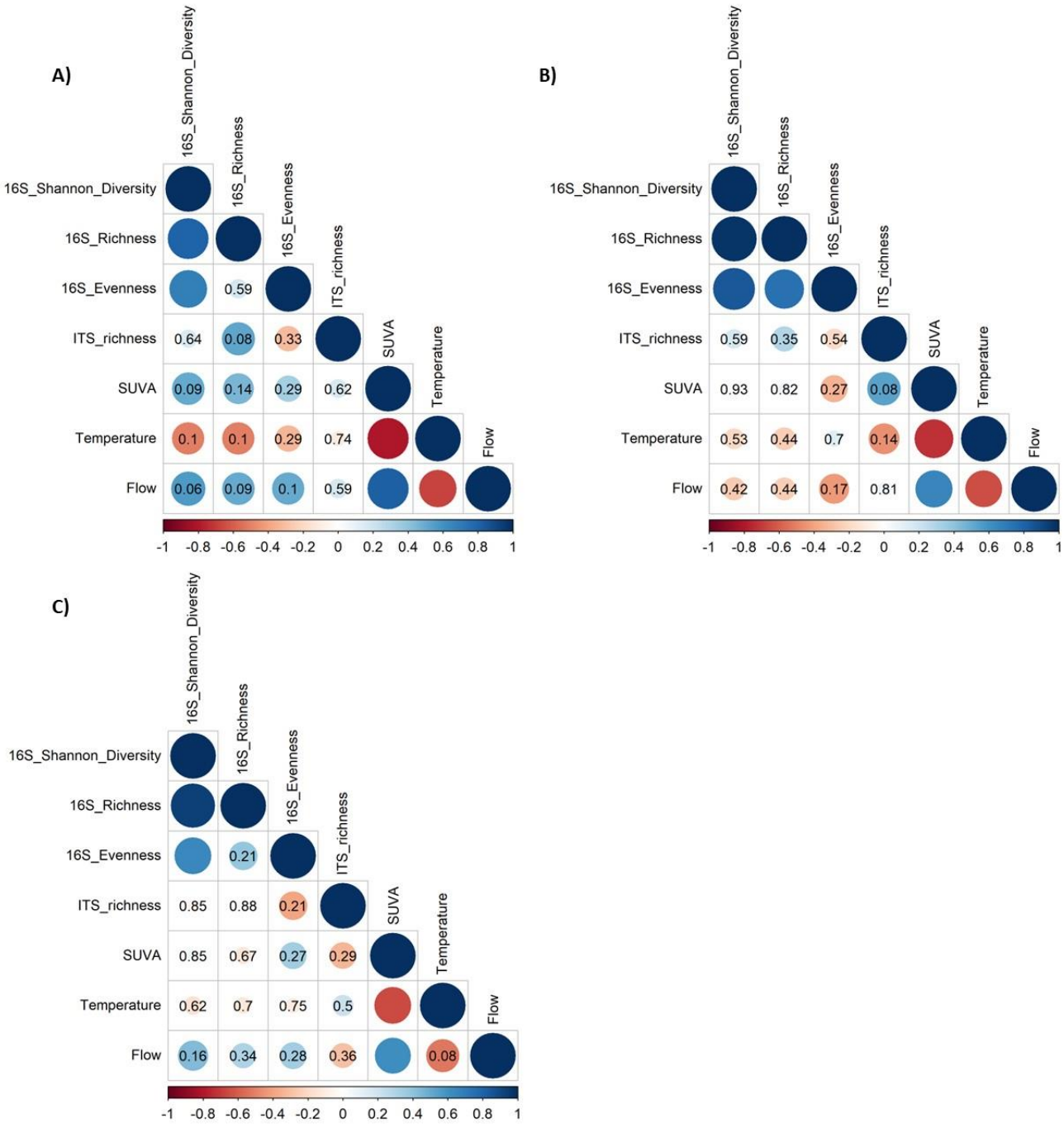

Figure A10. Pearson correlations between bacteria and fungi diversity metrics from leaf pack samples and stream habitat variables associated with increased cumulative defoliation in sites in the Gaspésie Peninsula, QC, Canada in **A)** 2019, **B)** 2020, and **C)** 2021. Blue circles represent a positive correlation and red circles represent a negative correlation, with darker shades and larger circles representing stronger correlations. P-values are displayed in the circle for all non-significant relationships and are not shown for significant relationships. Calculated based on average diversity from leaf pack samples (n=6/site/year) and average stream habitat (n=8 in 2019, n=10 in 2020, and n=2021).

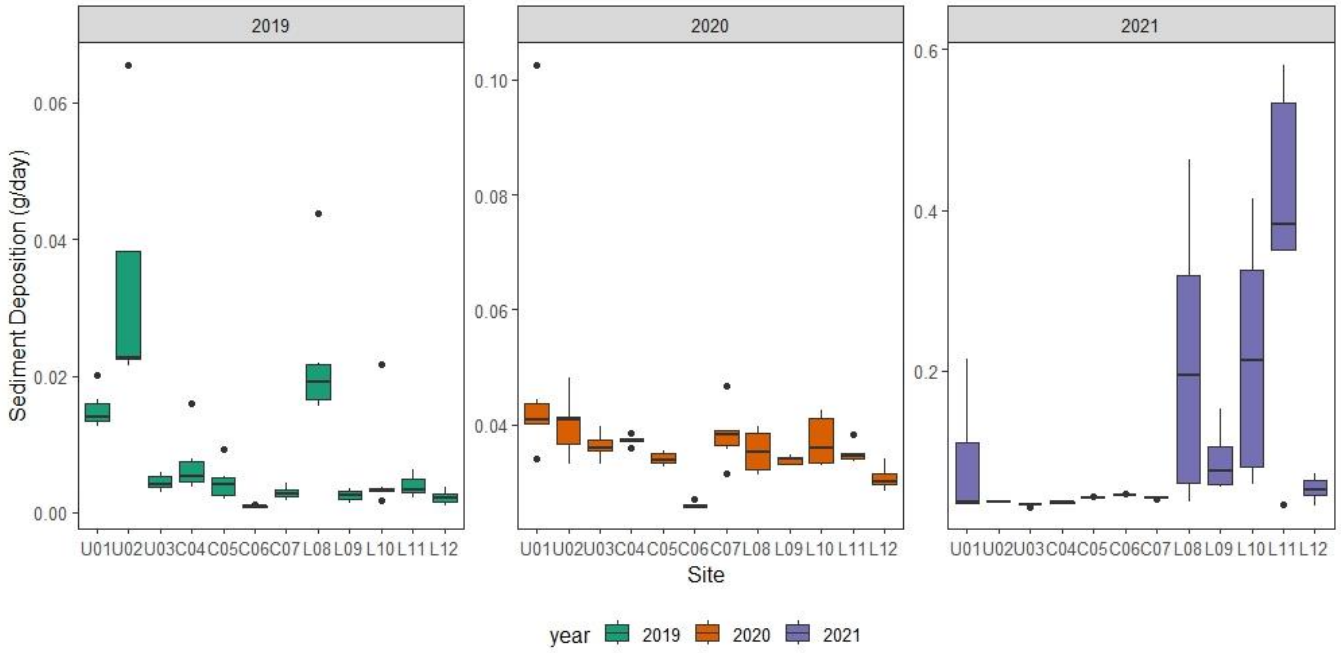

Figure A11. Boxplot of total sediment deposition rates (g/day) at each stream site in the Gaspésie Peninsula, QC, Canada in 2019, 2020, and 2021. Data represents n=6 replicates/site collected from mid-August-end September of each year, except for site U01 in 2019 (n=5), L09 in 2021 (n=4), and L11 in 2021 (n=5).

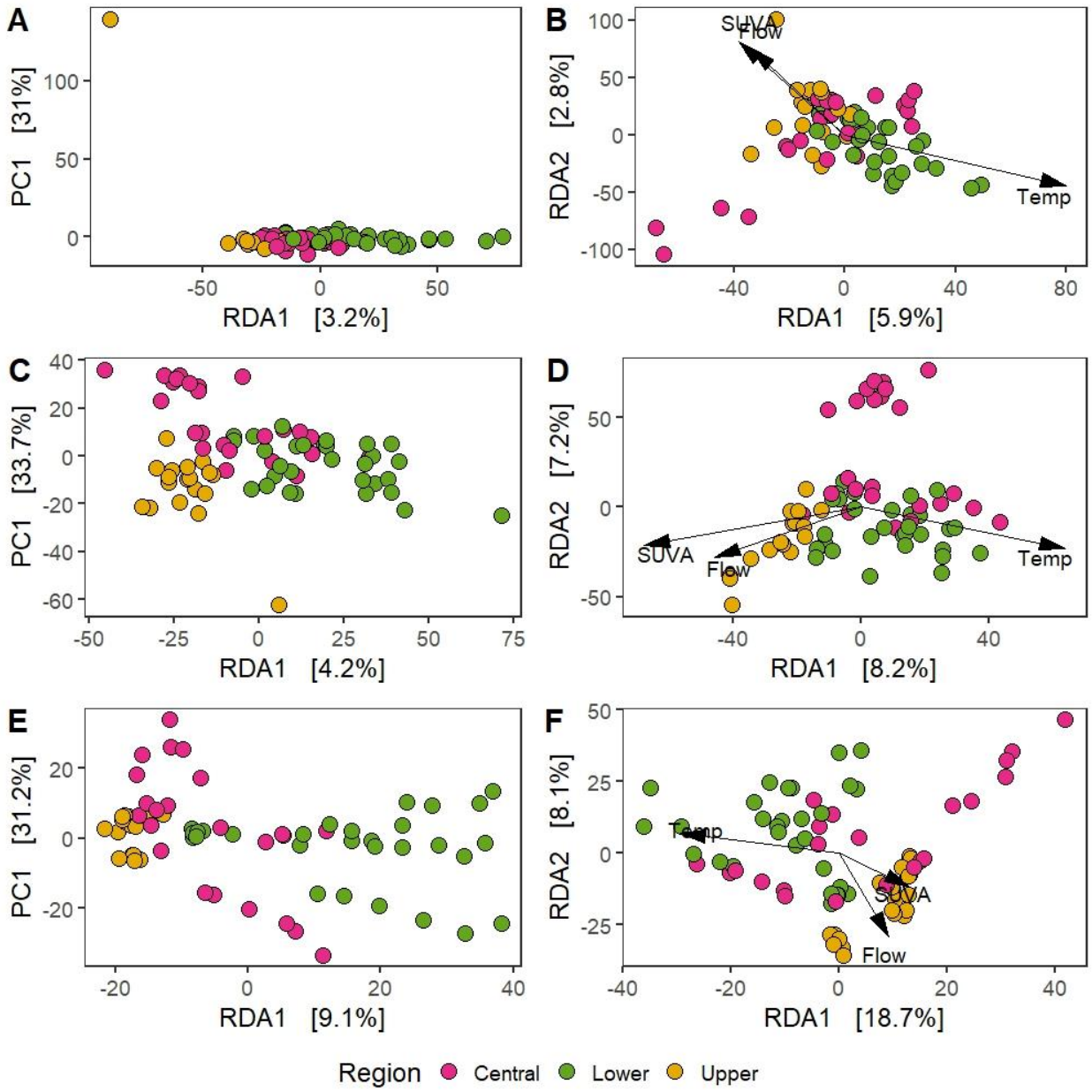

Figure A12. Comparison of bacteria community RDA plots constrained by **A), C),** and **E)** cumulative defoliation and **B), D),** and **F)** stream habitat variables associated with changes in cumulative defoliation (SUVA, flow, and temperature). Each row represents a different sample year, with panels A) and B) representing 2019, panels C) and D) 2020, and panels E and F) 2021. Each point displays a bacteria community from a leaf pack sample (n=6 replicates per site) and are coloured by geographic region in the Gaspésie Peninsula, QC, Canada. In panels constrained by cumulative defoliation (A, C, and E), the cumulative defoliation gradient is represented by RDA1 on the x-axis, while the y-axis shows other variability in the dataset (not explained by defoliation) represented by the strongest PCA axis (PC1).

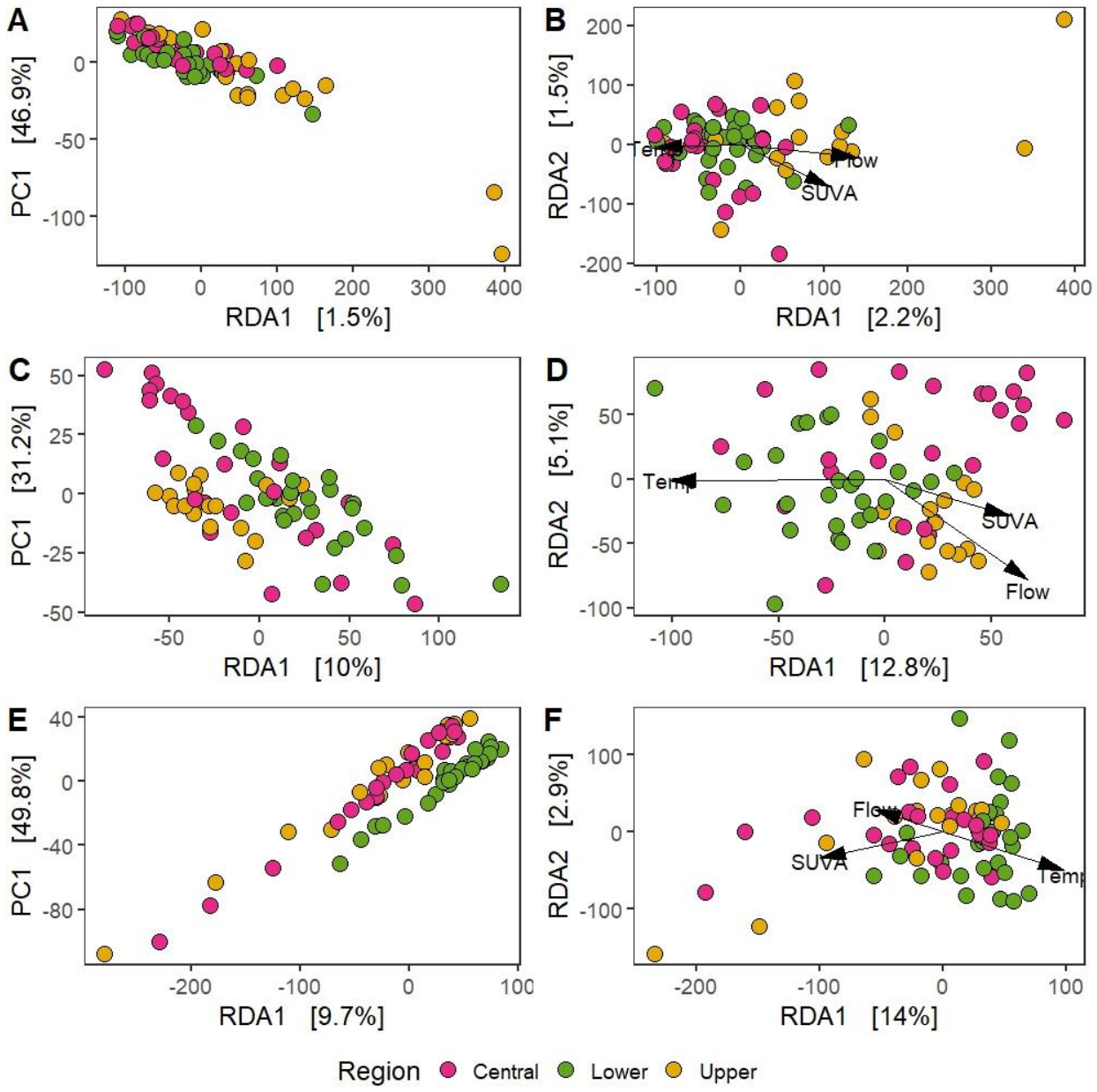

Figure A13. Comparison of fungi community RDA plots constrained by **A), C),** and **E)** cumulative defoliation and **B), D),** and **F)** stream habitat variables associated with changes in cumulative defoliation (SUVA, flow, and temperature). Each row represents a different sample year, with panels A) and B) representing 2019, panels C) and D) 2020, and panels E and F) 2021. Each point displays a fungi community from a leaf pack sample (n=6 replicates per site) and are coloured by geographic region the Gaspésie Peninsula, QC, Canada. In panels constrained by cumulative defoliation (A, C, and E), the cumulative defoliation gradient is represented by RDA1 on the x-axis, while the y-axis shows other variability in the dataset (not explained by defoliation) represented by the strongest PCA axis (PC1).

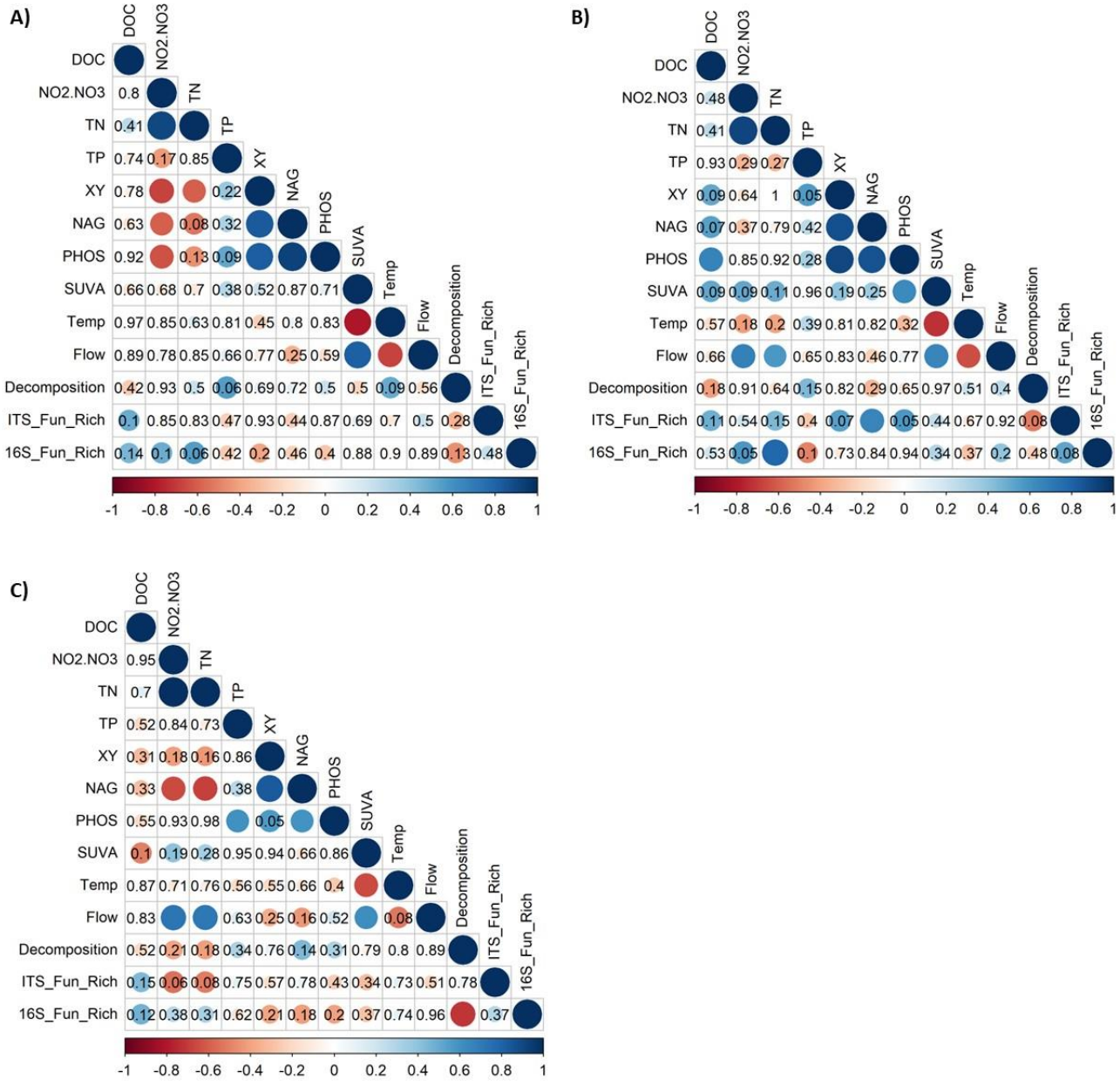

Figure A14. Pearson correlations between microbial function metrics and stream habitat variables in Gaspésie Peninsula, QC, Canada in **A)** 2019, **B)** 2020, and **C)** 2021. Metrics presented include extracellular enzyme activities (XY, NAG, and PHOS), leaf litter decomposition rates (mass loss per day), functional richness (16S and ITS), nutrients (TP, TN, NO_2-NO_3, DOM (DOC and SUVA), stream temperature, and stream flow. Blue circles represent a positive correlation and red circles represent a negative correlation, with darker shades and larger circles representing stronger correlations. P-values are displayed in the circle for all non-significant relationships and are not shown for significant relationships. Calculated based on averages of functional metrics from leaf pack samples (n=6/site/year) and averages of stream habitat data (n=8 in 2019, n=10 in 2020, and n=2021).